N O T I C E

THIS DOCUMENT HAS BEEN REPRODUCED FROM MICROFICHE. ALTHOUGH IT IS RECOGNIZED THAT CERTAIN PORTIONS ARE ILLEGIBLE, IT IS BEING RELEASED IN THE INTEREST OF MAKING AVAILABLE AS MUCH INFORMATION AS POSSIBLE

DOE/JPL-955079-80/1
Distribution Category UC-63

(NASA-CR-163884) DEVELOPMENT OF SIMPLIFIED PROCESS FOR ENVIRONMENTALLY RESISTANT CELLS Final Report, 8 Jun. 1978 - 30 Nov. 1980 (Kinetic Coatings, Inc.) 166 p HC A08/MF A01 CSCL 10A G3/44

N81-16575

Unclas 41186

Development of Simplified Process For Environmentally Resistant Cells

Final Report

December 1980

FEB 1981
RECEIVED
NASA STI FACILITY
ACCESS DEPT.

W. J. King

KINETIC COATINGS INCORPORATED
P. O. Box 416, S. Bedford Street
Burlington, MA 01803

JPL Contract No. 955079

"The JPL Low-Cost Silicon Solar Array Project is sponsored by the U.S. Department of Energy and forms part of the Solar Photovoltaic Conversion Program to initiate a major effort toward the development of low-cost solar arrays. This work was performed for the Jet Propulsion Laboratory, California Institute of Technology by agreement between NASA and DOE."

FOREWORD

This report was prepared by Kinetic Coatings, Inc., Burlington, Massachusetts 01803, and describes work performed from June 8, 1978 through November 30, 1980 on JPL Contract No. 955079.

Wm. J. King was Program Manager and was assisted in the research by E. R. Berman and P. J. Kramer.

Dale R. Burger was Technical Manager for JPL.

" This report was prepared as an account of work sponsored by the United States Government. Neither the United States nor the United States Department of Energy, nor any of their employees, nor any of their contractors, subcontractors, or their employees, makes any warranty, express or implied, or assumes any legal liability or responsibility for the accuracy, completeness or usefulness of any information, apparatus, product or process disclosed, or represents that its use would not infringe privately-owned rights."

ABSTRACT

This report describes a program to develop a simple, foolproof, all-vacuum solar cell manufacturing process which can be completely automated and which results in medium efficiency cells which are inherently environmentally resistant. All components of the completed cells are integrated into a monolithic structure with no material interfaces. The exposed materials (Si, Al_2O_3, Al, Ni) are all resistant to atmospheric attack and the junction, per se, is passivated to prevent long term degradation. Such cells are intended to be incorporated into a simple module consisting basically of a press-formed metallic superstructure with a separated glass cover for missile, etc., protection.

A 5 cm x 5 cm test cell configuration was designed in which the various efficiency loss factors were adjusted to yield a 10% AMI cell. Each of the cell elements was individually optimized for combination with the others. The basic cell consists of alloyed front (Al) and back (Ag plus Ni) contacts, a multi-purpose (AR, hermetic seal, implantation oxide) front surface coating of Al_2O_3, and an implanted front junction. Implantation damage annealing and contact alloying are carried out in a simple one step thermal treatment at 870°C using a resistance heated furnace in vacuum. Times at temperature as short as 15-20 seconds for complete cell activation were demonstrated in a related proprietary program.

The use of non-analyzed and semi-analyzed beams for fabricating these cells was developed by KCI for use on this contract. A final lot of 50 cells made using the semi-analyzed beam method had an average efficiency of 10.4% at AMI (28 ±1°C). An economic analysis predicts a manufacturing cost of $.45/peak-watt for these cells using a one machine automatic method.

TABLE OF CONTENTS

Section	Description	Page
1	Summary	1
2	Introduction	3
2.1	Program Background	3
2.2	Process Considerations	7
3	Technical Discussion	20
3.1	Program Plan	20
3.2	Combined Coating	25
3.3	Back Contact	66
3.4	Front Contact	78
3.5	Implantation and Heat Treatment	88
3.6	Interconnects	102
3.7	Demonstration Cells	110
3.8	Economic Analysis	149
4	New Technology	153
5	Conclusions and Recommendations	153
	REFERENCES	155
	APPENDIX 1	156

SECTION 1

SUMMARY

A comprehensive experimental program has been conducted to develop a simple foolproof manufacturing process which can be applied to the automated manufacture of solar cells hermetically sealed against typical terrestrial environments. The cells have a unique "integral" structure and are fabricated by ion beam sputtering (IBS) techniques using a patented (#4, 086, 102) inverse process involving the following basic steps for a P on N cell:

1. Apply front (Al) and back (Ag + Ni) contacts through appropriate masks.
2. Apply combined coating (Al_2O_3; AR, hermetic seal, implantation oxide) over front surface.
3. Ion-implant front junction using edge mask to provide passivated structure.
4. Heat treat to simultaneously electrically activate implanted ions and alloy contacts.

The basic concept was demonstrated in a pre-contract study at KCI. In the present program, each of the above steps was individually optimized for combination with the others to define the optimum cell. Detailed Milestone Technical Reports were submitted for each of the optimized steps. The present report summarized the results. All processes were conducted in vacuum without any wet chemistry except for texturizing the incoming material. Non-texturized material without any wet chemistry was also investigated.

All investigations and cells were made with slices from a single 2 Ω-cm, (100) N-type Cz crystal to eliminate material effects. None of the steps turned out to have any critical parameters and the final 50 cell demonstration lot averaged 10.4% efficiency at AMI (28 ±1°C) versus the goal of 10%. The ability to make cells with all vacuum processing was fully demonstrated.

In an extra-program effort, the ability of the basic process to make cells using non-analyzed ion beams was demonstrated by KCI and reported

at the 12th PIM at JPL-Pasadena. A final extension of this demonstration was the assembly by KCI of an implantation system using a semi-analyzed B beam, which was used to fabricate the final 50 cells.

SECTION 2

INTRODUCTION

2.1 Program Background

This development program was based on an initial unsolicited proposal submitted to JPL by KCI in December 1976 and subsequently funded under Task IV, Phase 2 as a low level, fixed-price contract. Because of program aberrations, the work performed under this contract has been discontinuous and has covered an elapsed period of 28 months rather than the originally scheduled 8 months. Additional non-program advances to the basic process have been made by KCI and where desirable (e.g. use of non-mass-analyzed and semi-analyzed ion beams), data on these advances has been included for completeness. All previous reports have been undistributed Milestone Technical Reports on the various process steps.

The primary rationale for KCI's method is that the 1986 production goals appear to be extremely difficult to achieve, both technically and economically, if standard cell structures and manufacturing methods are employed. Conventional cell structures use a sequence of steps and machines, each dependent on the previous one, each with its own failure probability and each requiring its own test and quality control procedures. KCI's approach, in contrast, is conceptually completely integrated such that raw material "in" to one end of a single machine is converted to cells "out", with only one final test before module fabrication. Proprietary methods for simple automatic fabrication of part of the module have been designed and partially developed for potential incorporation in the same machine.

Outside of module fabrication, only one yield parameter exists, that for completed cells. To do this requires that the cell structure and basic cell manufacturing process be essentially foolproof. The KCI method, which primarily involves processing by ion beam methods, approaches such a fool-proof method within the cell efficiency limitations while still being

automatable for low cost. While radical, the method is extremely simple and is ready for development of commercial level equipment.

The key to the automatic potential and the foolproof characteristic resides in the altered cell structure and processing sequency which severely limit the number of potential failure mechanisms. Not only are the amount of handling and number of steps drastically reduced, but the reliability of the various steps is also considerably improved. The preferred method, in the long run, involves the use of linear materials, some of which do not have the crystalline perfection of more classical silicon forms. The present program was restricted to Czochralski (Cz) material in an attempt to eliminate starting material factors from the results.

KCI's overall approach is best appreciated within the framework of more conventional fabrication methods. The problem of manufacturing cells in the enormous quantities required to produce significant power output (relative to present USA capacity of 4 x 10^{11} watts) has two primary components; the first to produce the necessary basic semiconductor material and the second to process the latter into functional cells. In addition to these, one has the associated requirements for encapsulation against the terrestrial environment and the need for low cost array fabrication methods. The major areas are therefore (ignoring power conditioning which is an electrical rather than a fabrication problem):

1) Material
2) Conversion to operational cells
3) Encapsulation
4) Array fabrication

In general, these are considered as separate tasks or requirements. The first more or less stands on its own although it does interact with the others which must be controlled or altered to conform with the starting material. The problem of reducing starting material costs to acceptable levels must be solved if the other areas are to have any meaning. The many material programs currently being funded by industry and DOE will hopefully provide the necessary

ORIGINAL PAGE IS
OF POOR QUALITY

material at much reduced costs. Conversion techniques which reduce the requirements on the starting material will obviously make this task easier.

In contrast, factors 2, 3, and 4 are, of necessity, clearly interrelated. Encapsulation requirements are clearly dependent on the contact material and bond strength, the AR coating materials and related bond strength, the junction depth and configuration etc. Array fabrication methods are just as clearly dependent on contact configuration and materials. If extremely low cost production is to be achieved, it would appear that these separate problems should be treated as one with the intent of achieving a more or less unified manufacturing concept.

Equally important is the need for a major reduction in the number and complexity of processing steps, the degree of manual handling, and the wet chemistry involved in producing a cell. A simple reworking of existing processes or automation of certain steps is unlikely to achieve the neccessary cost reductions. If one looks at typical cell processing sequences, one cannot help but notice the sophistication of the processing versus the desired cell goals of extreme ruggedness and low cost.

The major conclusion from the above is that meeting the projected DOE goals will require a manufacturing concept which is unified, automatic and simple. Corrollaries to this are that it must be consistent with different starting materials, essentially fool-proof for very high yield, and amenable to simple scaling to required manufacturing levels without additional development of the basic process. The requirement for fool-proof processing is basically inconsistent with present cell manufacturing methods. Front contacts, for example, usually involve multiple layers bonded to surfaces which may or may not be adequately cleaned. Bond strength and resistance to atmospheric attack are suspect even under correct processing conditions and can deteriorate badly if the processing is off-peak. Similar considerations hold for the AR coating and for back contacts. Encapsulating everything can help to reduce the effects of atmospheric humidity and chemicals etc., but also introduces an additional

interface subject to degradation. It is highly desirable that interfaces such as these which are basically surface bonded be eliminated from the basic cell structure. A fully "integrated" structure is highly desirable and for long term stablility may be absolutely necessary.

In general, it is assumed that the cell components (contacts, AR coating etc.) will be made as reliably and cheaply as possible but that it will be necessary to encapsulate the cells and/or module in order to make them withstand normal terrestrial conditions. KCI's method involves making the cell and its component parts, as well as the interconnects and module structure in such a manner as to be extremely weather resistant, thereby precluding the need for additional encapsulation. The only additional protection needed would be a missile (hail stones, rocks etc.) shield such as a glass plate or plastic diaphragm. Inherently, modules made with such cells must be much cheaper than modules made with cells of conventional geometry.

It is also necessary that the processing be capable of using starting material as grown (Dendritic, EFG etc.) or with minimum processing, such as sawed-etched surfaces for conventional material (e.g. Cz). Texturizing, if required, can and should be done as part of the etching to remove saw damage without the need for surface polishing.

These requirements on processing seem much more achievable if one adopts the philosophy of trying to manufacture cells of "acceptable" efficiency (defined here as > 10% AMI) at very low cost, rather than relatively high efficiency at relatively high cost. In view of the process sophistication involved, even if one could double the efficiency ,the price in terms of the added manufacturing cost is almost certainly going to be much more than twice that achievable with a simple automatic process for low cost cells. The latter also would not preclude improvements in average efficiency due to subsequent associated improvements, e.g. better starting material

The KCI cell configuration and approach, as used in this program, are based on two ion beam processes, ion beam sputtering (IBS) and ion implantation (II). The use and techniques for these processes as applied to

solar cells and other semiconductor devices were originally conceived and developed by one of the principals of KCI and his group while an employee of Ion Physics Corp. in the early 60's. Although II is now a well developed and accepted semi-conductor technology, there is a significant difference between the application method in the KCI method (see Section 2.2) and those of other development laboratories. An important factor in simplifying the cell manufacturing process is the use of IBS to produce a completly integrated anti-reflective (AR) and encapsulation (E) coating that stays integrally bonded (in fact becomes better bonded) when subjected to high temperature (800°C-1070°C) thermal treatment. The same coating also acts as an implantation oxide (to place peak concentration at silicon surface) and to provide mass separation of unwanted ion species in non-mass-analyzed or semi-analyzed ion beam cell fabrication. A summary of the KCI technique and an overview of the projected manufacturing concept are given in the following section.

This report is not intended to be a definitive document on the detailed characteristics of the KCI method or its primary advantages. The original proposal for this contract contained an extensive development of the theory and practical aspects of the KCI cell and module fabrication techniques. These extended considerations and projections on machines, modules etc. are not part of this program and have not been included in this report. The latter is restricted to technical results of the actual program with the addition of selected data from proprietary KCI developments. Details of the cell fabrication process, per se, may be found in the patent (#4,086,102)

2.2 Process Considerations

Basic Process

The basic process in its final form for P on N cells is represented in Fig. 1 and consists of the following sequence carried out under vacuum conditions:

1) Apply front (Al) and back (Ag + Ni) contacts through appropriate masks.
2) Apply combined coating (Al_2O_3; AR, hermetic seal,

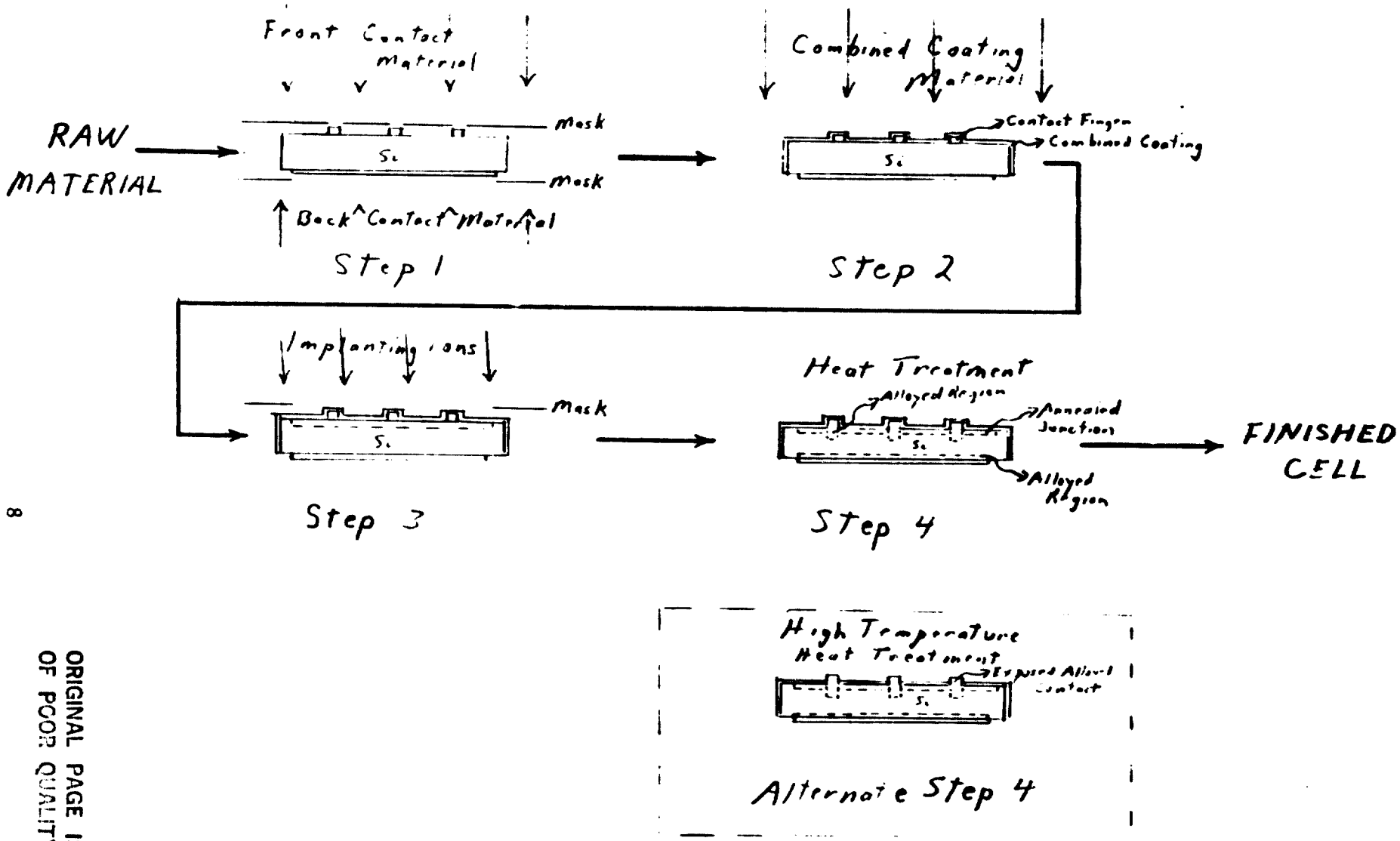

Figure 1 - Manufacturing Process Sequence

ORIGINAL PAGE IS
OF POOR QUALITY

implantation oxide) over front surface.

3) Ion-implant (B) front junction using edge mask to provide passivated structure.

4) Heat treat to simultaneously electrically activate implanted ions and alloy contacts.

In this program the contacts have been applied sequentially using the same deposition system. An automatic system would likely apply them simultaneously. All developments have been conducted using ion beam sputtering (IBS) as the deposition technique. This is particularly important for the Al_2O_3 combined coating which must be optically clear, integrally bonded, of the correct index of refraction, and able to withstand thermal excursions of up to 1,000°C without delaminating.

The choice of N-type substrates allows the use of alloyed Al as the front contact. In this form the front contact itself forms a rectifying junction with the substrate and cannot short the implanted junction unless it penetrates all the way to the back. The Ag (3% As doped) alloys with the silicon, followed by the Ni which is intimately bonded to the Ag by the IBS process. Finally, the Al_2O_3 reacts with the SiO_2 on the slice surface to form an integral layer. After heat treatment, which must be above 830°C to alloy the Ag, the entire structure is integral and can only be destroyed by physical destruction or etching. Even if fractured, the component parts continue to operate as similar cells of smaller size.

The contact materials were also chosen to be bondable by ultrasonic or parallel gap welding techniques. The former is very successful on the front contacts, but neither was very successful on the back due to the relative thinness of the alloyed layer. In a related in-house program, KCI has developed a simple vacuum method of attaching integral interconnect strips to the back and/or the front contacts to permit partial module fabrication in the same machine as the cell manufacture. These interconnect strips are Ni (or Ni alloy) which is readily weldable by any method.

The process was originally conceived for use with as-grown, linear materials in order to provide automatic masking and linear flow through a

single machine. Although linear material is preferred from a manufacturing point of view, the process may be readily adapted to other forms. The cells are basically designed to be extremely rugged and self-encapsulated and are conceptually integrated with a simple, inexpensive module having the cells themselves partially exposed to the environment and convection cooled. Even if used in a more conventional module, the cells have the advantage of inherent resistance to the encapsulating and interconnecting etc. procedures and materials. As a factor in the overall photovoltaic program. the cell manufacturing process, per se, is therefore capable of standing on its own merits.

Elaborate theoretical and practical considerations went into the cell structure and materials as well as into the individual process steps. Full consideration of these factors is beyond the scope of this report but the following sections cover some of the more important details. It is important to recognize in all of these considerations that the criterion is acceptable performance with very simple, foolproof processing and low cost, rather than highest efficiency independent of the complexity of the process. The intent is to reduce the manufacture of solar cells to a process resembling conventional manufacturing (e.g. glass or steel production systems) on a large scale more than it does conventional semiconductor processing. All of the in-house and contract developments relating to the KCI process have been carried out under what, at best, can be described as medium dirty factory conditions with no clean rooms, clean benches, or other specialty clean conditions.

The simplicity of the process results from the fact that it is completely additive. Nothing applied directly to the cell (cp. diffusion oxides, photoresist layers, edge cutting after junction formation) is ever removed after application.

Combined Coating

The combined coating material simultaneously provides anti-reflection (AR), encapsulation, and implantation oxide functions. In addition (see below), and especially for B, for the use of a non-mass-analyzed

or semi-analyzed implantation system (see Section 3.7), it also acts as a mass analyzer to prevent heavy metallic ions or complex molecules from reaching the silicon surface.

For the anti-reflective function, the index of refraction (n) must only be near the optimum value. Theory gives a minimum reflectivity value of 9.7% for a SiO_2 anti-reflective layer and 1.6% for Al_2O_3 versus 0% with a perfectly tuned n value. These are peak values which increase as one goes off peak wavelength, but detailed calculations show that this fall-off in performance is relatively minor over the wavelength (λ) range of cell operation. In the same way, the thickness of the AR layer is quite non-critical except when striving for the highest efficiency.

As an encapsulant, the coating material must be inherently hermetic and suitable for application to Si in hermetic form and with high optical clarity for maximum light transmission. The latter factor is determined by the deposition system which dictates the properties of the deposited material. IBS as practiced by KCI provides Al_2O_3 coatings with the necessary optical and hermetic properties. Although the best encapsulation will be achieved on smooth surfaces, the cell structure is such that small imperfections are unlikely to seriously affect cell performance, and texturized surfaces were emphasized in the program. In the long run, as-grown or sawed-etched surfaces are the most likely surface conditions.

In general, implantation for these cells has been carried out through the oxide in order to fix the surface states rather than leaving them subject to modification by subsequent application of the combined coating. Pre-coating implants can be achieved with lower energies and doses but initially it was not clear that implanting just would not affect the bonding characteristics of the Al_2O_3 layer at the very high thermal temperatures used for thermal treatment.

As an implantation oxide, the function of the coating is to place the peak of the implanted distribution near the coating-Si interface. If the ion energy is too low for the coating thickness, fewer ions will end up in the Si and

the doping levels will be lower for a given incident flux. If too high, the peak will be within the Si and there may be a reverse drift field at the Si surface tending to reduce carrier collection efficiency. Since the lifetime at the surface is always small in any event, the latter factor is considered to be of little significance and the implantation energy is usually adjusted to place the peak well beneath the Si surface. Because of the alloyed front contacts which penetrate many microns below the implanted junction, the front contacts always contact the implanted layer at the peak of the distribution. It is impossible for the contact resistance to be anything but essentially zero (cp. surface layer techniques).

As a mass analyzer, the coating must be thick enough so that the range of undesired heavy ions is too low for penetration to the Si surface. This condition is easily met for most of the more undesirable contaminating ions such as heavy metals from source electrodes etc. The major disadvantage in using the method is that the contaminant ions stopped in the oxide can act as absorbers and reduce the amount of light reaching the cell. This is also true of doping ions and is another reason for pushing the implanted peak below the Si surface.

A special case occurs when Al is used as the alloyed front contact and and the Al_2O_3 coating is put on over the entire front surface, including the contact. If the cell is heat treated, some of the Al from the Al_2O_3 over the contacts segregates and alloys, the rate being determined by the temperature but apparently speeded up by the Al-Si liquidus below. The O_2 evolves or is absorbed in the alloy as a minor constituents in the thick alloy region. The resulting surface can be contacted easily, including attaching Al interconnect leads by ultrasonic bonding methods. The Al_2O_3 over the implanted regions stays essentially the same, except that it becomes integrally bonded, probably due to some slower Al migration.

The reasons for using Al_2O_3 as the combined coating material are basically:

1) thermal compatibility with Si
2) absence of optical absorption in λ region of interest
3) hermeticity in thin IBS deposited layers

ORIGINAL PAGE IS
OF POOR QUALITY

4) formation of completely integral structure with high temperature heat treatment

5) resistive to chemical and abrasive (harder than SiO_2 or sand) attack

6) performance as AR coating nearly equal to SiO for Si to air conditions

7) hydrophobic; self cleaning under rain conditions

Implantation

In the preferred configuration, the ions must be sufficiently energetic to place the peak of the distribution below the Si surface. For boron ions, and Al_2O_3 layers in the 900-1,100 mμ thick range, energies of the order of 60-80 keV are required.

A more important consideration, in the long run, is the need for large total available ion currents, in the range of 2-3 A (at doping level of 10^{16} ions/cm^3 - production level 5 x 10^8 watts) in the 1986 time frame to orders of magnitude more for subsequent periods. Current machines, with their highly sophisticated analyzing and beam handling systems, and short up times, do not look attractive for these future applications. The use of non-analyzed or semi-analyzed beams combined with the foolproof cell structure and simple processing can obviate this problem if properly applied. This problem has been addressed in an in-house KCI program with significant success for the process under study. The final 50 demonstration cells were, in fact, made with a highly contaminated semi-analyzed beam.

Contacts

The contact materials were chosen to alloy with the Si at temperatures compatible with implant annealing. In addition, they must be readily available, environmentally resistant, and amenable to interconnection by methods (e.g. ultrasonic bonding) providing joints which themselves are resistant to atmospheric attack. As long as the cell reaches the minimum temperature (830°C for Ag) needed for alloying, the cell becomes integral.

The alloy material for the front contact is even more resistant to attack than the Al itself while the back has a combination material, primarily nickel, exposed.

A very important feature results from the alloyed junction front contact-implanted junction technique. In standard implantation procedures, it is necessary to maintain clean conditions in order to avoid beam "shadowing" due to dust particles or surface irregularities. As shown in Fig. 2(a), if, for example, a dust particle of diameter greater than the junction depth equivalent to the implanting ion energy is on the surface, it will shadow the beam (essentially plane parallel even allowing for off normal implant) and leave an unimplanted region. This unimplanted region is the same type as the original bulk material and acts as a "pipe" from the front surface to the bulk material. If a conventional metal contact is now applied to the front, and is deposited over this unimplanted spot or spots, there will be a shorting effect across the junction, degrading the device characteristics. Since implanted junction depths are usually in the 0.1 - 1 micron range, dust particles of this size can cause this problem. Clean conditions are required to reduce the number of such particles to the point where high yield conditions are obtained. This can be a particularly bad problem with solar cells because of the large area of the front contact.

The procedure outlined above, in which the contact is applied first and alloyed to form its own junction, completely avoids this problem (see Figure 2(b)). The entire front surface is exposed to the implanting ion beam such that implantation occurs right up to the alloyed contact to form a continuous junction. The areas under any dust particles, etc., although not implanted have no effect on the junction characteristics, since they are not statistically likely to be touching the contact, and even if they were, the contacts themselves are rectifying to the bulk material. The high temperature annealing promotes complete interconnection of the alloyed and diffused junctions to provide perfect contact to the "active" implanted area.

The same technique can be used to facilitate the use of less

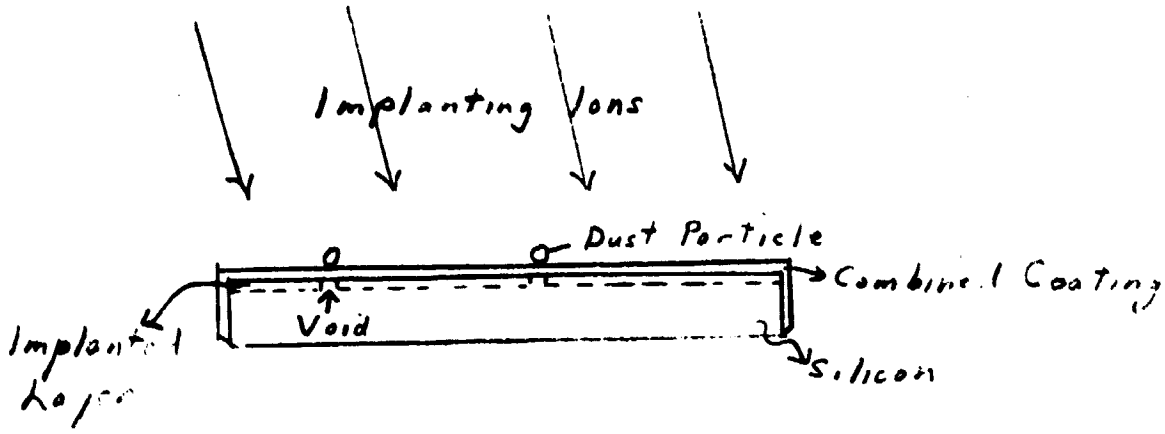

Fig. 2 a) Dust Particle Problem
- Post Implant Contact

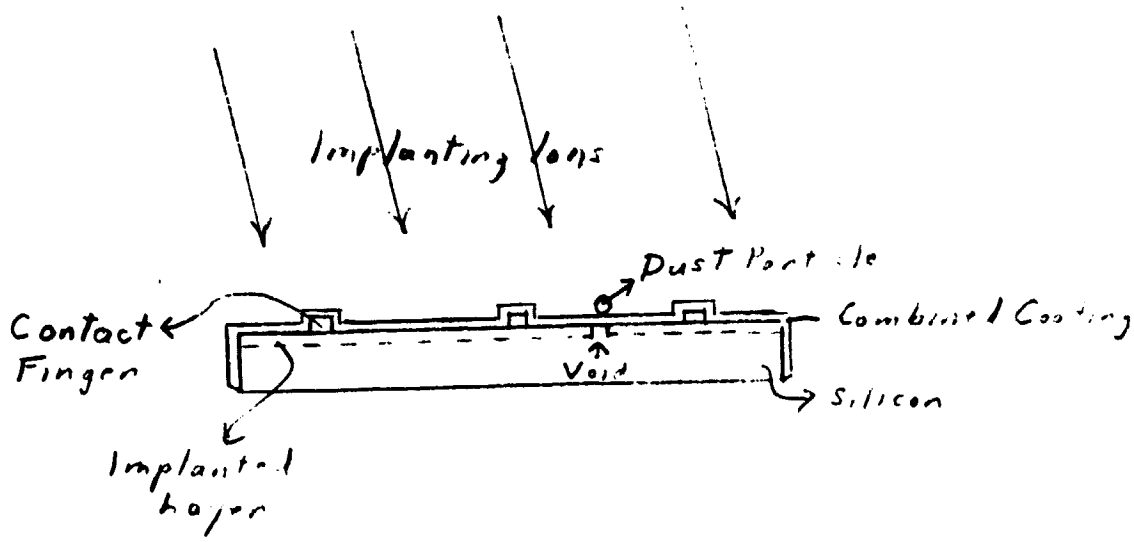

Fig 2 (b) Dust Particle Effect
- Pre Implant Contact

Figure 2 - Beam Shadowing by Dust Et.

ORIGINAL PAGE IS
OF POOR QUALITY

processed, cheaper starting material for manufacturing solar cells. For example, sawed-etched surface can cause beam shadowing since the beam usually intercepts the surface at a non-normal angle (e.g. 7° to <111>). Since there are many spots on a sawed-etched surface where this can occur, the probability of significant junction shorting with a conventional, post-implantation contact is very high. The pre-implant, alloyed contact method completely avoids the problem. Sawed-etched material solar cells have been successfully fabricated by this method.

Another variation of this technique is its use on poorer quality starting material such as dendritic or EFG, which can contain sections or regions having defects which are highly doped and may not be "overcompensated" by the implanted or diffused atoms to create the necessary P-N junction, with pipes or shorting areas resulting from this lack of overcompensation. Again the pre-implant alloyed contacting method avoids the problem because of the very high level of doping introduced by the alloyed region, which will always overcompensate the bulk material (which has a doping level below a solid state "saturation value"). In order to achieve the ultimate in automation and low cost processing the ultimate process may combine linear material and the basic sequence outlined in this section.

Thermal Treatment

The thermal requirements for the present process were to produce adequate cell performance in the shortest possible time, the object being to provide very simple in-line annealing in an automatic machine. In contrast to diffusion, where some doping atoms must diffuse to the full junction depth (.1 - 1 μ in general for solar cells), the implanted ions are already near their final positions and are nominally one atom spacing from an active lattice site. In principle, the activation energy to transfer the doping atoms to the lattice site must be applied only long enough for a movement of one atom spacing. Annealing the associated radiation damage caused by the incoming ions can require longer thermal treatments due to damage clusters at the end of the ion range.

As is well known from the many studies which have been done, the exact conditions and times for proper annealing can be complex functions of the doping ions, doses, energies, substrate characteristics, etc. In some cases this has led to sophisticated annealing cycles in attempts to achieve the optimum crystal perfection and doping conditions for highest cell efficiency, Such complicated cycles have been categorically rejected in this program as incompatible with a simple, foolproof, cheap manufacturing process.

In general, only a few atom spacings must be traversed in order to restore the lattice to some semblance of the original condition. Such spacings are still two to three orders of magnitude less than those of even a shallow (0.1 μ) diffused junction. The lattice regrowth rate is a strong function of temperature and goes up rapidly at higher temperatures. The time at temperature, particularly for high temperature treatment of boron implants, can therefore be quite short, in the order of seconds or less for "acceptable" performance. Although most of the contractual program was carried out with 10 minute annealing cycles (value from various thermal treatment studies in program), a subsequent in-house study by KCI, using a proprietary implant procedure, demonstrated clearly that 15-22 second anneals at temperature (870°C) could be used to achieve cells of greater than 10% AMI efficiency. Shorter times are likely to be successful, but could not easily be studied with the vacuum furnace being used because of limitations in the slice transfer system. In any event, for the projected manufacturing machines having a 1 meter wide strip of material moving at .5 meter/minute, the required central hot zone would only be 15-20 cm. long and the total hot zone 50-60 cm. long.

Since the furnace is in vacuum, conduction and convection losses are low and efficiency of a simple resistively heated furnace using reflectors can be quite high. It is only necessary to raise the implanted layer and contacts, which are on the outside, to the desired temperature. The core does not have to come to temperature and preferably should not since higher temperatures can only lead to lifetime etc. degradation. The required temperature rise can be

provided by any appropriate method including electron beams and lasers, two of the more exotic methods currently being developed. Such sophisticated methods are considered by KCI to be unnecessarily complicated for the simple annealing problem presented here if manufacturing reliability and very low cost are to be achieved.

Because of the small time required in the hot zone the actual energy delivered to the cells being processe can be small if required. However, the laiter is irrelevant because for any large scale automatic processing method operating in vacuum, the real power consumption will be determined by the heaters on the pumps, standby power in the power supplies, electron beam for evaporation or equivalent energy etc., not by the power actually delivered to the device. The energy recovery period will be determined by the total of such power consumption divided by the throughput of the machine.

Boron ions (i.e. a P on N cell) are preferred because of the lower implantation energies and annealing temperature required. The other important thermal consideration is that of the temperature of the silicon substrate during implantation. Cells implanted at liquid N_2 temperatures in early Ion Physics Corporation studies[1-4] consistently had higher short circuit currents and fill factors than cells implanted in similar material at room temperature. This effect appeared to be due to a stiffening of the lattice at the lower temperature and associated reduction of radiation damage, or to reduced vacancy enhanced diffusion which tends to generate recombination centers in the surface and space charge regions. The total effect, which was repeatedly observed, was a difference of 3-4% (relative) in efficiency. If a "high efficiency" approach were pursued the difference could be significant. However, for the "lowest cost" approach, room temperature implants are preferred.

The advantages of this cell manufacturing methods may be summarized as:

1) Extreme simplicity.
2) Completely integral cell-no surface bonded interfaces-all exposed materials environmentally resistant

3) Foolproof processing - high yield.

4) Completely automatable in one vacuum chamber and capable of very large scale production.

5) All conventional silicon starting materials may be used - may also be preferred method for thin film materials.

6) All materials used are readily available and consistent with low cost processing in quantities used.

7) Compatible with simple module fabrication.

Results of this development program indicate clearly that these advantages can be achieved in full scale production.

SECTION 3

TECHNICAL DISCUSSION

3.1 Program Plan

This program's basic objective was to develop a simple manufacturing process which could be applied to the automated manufacture of integral solar cells hermetically sealed against typical terrestrial environments. The key words in this objective were simple and hermetically sealed and as such they represented the major goals of the program. A corollary to these goals was that the cells should have the highest efficiency consistent with the limitations of the processing and that the cell interconnect method should also be inherently environmentally stable. The latter problem was addressed by designing the cells to have weldable (i.e. weld or ultrasonic bond) front and back contacts.

Overriding the program's objectives was the requirement that the cell manufacturing process be completely automatable in one machine which would take in prepared silicon (linear materials or sawed-etched Cz material) and feed out completed solar cells. The intent was to provide a cell manufacturing process which is essentially foolproof and which requires an absolute minimum of handling and personnel (one machine). Very high yields and relatively low cost per cell are expected to more than compensate for the somewhat lower average efficiencies expected from the compromises necessary to achieve the basic processing and cell characteristics. Additional manufacturing cost savings are ultimately expected to accrue through simplified module construction, and the present program, which was limited to cell processing, addressed this problem through the requirements of hermeticity and weldable contacts. Investigations on the latter were limited to available equipment.

For a fully automated, one machine process, the 1986 goal of $500/kW appears achievable with a minimum cell efficiency of 10% AMI and this was established as a program goal. Calculations on the test cell configuration (see below) were based on this goal.

Independent of the verification samples needed for the individual process steps (see Section 2) the program included the following key Tasks in chronological order:

A) Optimize combined coating

B) Optimize back contact

C) Optimize front contact

D) Optimize ion implantation

E) Optimize heat treatment

F) Fabricate 50 complete test cells

G) Test contact weldability

H) Make economic forecast analyses and evaluations

I) Fabricate 50 demonstration cells for environmental test

J) Submit Final Report

For convenience this technical discussion of results combines all demonstration cells in one section followed by contact weldability and economic forecasts. Some KCI data on the semi-analyzed implant machine is included in the demonstration cell section.

The process verification procedure was organized so that each of the process steps (Tasks A-E) could be individually optimized and then combined with the others to define the optimum cell in terms of efficiency and environmental stability. Of necessity, Task E ran concurrently with Tasks A-D.

The individual "process" tasks were designed to allow optimization of each of the process elements without interaction with the others, with the exception of heat treatment. Since all cell elements eventually had to be simultaneously exposed to the same thermal treatment, the combined coating, contacting, and implantation developments were conducted as a function of heat treatment as well as of other critical factors.

In order to be consistent with available fabrication and testing equipment and to permit easy but accurate analysis of the effects of parameter changes, a 5 cm x 5 cm test cell structure, as shown in Figure 3, was chosen. This size is obtainable from a conventional 3" round slice and has the particular

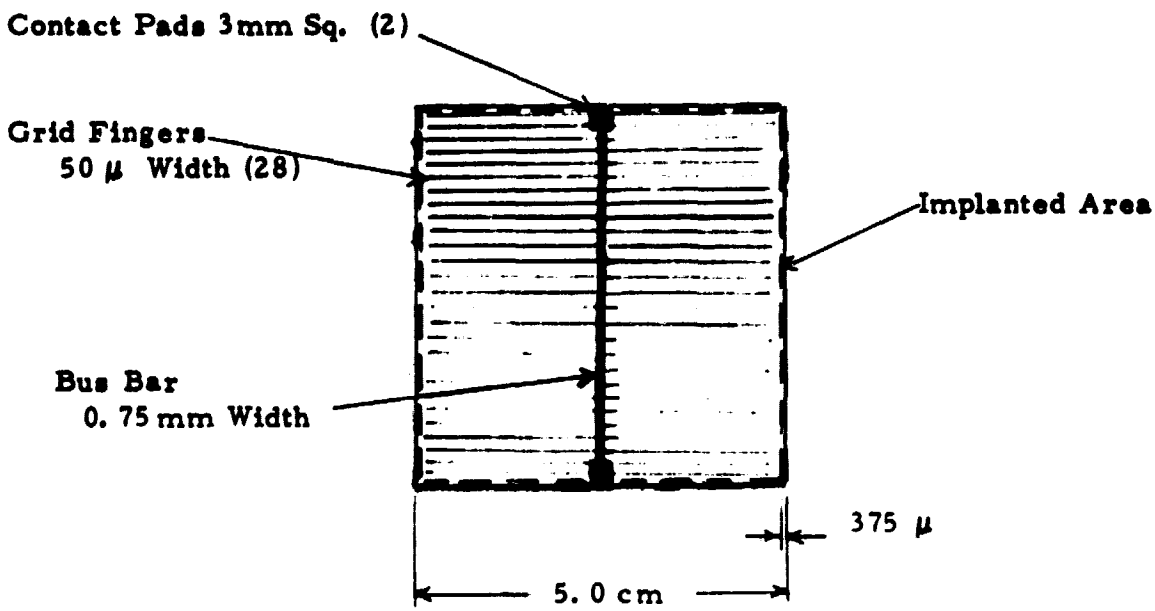

Front

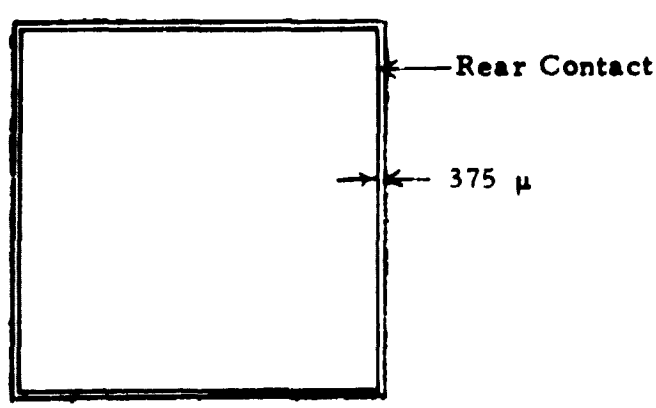

Rear

ORIGINAL PAGE IS
OF POOR QUALITY

Figure 3

TEST CELL CONFIGURATION

advantage of being an acceptable sample size for a Beckmann DK-2A spectrometer which was used for measuring the front surface reflectivity in the combined coating studies. All of the data necessary for other cell sizes or configurations can be obtained from this basic cell and the individual task results.

To obtain a passivated structure, the front surface was masked during implantation, with the frame width originally designed at 250 μ but later changed to 375 μ. The cell has a picture frame back which originally had a frame width design value of 1 mm. The economics of the program dictated the use of the implant mask for the back contact mask and led to some potential edge shorting problems due to mask undercutting. The latter apparently did not occur, however, to any significant extent. The combined coating, which provides an encapsulating function, had to be continuous to the outside edges of the cell, i.e. to beyond the implanted region, and was applied without any masking.

Assuming that the area outside the junction edge does not contribute current, the total shadowed or non-active area on the front surface is 6.7% (with 250 μ border) of the total. Materials used were Al_2O_3 for the combined coating, Al for the front contact and a combination of As doped Ag overlaid with Ni for the back contact. All changes in AR etc. characteristics and resistance characteristics of the contacts were made only through changes in the appropriate material thicknesses and subsequent heat treatment (H.T.). The implanted layer was boron.

Reasonable goals for the program were set up by evaluating the various loss factors affecting cell efficiency and assigning maximum loss values consistent with a required minimum cell efficiency of 10% AMI. It is important to note that some loss factors were more important in the cell configuration being developed here for simplicity and environmental stability, than in cells designed for optimum efficiency. Among these loss factors were potential reflectivity losses due to the imperfect index of refraction of the AR coating, potential light absorption losses in the AR coating due to boron doping (from

implantation) or to thermal treatment, and larger than normal R_s (series resistance) losses in the front grid due to the use of a semiconductor metal alloy rather than a pure metallic conductor. A small compensating factor for the latter was the fact that R_c (resistance between contacts and silicon) is negligibly small for both front and back contacts because of their fully alloyed nature. In the present cell, the major loss factors considered were:

1. F_L = fraction of light lost due to reflection or absorption in the AR coating.
2. F_s = fraction of current lost due to shadowing by front contact and to non-implanted frame.
3. F_G = fraction of power lost due to voltage drop in the grid made of conductor having resistivity ρ_G (ohm-cm).
4. F_I = fraction of power lost due to voltage drop in implnnted layer having sheet resistance ρ_I (ohms/square)

Since F_L can be somewhat greater than in conventional cells, the available current density at maximum power was arbitrarily estimated as 26.5 mA/cm^2 at 100 mW/cm^2 input. This turned out to be close to the real value.

With an assumed voltage at maximum power of .46 V (final value .41-.43 V), for a minimum efficiency of 10% the effective current density after loss factors F_S, F_G, and F_I were applied had to be at least 21.7 mA/cm^2. The total of F_S, F_G, and F_I was arbitrarily set at a maximum of 16.5%, which if achieved, would have resulted in an effective current density of 22.1 mA/cm^2 and efficiency greater than 10%.

To achieve these minimum specifications the necessary calculations on projected performance were made using an RCA[5] treatment, and the following individual goals established:

1. F_L Total loss of available incident light due to reflection and/or absorption in the combined coating was to be less than 15% for non-textured surfaces and 10% for textured surfaces.
2. F_s Total loss due to grid shadowing and/or non-implanted area was set at 6.7% by the test cell configuration.

3. F_G Total loss due to resistance losses in front and back contacts was to be 8% or less. To achieve this, individual goals for the front and back contacts were established as .046 ohms and .035 ohms per square, respectively.

4. F_I Total loss due to resistivity of implanted layer was to be 1.8% or less. To achieve this the sheet resistance of the implanted layer had to be 77 ohms/square or less.

The sum of the F_S, F_G, and F_I goals was therefore a maximum of 16.5% as required. The modification in the implant mask size to a border of 375 μ increased F_S to 7.8% and the overall loss factor to 17.6%. This used up the .4 mA/cm^2 margin of error allowed in the original calculations.

The program was restricted to (100) Cz material of 2 Ω-cm nominal resistivity. All starting cell material was obtained from a single 3" diameter Wacker crystel with each slice (375 μ thick) being sawed-etched on one side and polish-etched on the other. Although slice differences along the crystal were possible, these were expected to be minor so that the various task results could be interpreted without the complication of starting material variations. The program results therefore reflect optimization of the basic process procedures and parameters rather than of material or geometry. The material was purchased off the shelf. Although it was supposed to be high quality single crystal, patterns formed during heat treatment (coating study) indicated a possibility of multi-crystalline structure with core defects.

Overall organization of the cell optimization program is shown in Fig. 4. Details of the various stages are discussed in the appropriate following sections. The primary factor running through the program was the use of very simple measurements to evaluate and optimize the individual cell parameters. Results, in general, were quite close to the predicted values.

3.2 Combined Coating

Optimization Procedure

The basic experiment performed involved depositing a

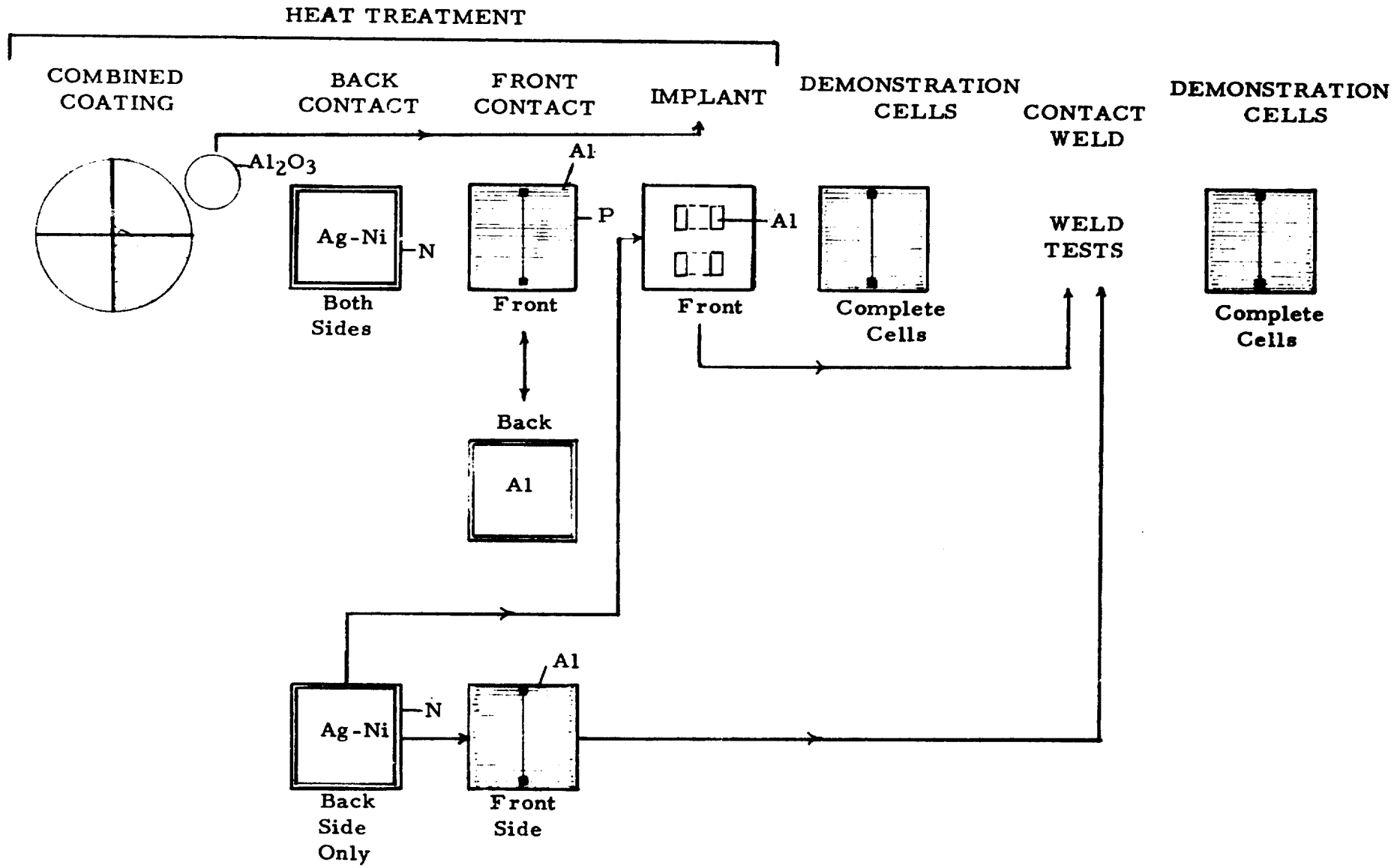

Figure 4. WAFER CONFIGURATION and FLOW for PROCESS OPTIMIZATION

combined coating (AR, environmental protection, implantation oxide) of Al_2O_3 on silicon and subsequently heat treating the structure at temperatures equivalent to those likely to be used for the final multi-purpose heat treatment.

In order to obtain the maximum amount of information about the AR characteristics of different surfaces, the combined coating experiment had the slices sectioned into four quadrants as shown in Figure 5. Two of the quadrants were texturized and the other two were left as received (no chemical treatment) so that the four different surfaces were polish-etched (p), sawed-etched (se), polish-etched-texturized (pt), and sawed-etched-texturized (set).

Texturing was done with commerical (Transene Co., Inc.) hydrazine in a commercial(Transene Co.,Inc.) reactor. In order to optimize the texturing procedure, time and temperature were systematically varied,with the silicon surface total reflectivity being measured for each combination. Reflectivity for this optimization procedure, and for all AR coatings etc., was measured on a Beckman DK-2A spectrometer having an integrating sphere which integrates light reflected at all angles for an incident angle of 5°. Optimum performance, i. e. lowest average reflectivity, was obtained with approximate time and temperature of 20 minutes and 110°C, respectively.

The AR coating thicknesses to be investigated were chosen by comparing the photon flux spectrum with the response curve of a texturized cell. In principle, for lowest average reflected light, the wavelength of mimimum reflectivity should be roughly at the maximum of the product of the photon flux spectrum and the cell quantum efficiency response curve. The latter was not known for the cells being developed in this prograr . However, it was known that the response curve for a reasonable non-AR coated texturized cell is fairly flat from less than 600 to greater than 800 mμ. As an example, the reader is referred to Fig. 3 of RCA Quarterly Report No. 3 on Contract ERDA/JPL-954352. Fig. 2 from the same reference gives the photon flux spectrum for air mass (AM) 0, 1 and 2, and for conveninece is reproduced here as Figure 6. From Fig. 6, for a cell with a flat quantum efficiency

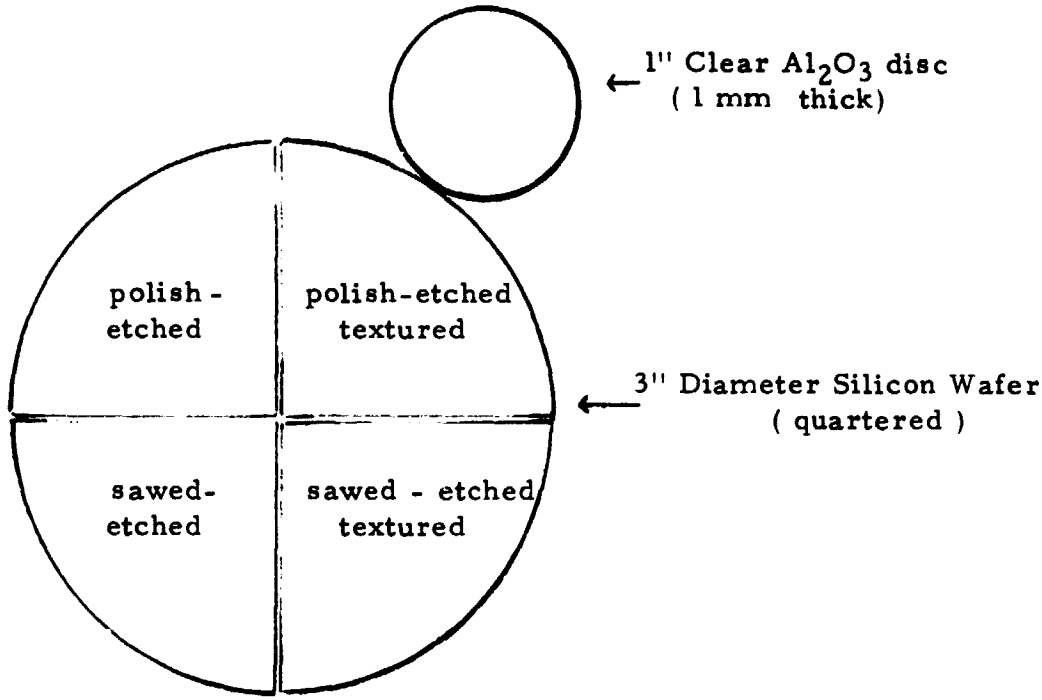

ORIGINAL PAGE IS
OF POOR Q

Figure 5. Basic Combined Coating Experiment

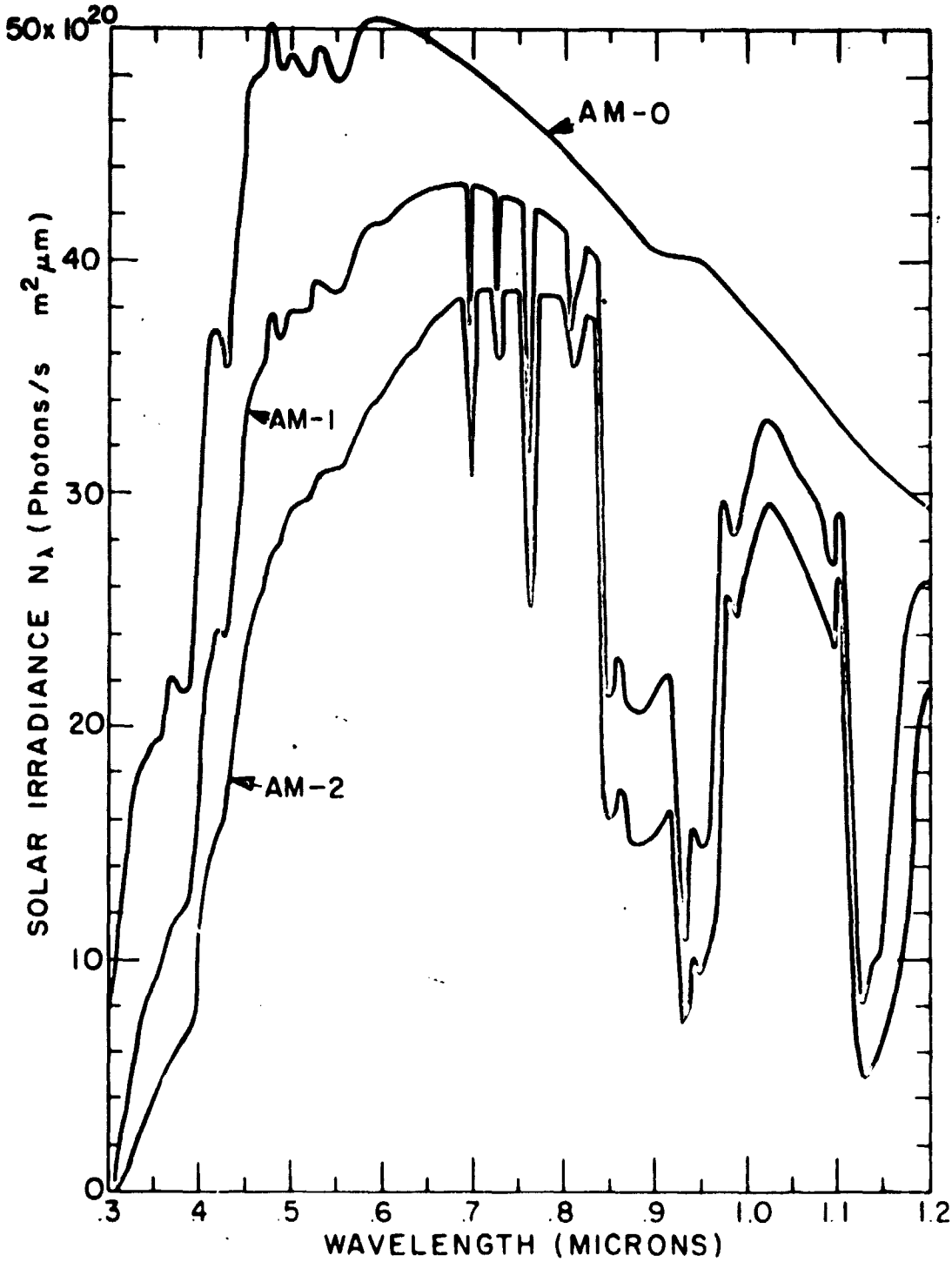

Figure 6. Solar irradiance expressed in terms of photon flux. (Reprinted from RCA Quarterly Report No. 3 on ERDA/JPL -954352; Sept. 1976; B. F. Williams)

response, the wavelength of minimum reflectivity should be approximately 700 mμ for AM1 and 750 mμ for AM2. On the assumption that AM2 would be the highest terrestrial air mass value, it was therefore decided to conduct the parametric study with Al_2O_3 thicknesses corresponding to minimum reflectivity wavelengths (λ_{min}) of 650, 675, 700, 725, and 750 mμ.

Assuming an index of refraction (n) of 1.76 for the deposited Al_2O_3, the corresponding Al_2O_3 thicknesses used were therefore:

λ_{min} (mμ)	Al_2O_3 Thickness ($\lambda_{min}/4n$-mμ)
650	92.3
675	95.9
700	99.4
725	103.
750	107.

One additional sample set corresponding to an initial (before heat treatment) λ_{min} of 800 mμ was made to have available in case of appreciable thinning of the Al_2O_3 during heat treatment. It was found to be unnecessary and was not followed in detail.

A 2.5 cm diameter, 1 mm thick polished disc of pure Al_2O_3 was included with each four quadrant set, as shown in Figure 5, and simultaneously received a deposited layer of Al_2O_3 of the same thickness. By measuring the transmittance of the discs before and after deposition of the AR coating, and after each heat treatment, the transmittance of the AR coating as a function of heat treatment could be directly evaluated. In this way, it could be directly determined if any decrease in reflectivity was caused by light absorption in the AR coating.

The coatings were applied in a small experimental ion beam sputtering (IBS) system. After coating with Al_2O_3 to the desired thickness, all silicon sample sets (i.e. for all thicknesses) and all Al_2O_3 discs were simultaneously heat treated in vacuum at successively higher temperatures

of 870°C, 970°C and 1070°C. After vacuum(roughing level - approximately 5 microns or less) was reached, the samples were inserted directly into the hot zone and held at temperature for 10 minutes. They were then removed to the end of the furnace tube(3" diffusion type) which was immediately back-filled with Ar gas to atmosphere. Complete reflectance and/or transmittance data, as appropriate, were taken for each sample after each thermal treatment.

In summary, the complete parametric reflectance study included 5 different AR layer thicknesses on 4 different surfaces, with thermal treatment at 3 temperatures. Transmittance was measured for 5 different AR layer thicknesses with thermal treatment at 3 temperatures.

Experimental Results

The data generated in this development study were quite extensive and, for each silicon surface, included reflectance vs. λ vs. thermal treatment for each λ_{min}, and reflectance vs. λ vs. λ_{min} for different thermal treatments. In addition, transmittance vs. λ vs. λ_{min} for different thermal treatments was measured for the 1" Al_2O_3 discs. All curves are not reproduced here, nor is any attempt made to explain all of the factors affecting each graph or parameter. However, certain important conclusions were obvious when the results were viewed sequentially and systematically, particularly with respect to the degree of process control needed for "acceptable" results. In essence very loose limits can be used.

The following symbolism has been used in the pertinent graphs:

SYMBOL	MEANING
	General
Cal.	100% Calibration Line
Z	Zero Calibration Line
R	Reflectance (integrated)
T	Transmittance
H. T.	Heat Treatment
λ	Wavelength
λ_{min}	Wavelength of minimum reflectance (calculated)
	Surfaces
p	Polish-etched
se	Sawed-etched
pt	Polish-etched-texturized
set	Sawed-etched-texturized
	Constant λ_{min} Graphs
0	No AR; no H. T. ; Standard
1	AR; no H. T.
2	AR; 870°C H. T.
3	AR; 970°C H. T.
4	AR; 1070°C H. T.
	Constant H. T. Graphs
0	No AR; no H. T. ; Standard
2	AR; λ_{min} - 650 mμ
3	AR; λ_{min} - 675 mμ
4	AR; λ_{min} - 700 mμ
5	AR; λ_{min} - 725 mμ
6	AR; λ_{min} - 750 mμ
	Transmittance Graphs
2	AR; λ_{min} - 650 mμ
3	AR; λ_{min} - 675 mμ
4	AR; λ_{min} - 700 mμ
5	AR; λ_{min} - 725 mμ
6	AR; λ_{min} - 750 mμ
S1	Standard Al_2O_3 disc; no H. T.
S2	Standard Al_2O_3 disc; H. T.

All sample sets used in the investigation and a set of standards were texturized at the same time. After scribing into quadrants, the samples for texturizing were placed in the hydrazine reactor without any intermediate steps. Following texturizing the samples were quenched in distilled water, then dried using dry N_2 gas. The set to be used for standards was then measured for R vs. λ and set aside (Note: the four quandrants from each slice were kept together as a sample set).

Fig. 7 gives R vs. λ for the standard set taken before the AR measurements were made. The Beckman DK-2A used for all R and T measurements is an older instrument which has linearity charcteristics which are strongly dependent on internal gain pot settings, optical alignment etc. In spite of constant checks on the 100% and zero calibration levels, changes in R of ± 5 % relative are possible at the low end of the scale due to linearity changes. To avoid this, the internal gain settings were kept fixed throughout the experiment to ensure that relative changes were correct. With this procedure, the standard (no AR; no H. T.) curves were quite reproducible throughout the extended experiment. The machine was realigned after the experiment was completed, after which the curves for the same set of standards ran approximately 10% higher on a relative basis. Other shifts are possible due to variations in the exact spot on the sample used for measuring reflectance, orientation etc. However, as is obvious from Figures 8-15, these shifts have negligible effect on the conclusions to be drawn. MgO, which is quite good in the critical .35-1.1 μ range, was used as the reference standard in all cases.

For most cases data was taken from .5-1.5 μ. Due to detector characteristics the spectrometer could not be adjusted to go to lower wavelengths (i.e. farther to blue end) in a single scan. Where important, data was also taken in a range from .35-.8μ. Data taken over this range using a different detector, in general agreed better in absolute values with the absolute values taken for the .5-1.5 μ range after realignment. Agreement at very low R values (<2%) was quite good in all cases, with the worst non-linearity effects being in the 5-35% range.

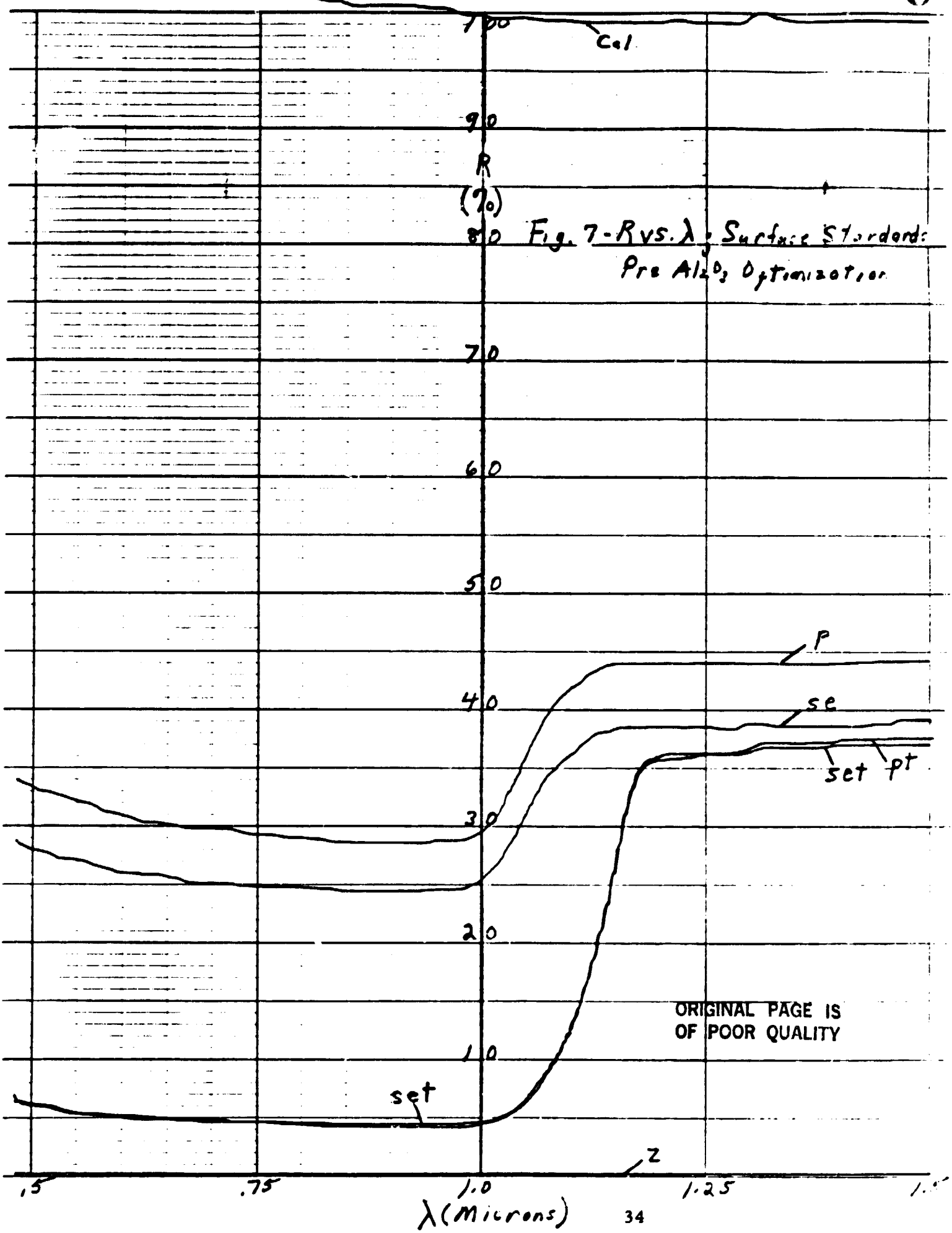

Fig. 7 - R vs. λ; Surface Standards
Pre Al_2O_3 Optimization

ORIGINAL PAGE IS
OF POOR QUALITY

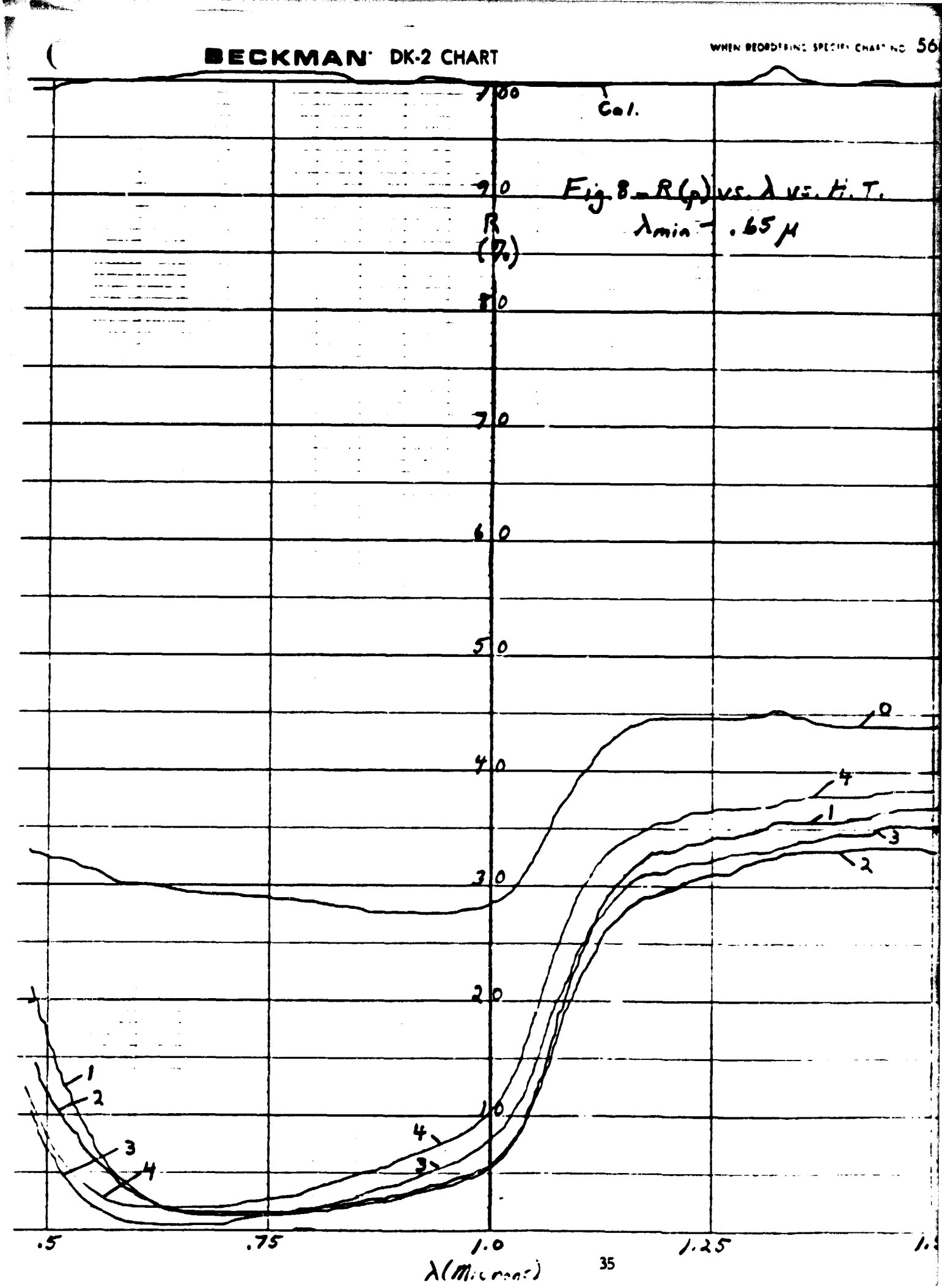
BECKMAN DK-2 CHART
WHEN REORDERING SPECIFY CHART NO. 56
Col.
Fig. 8 - R(p) vs. λ vs. H.T.
λmin - .65 μ
R (%)
100
90
80
70
60
50
40
30
20
10
.5
.75
1.0
1.25
λ (Microns)
0
4
1
3
2
1
2
3
4
4
3

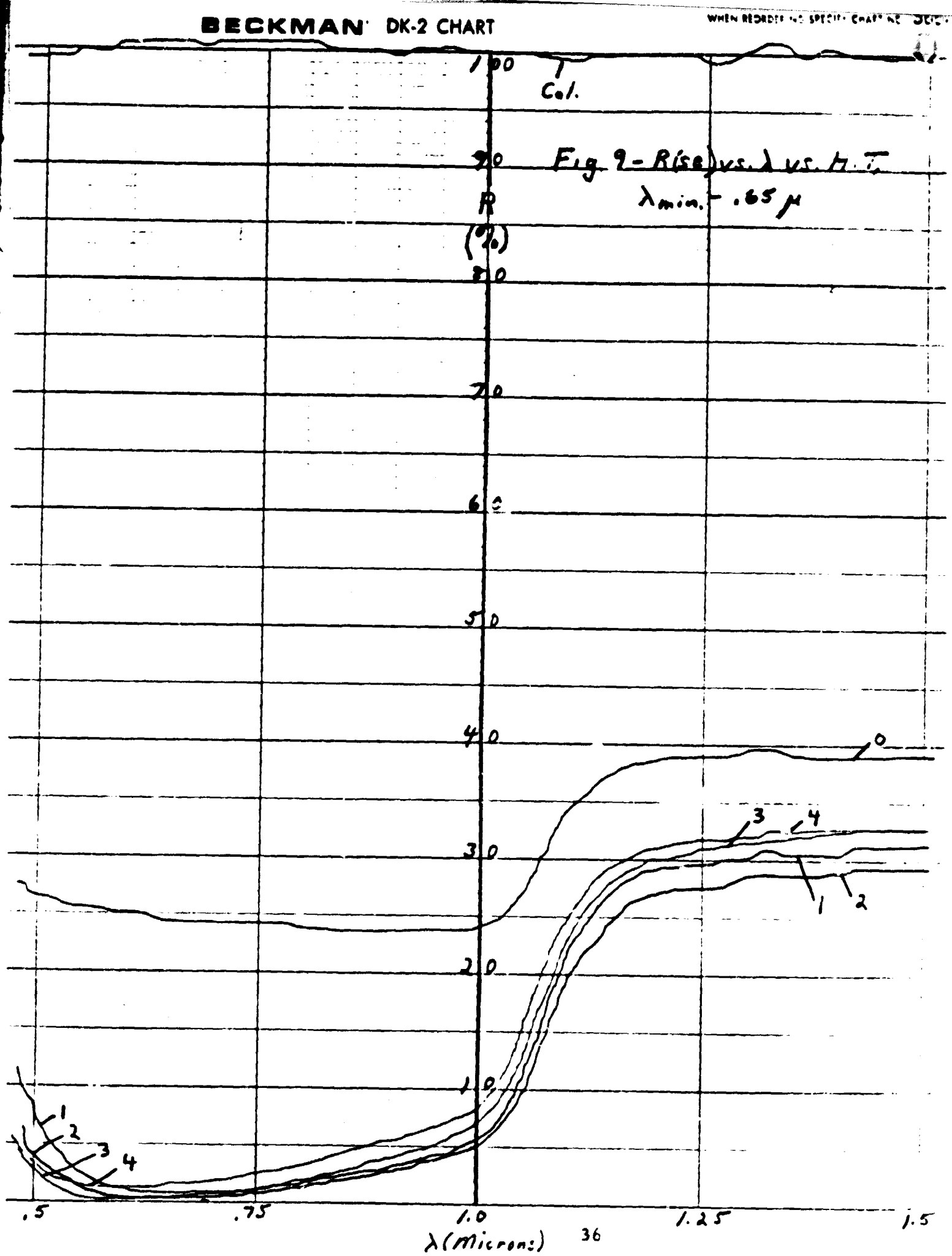
BECKMAN DK-2 CHART
Cal.
Fig 9 - R(se) vs. λ vs. H.T.
λmin. - .65 μ
R
(%)
100
90
80
70
60
50
40
30
20
10
0
3
4
1
2
.5
.75
1.0
1.25
1.5
λ (Microns)

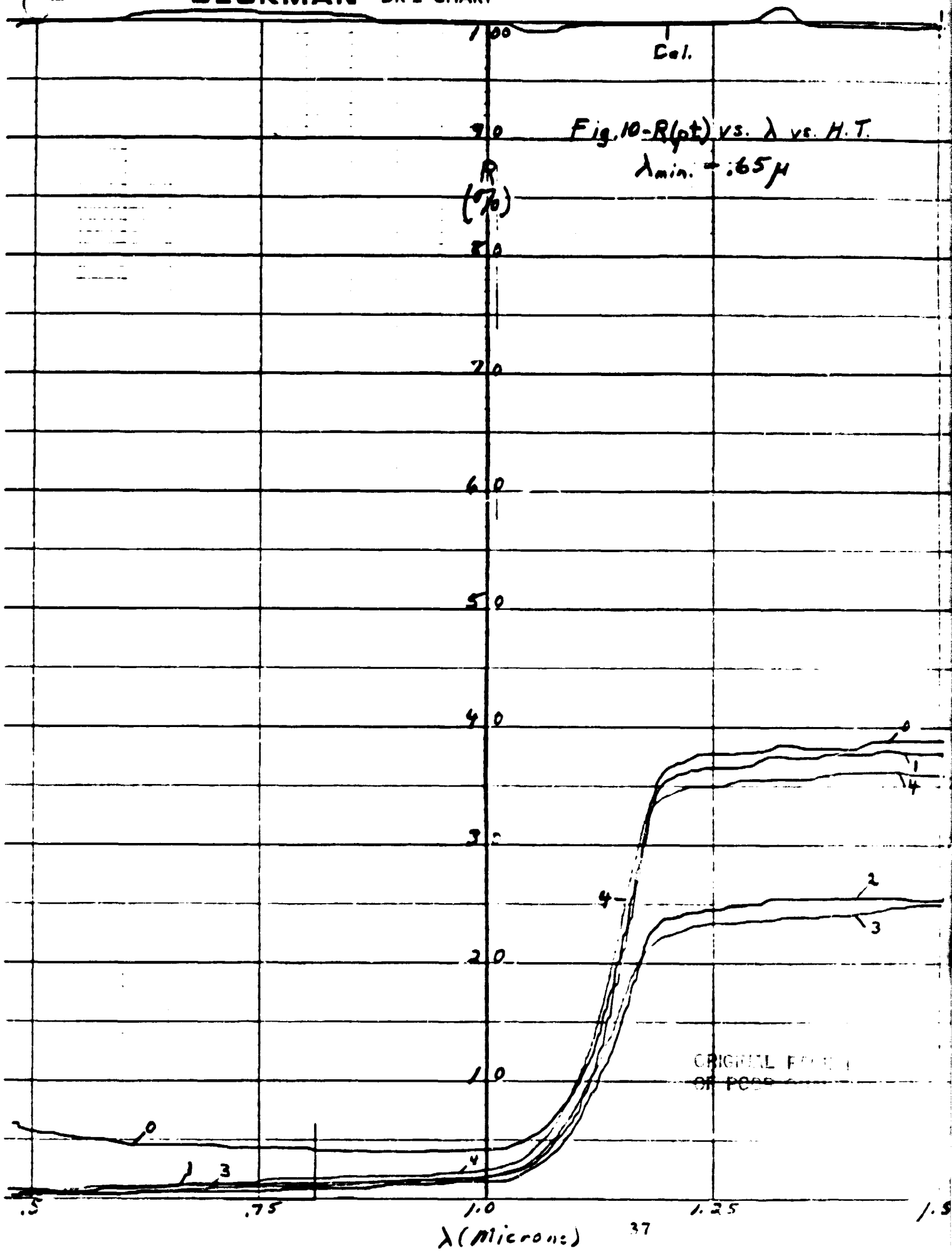
BECKMAN DK-2 CHART
Cal.
Fig. 10-R(pt) vs. λ vs. H.T.
λmin. = .65μ
R (%)
100
90
80
70
60
50
40
30
20
10
0
1
4
2
3
.5
.75
1.0
1.25
1.5
λ (Microns)

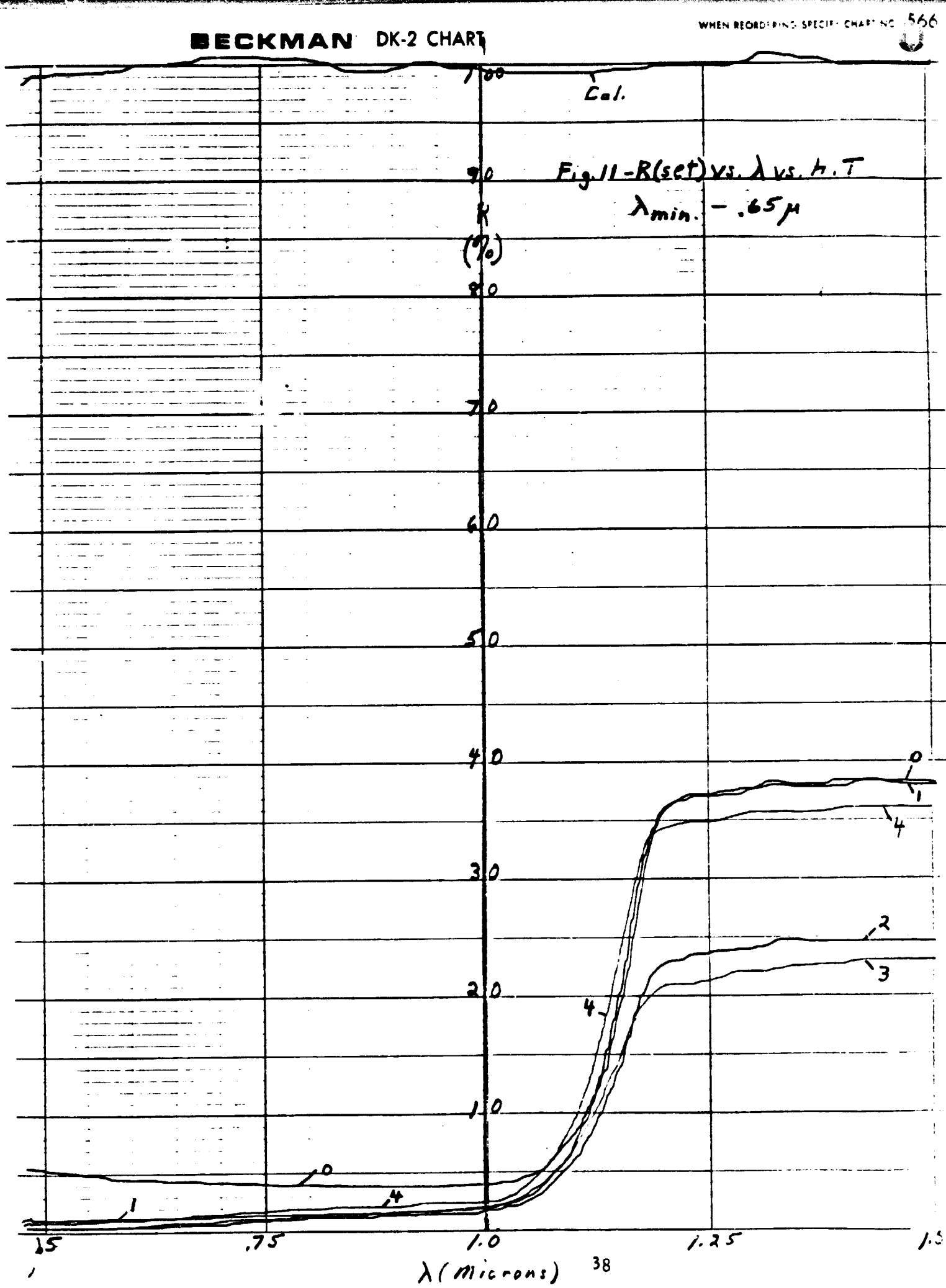
BECKMAN DK-2 CHART
WHEN RECORDING SPECIFY CHART NO. 566
Cal.
Fig. 11 - R(set) vs. λ vs. h.T
λmin. - .65μ
R (%)
100
90
80
70
60
50
40
30
20
10
.75
1.0
1.25
λ (Microns)
0
1
2
3
4

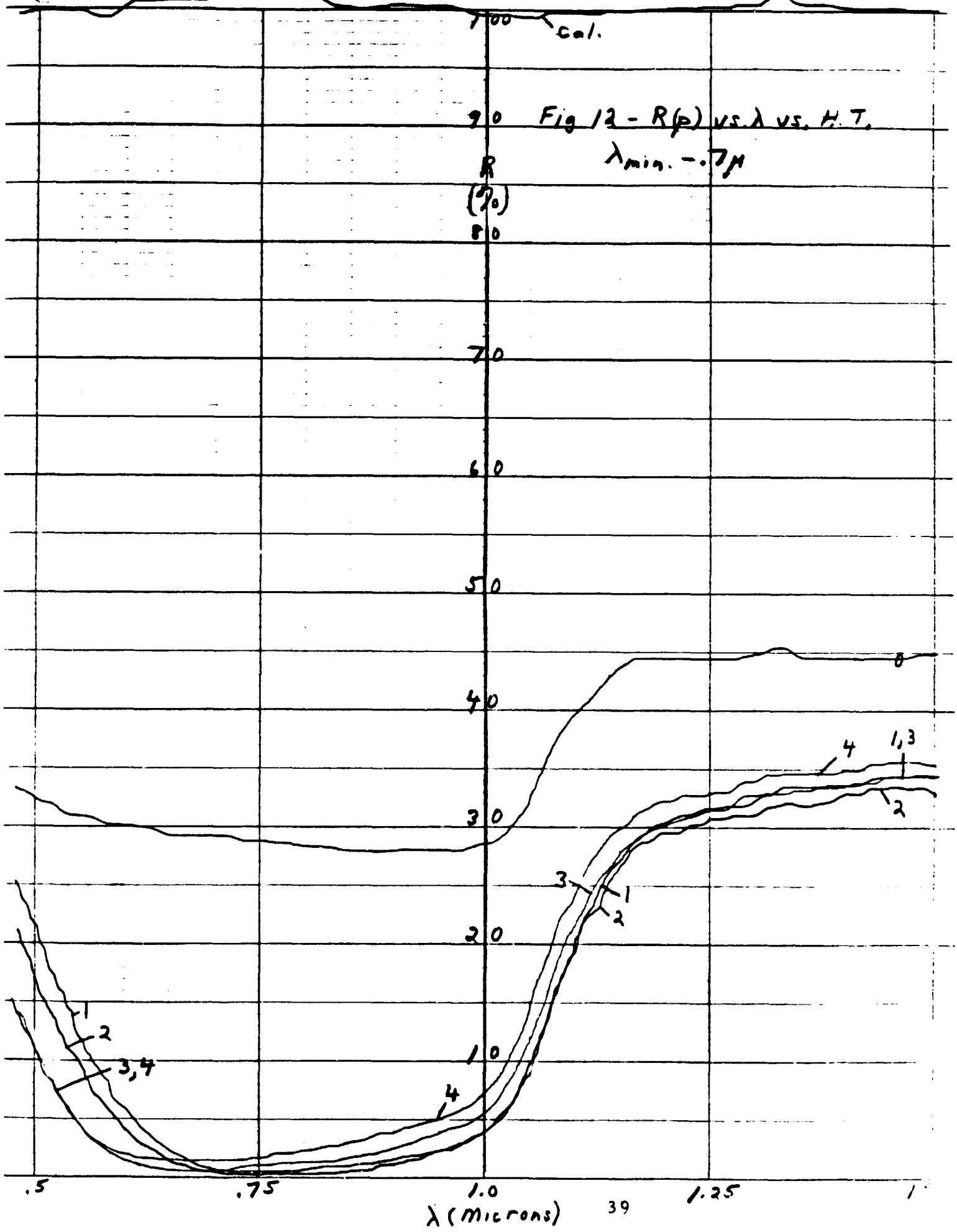
Fig 12 - R(p) vs λ vs. H.T.
λmin. - .7μ
R (%)
100
Cal.
90
80
70
60
50
40
30
20
10
0
4
1,3
2
3
1
2
1
2
3,4
4
.5
.75
1.0
1.25
1
λ (Microns)

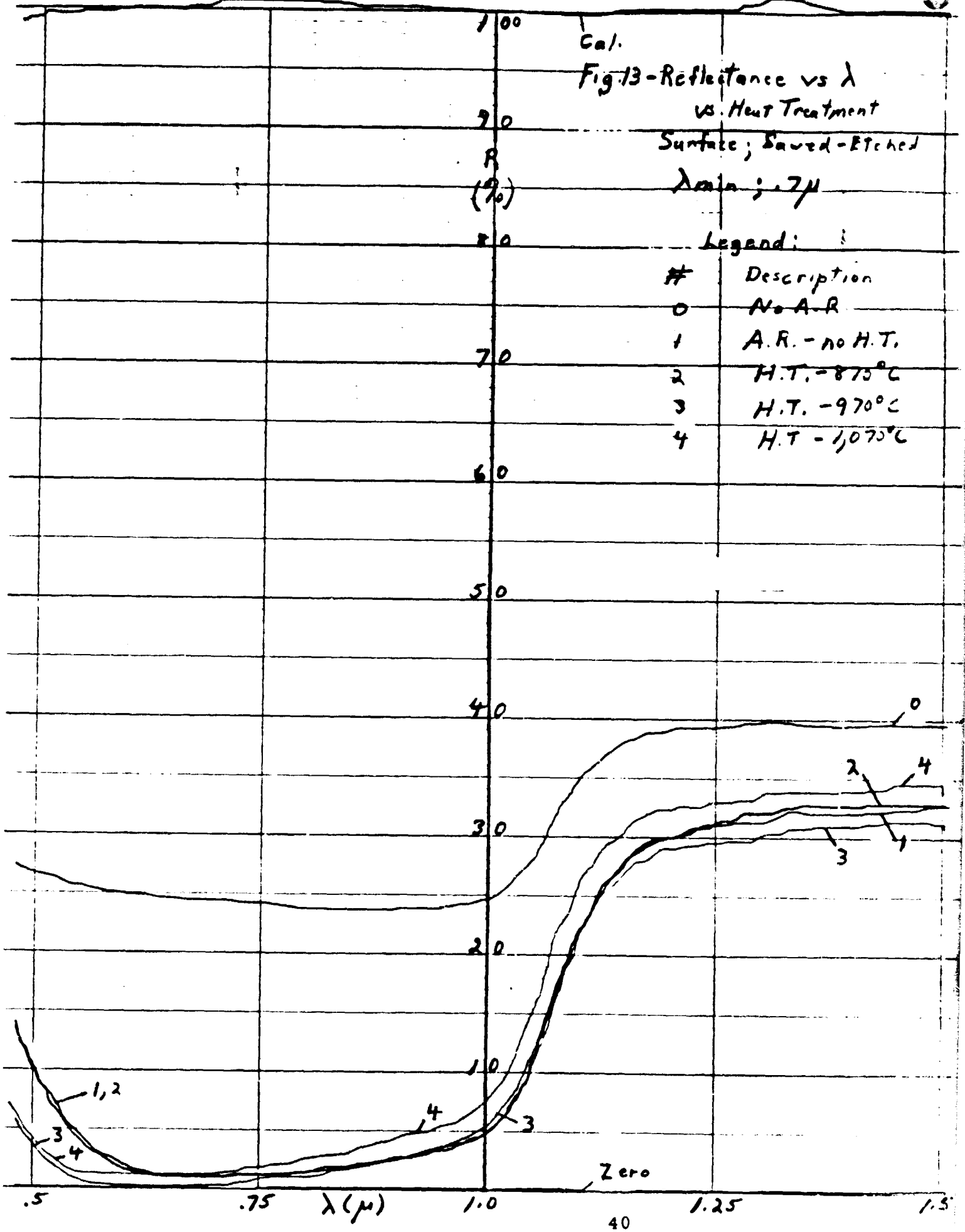
Cal.
Fig 13 - Reflectance vs λ
vs. Heat Treatment
Surface; Sawed-Etched
λmin; .7μ
Legend:
Description
0 No A.R.
1 A.R. - no H.T.
2 H.T. - 875°C
3 H.T. - 970°C
4 H.T - 1,075°C
R (%)
100
90
80
70
60
50
40
30
20
10
Zero
.5
.75
λ (μ)
1.0
1.25
1.5
0
2
4
1
3
1,2
3
4
4
3

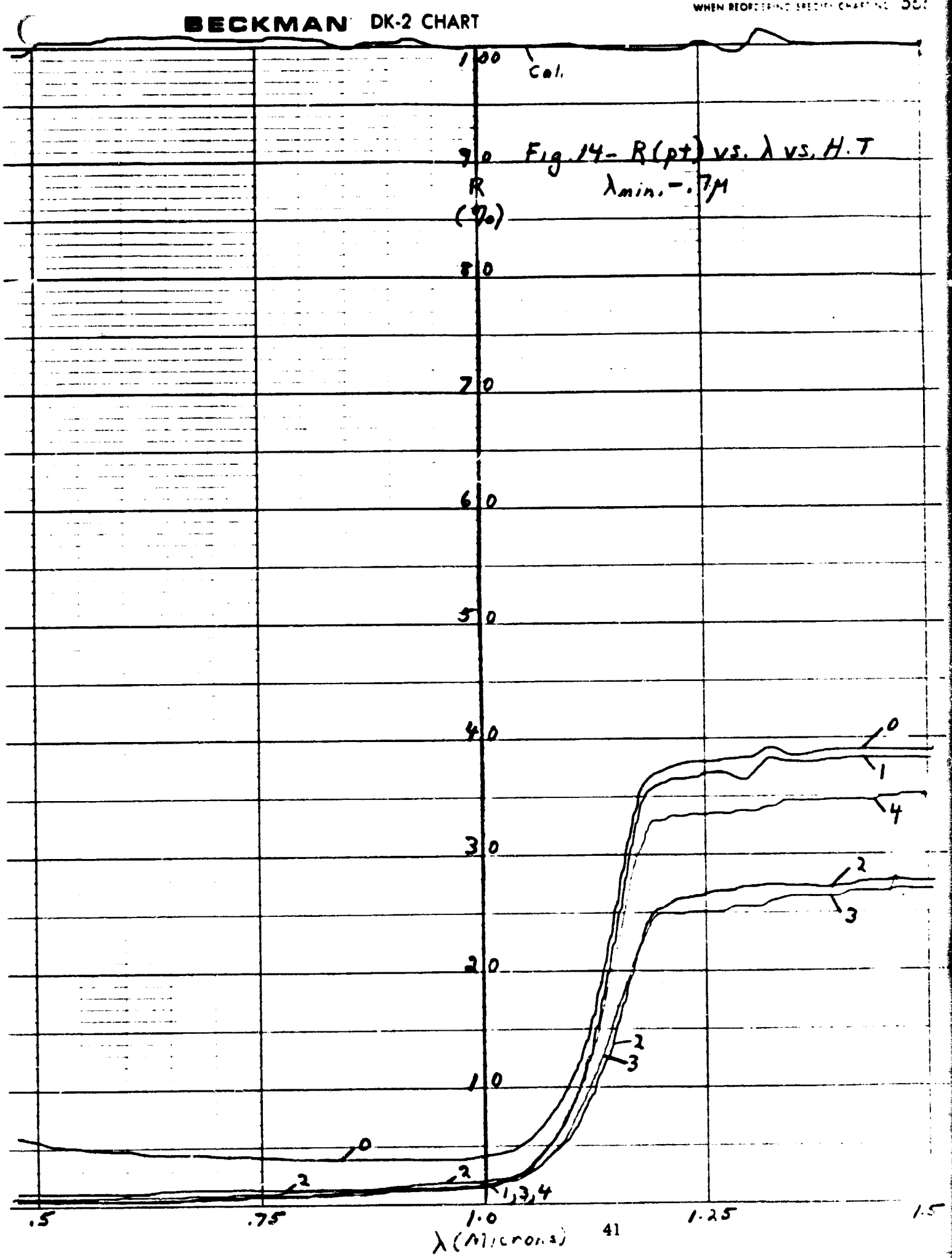
BECKMAN DK-2 CHART
Col.
Fig. 14- R(pt) vs. λ vs. H.T
λmin.-.7μ
R
(%)
100
90
80
70
60
50
40
30
20
10
0
2
1,3,4
.5
.75
1.0
1.25
1.5
λ (Microns)

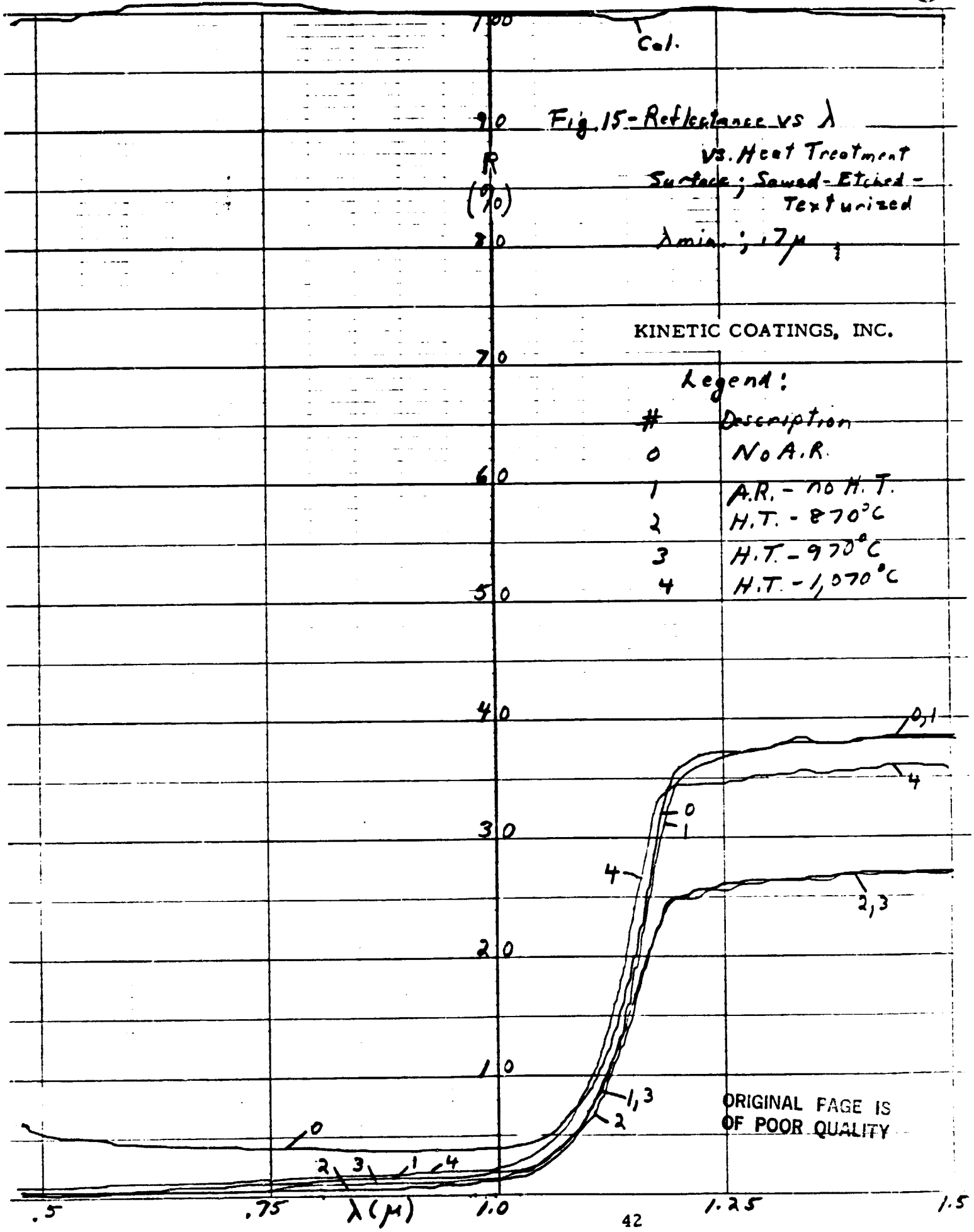

ORIGINAL PAGE IS OF POOR QUALITY

Data in Figs. 8-11 sequentially give R vs. λ vs. H.T. for p, se, pt, and set surfaces at a λ_{min} of .65 μ. Very similar data was obtained for the other 4 λ_{min} values and for comparison Figs. 12-15 give the curves for a λ_{min} of .7 μ. The latter was the value used for cell fabrication and corresponds to an Al_2O_3 thickness of 99.4 mμ.

Figure 8 for the polish-etched surface and λ_{min} of .65 μ shows a normal sharp reduction in reflectance to approximately 1.6% at the minimum point with no H. T. (curve 1). This is in excellent agreement with the calculated value(1.6%) for an AR coating having an n value of 1.76. With heat treatment the curve shifts to shorter λ's and to lower values of R until 970°C is reached. (Note: Whenever absolute R values got extremely low as in curve 3, the zero calibration for the instrument was immediately rechecked and in some cases actually plotted for reference - see e.g. Fig. 13).

The shift to shorter λ's may be due to thinning of the AR coating at the higher temperatures. However, the shift to lower R values(curve 3) implies a shift in n to higher values. After 1070°C H. T. the whole curve lifts up to somewhat higher values of R. Since the maximum H. T. temperatures for complete cells were likely to be in the 850-900°C range, and highly unlikely to be above 1,000°C, higher values of temperature were not used.

At 970°C there was an apparent staining of the silicon surface under the AR coating. This stain was not apparent at 870°C and was originally thought to be due to material left on the silicon after etching by the manufacturer. However, separate samples which were HF dipped before AR coating to test this hypothesis gave the same result. Subsequent tests on 3" diameter samples which were heat treated while supported horizontally, rather than standing vertically as in the four quadrant cases, showed the effect to be strongly reduced. The staining patterns indicated possible multi-crystalline structure and core defect effects.

This coupled with close visual evaluation of the surface led to the tentative conclusion that the Al_2O_3 coating was "decorating" dislocations at the higher temperatures. Since the stain apparently involves a large number of brighter spots, it is possible that the increase in R at 1070°C is due to the collective reflectance of the stained area. This effect also appeared on se samples but was not apparent on pt or set samples. Since there was little effect on performance, no further attempt was made to interpret or remove this phenomenon.

Fig. 9 gives comparable R curves for the se surface. These are similar to those for the p surface, with a significant shift to lower R values at the shorter λ's and very low R values (<1%) at the minimum point with 870°C or 970°C H. T. The pt and set surfaces (Figs. 10 and 11, respectively) give extremely good performance across the active spectrum, with R averaging considerably less than 2% for the .5-1.1 μ region at all temperatures. Similar data for the overlapping scan over the .35-.8 μ (see Figs. 18-20) shows that this excellent performance extends over the complete active spectrum. Values of R, in fact, range from .5-1% over most of this region. The slight increase in R with the 1070°C H. T. is also apparent for the pt and set samples and in general was found to occur for almost all samples tested.

Similar data (Figs. 12-15) for the sample sets for the other four λ_{min} values, in general is extremely similar to that for the λ_{min} of .65 μ. The only apparent change is a shift to higher λ's for the minimum reflectivity area for p and se samples as the AR coating thickness increases, accompanied by by an increase in R values at shorter λ's.

It was very informative to plot R vs. λ vs. λ_{min} for a given H. T. as in Figs. 16-28. Fig. 16 shows the .5-1.5 μ region curves for the pt samples after the 1070°C H. T. The extreme similarity of the curves for the 5 different Al_2O_3 thicknesses is immediately obvious. Figs. 17-20 show the shorter λ region after no H. T., 870°C, 970°C and 1070°C, respectively. Again the curves are essentially the same for practical purposes. The 970°C case is particularly striking since R is extremely low in all cases right down to .35μ. Obviously for the pt case, the thickness of the Al_2O_3 AR coating is a non-critical factor after H. T. (cp. Fig. 17 for no H. T.). Although there is a

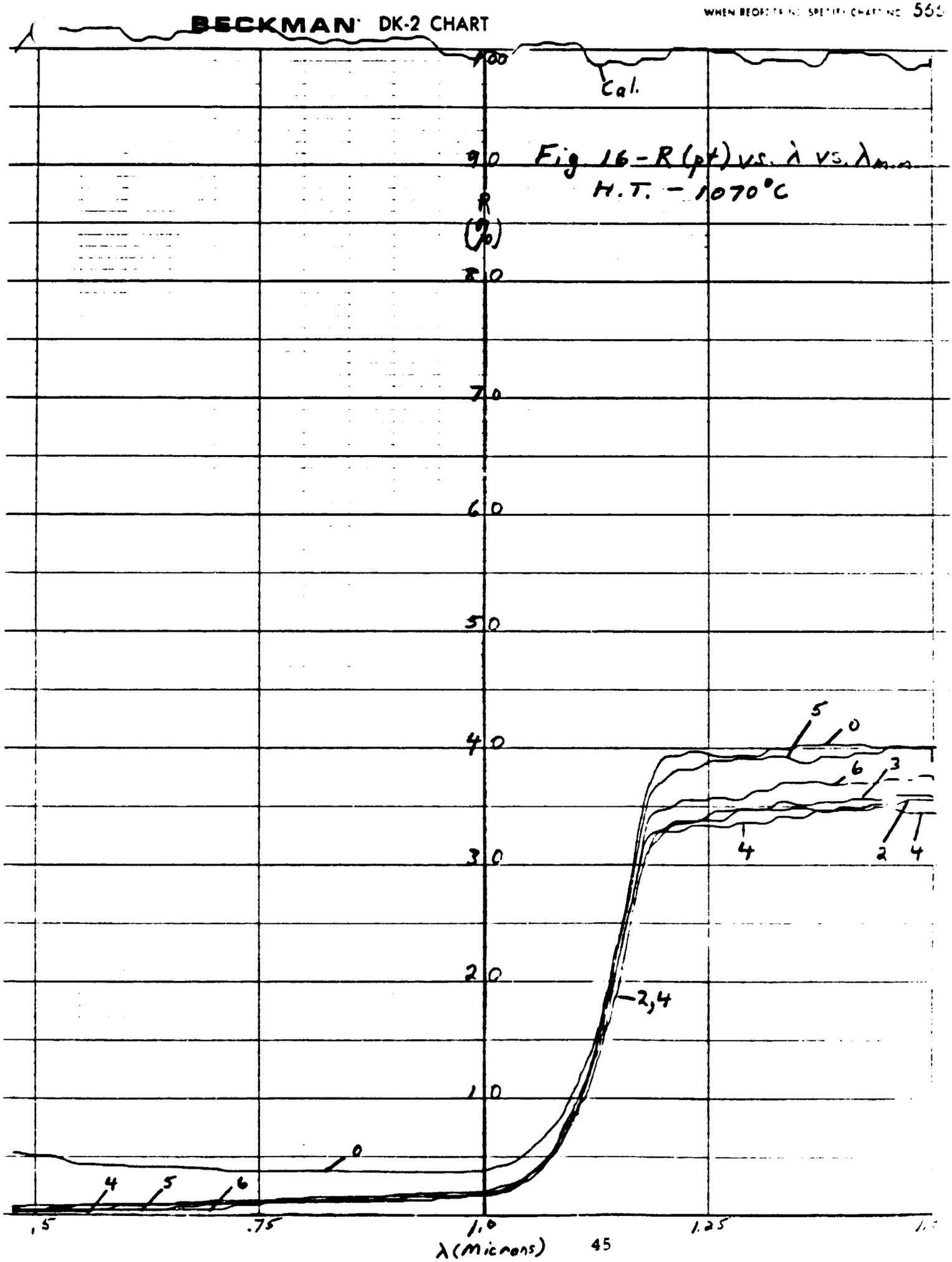
BECKMAN DK-2 CHART
Cal.
Fig 16 - R (pt) vs. λ vs. λm.a
H.T. - 1070°C
R (%)
100
90
80
70
60
50
40
30
20
10
5
0
6
3
4
2
4
2,4
0
4
5
6
.5
.75
1.0
1.25
λ (Microns)

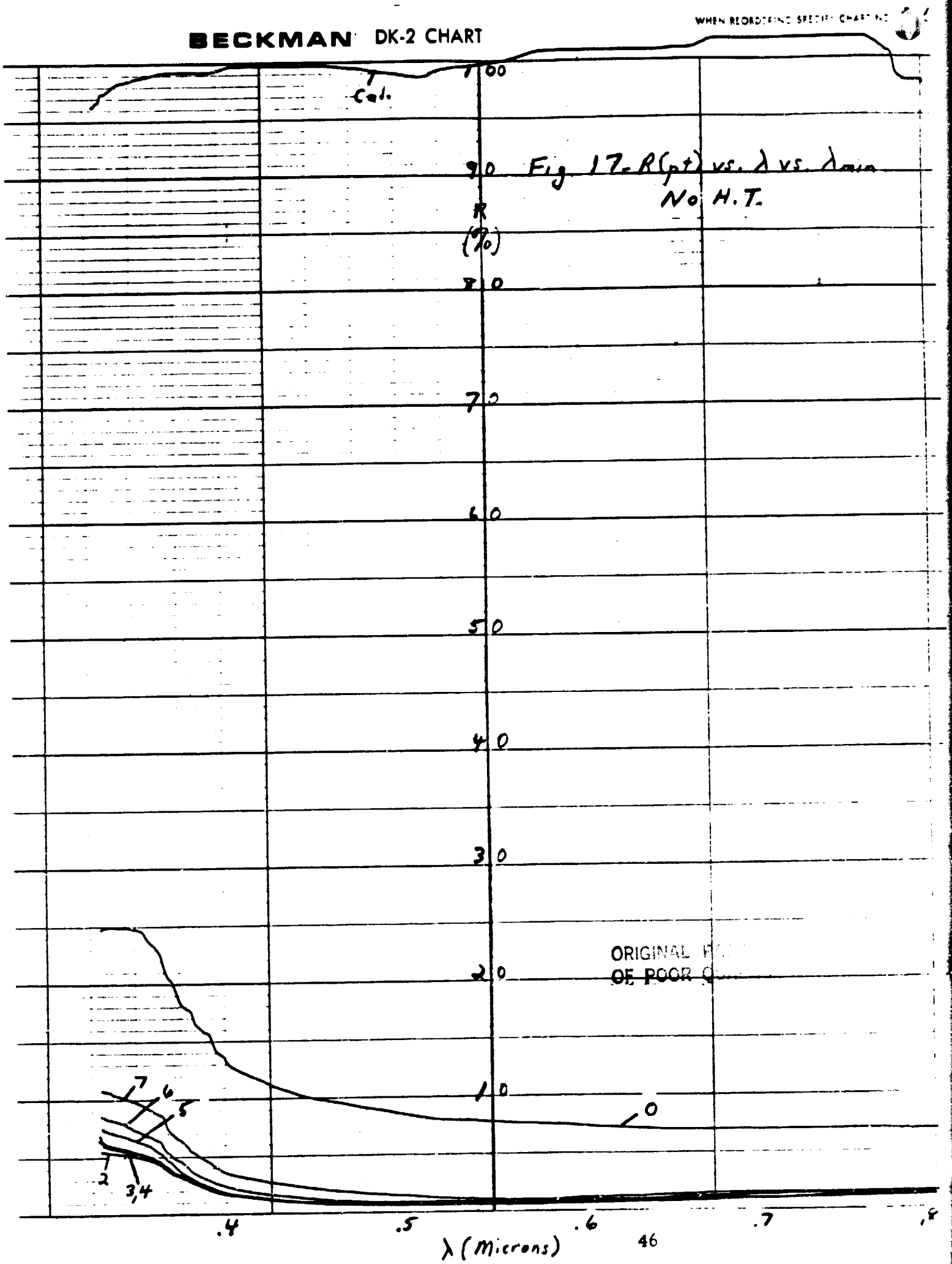

Fig 17 - R(pt) vs. λ vs. λ min
No H.T.

ORIGINAL PAGE IS
OF POOR QUALITY

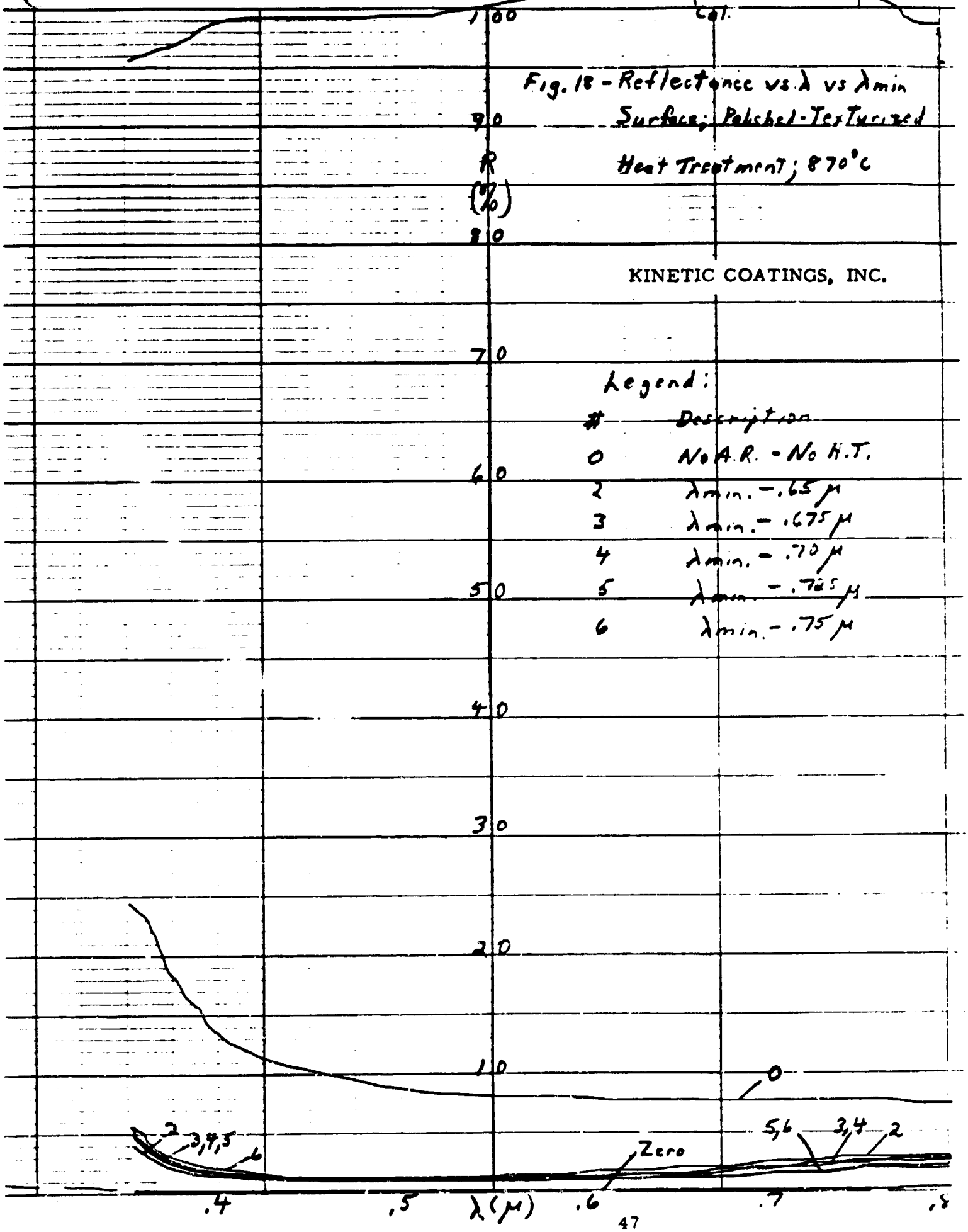
Cal.
Fig. 18 - Reflectance vs. λ vs λmin
Surface; Polished-Texturized
Heat Treatment; 870°C
KINETIC COATINGS, INC.
Legend:
Description
0 No A.R. - No H.T.
2 λmin. - .65 μ
3 λmin. - .675 μ
4 λmin. - .70 μ
5 λmin. - .725 μ
6 λmin. - .75 μ
R (%)
100
90
80
70
60
50
40
30
20
10
0
2
3,4,5
6
Zero
5,6
3,4
2
.4
.5
λ(μ)
.6
.7
.8

BECKMAN DK-2 CHART

WHEN REORDERING SPECIFY CHART NO. 566

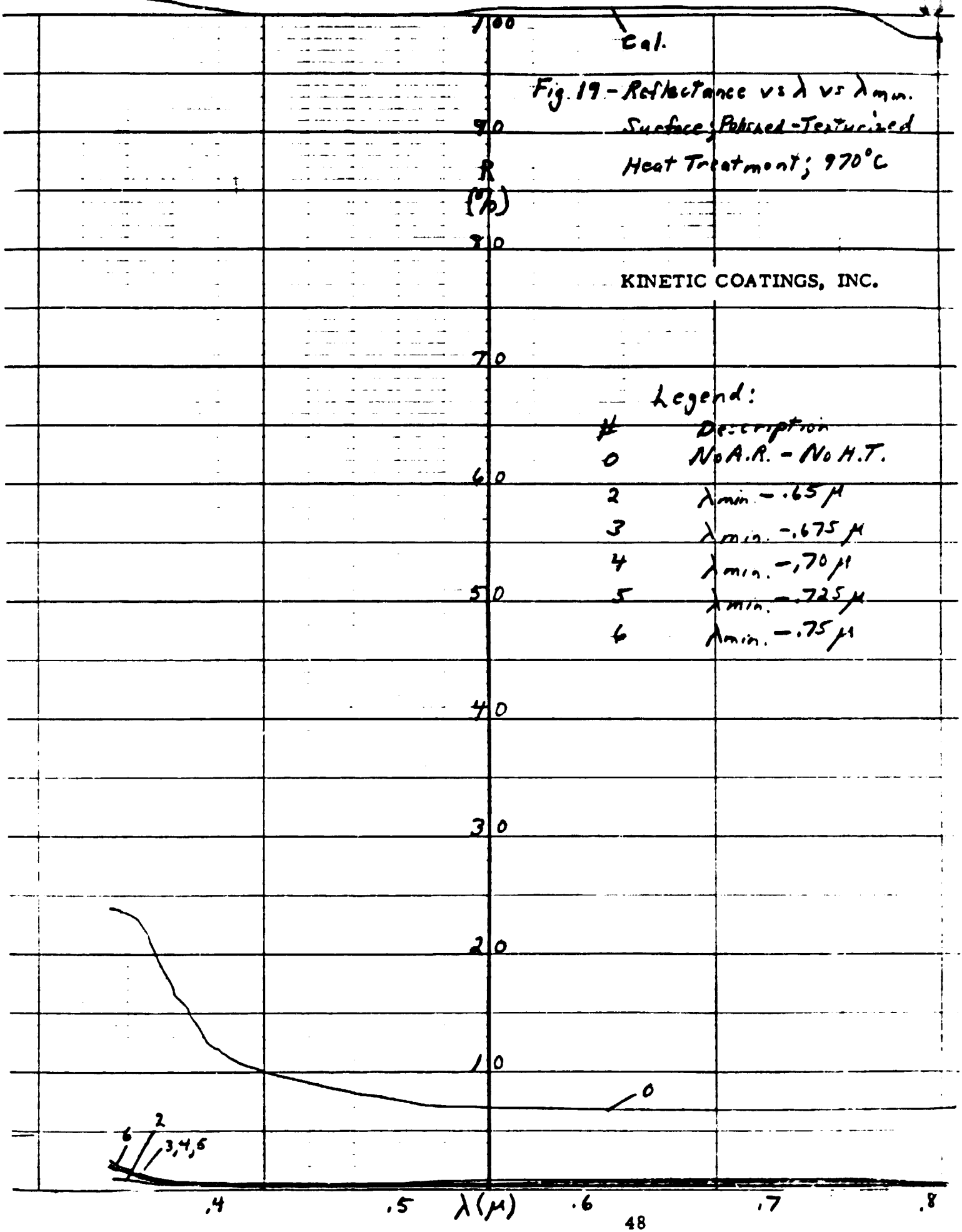

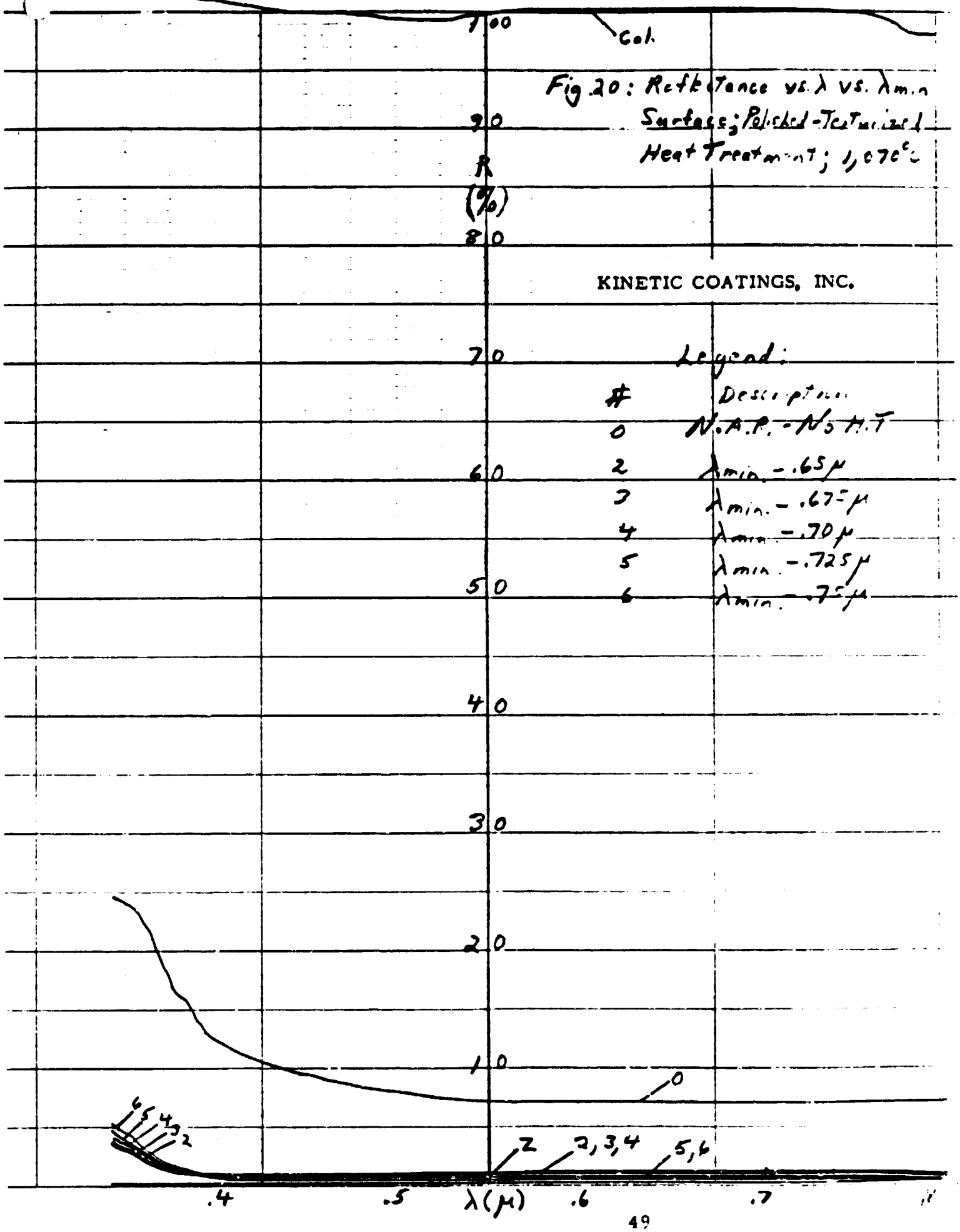
Col.
Fig 20: Reflectance vs. λ vs. λmin
Surface: Polished-Texturized
Heat Treatment; 1,070°C
R (%)
100
90
80
70
60
50
40
30
20
10
KINETIC COATINGS, INC.
Legend:
Description
0 N.A.P. - No H.T
2 λmin. - .65μ
3 λmin. - .675μ
4 λmin. - .70μ
5 λmin. - .725μ
6 λmin. - .75μ
0
6 5 4 3 2
2
2, 3, 4
5, 6
.4
.5
λ(μ)
.6
.7

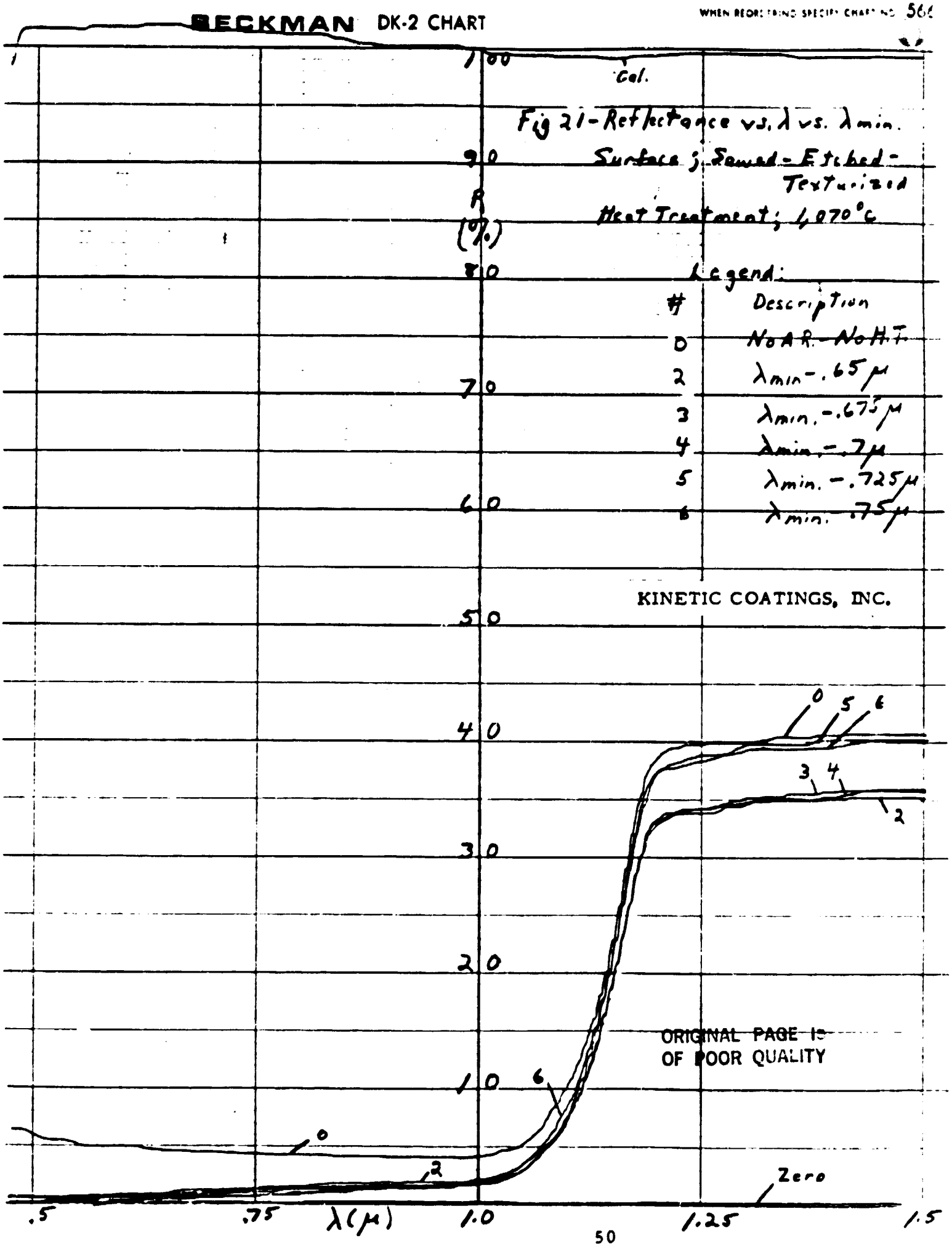
BECKMAN DK-2 CHART
WHEN REORDERING SPECIFY CHART NO. 566
Col.
Fig 21 - Reflectance vs. λ vs. λmin.
Surface; Sawed - Etched - Texturized
Heat Treatment; 1,070°C
Legend:
Description
0 NoAR - NoH.T.
2 λmin - .65 μ
3 λmin. - .675 μ
4 λmin. - .7 μ
5 λmin. - .725 μ
6 λmin. .75 μ
KINETIC COATINGS, INC.
R (%)
100
90
80
70
60
50
40
30
20
10
.5
.75
λ(μ)
1.0
1.25
1.5
0
5
6
3
4
2
Zero
ORIGINAL PAGE IS OF POOR QUALITY

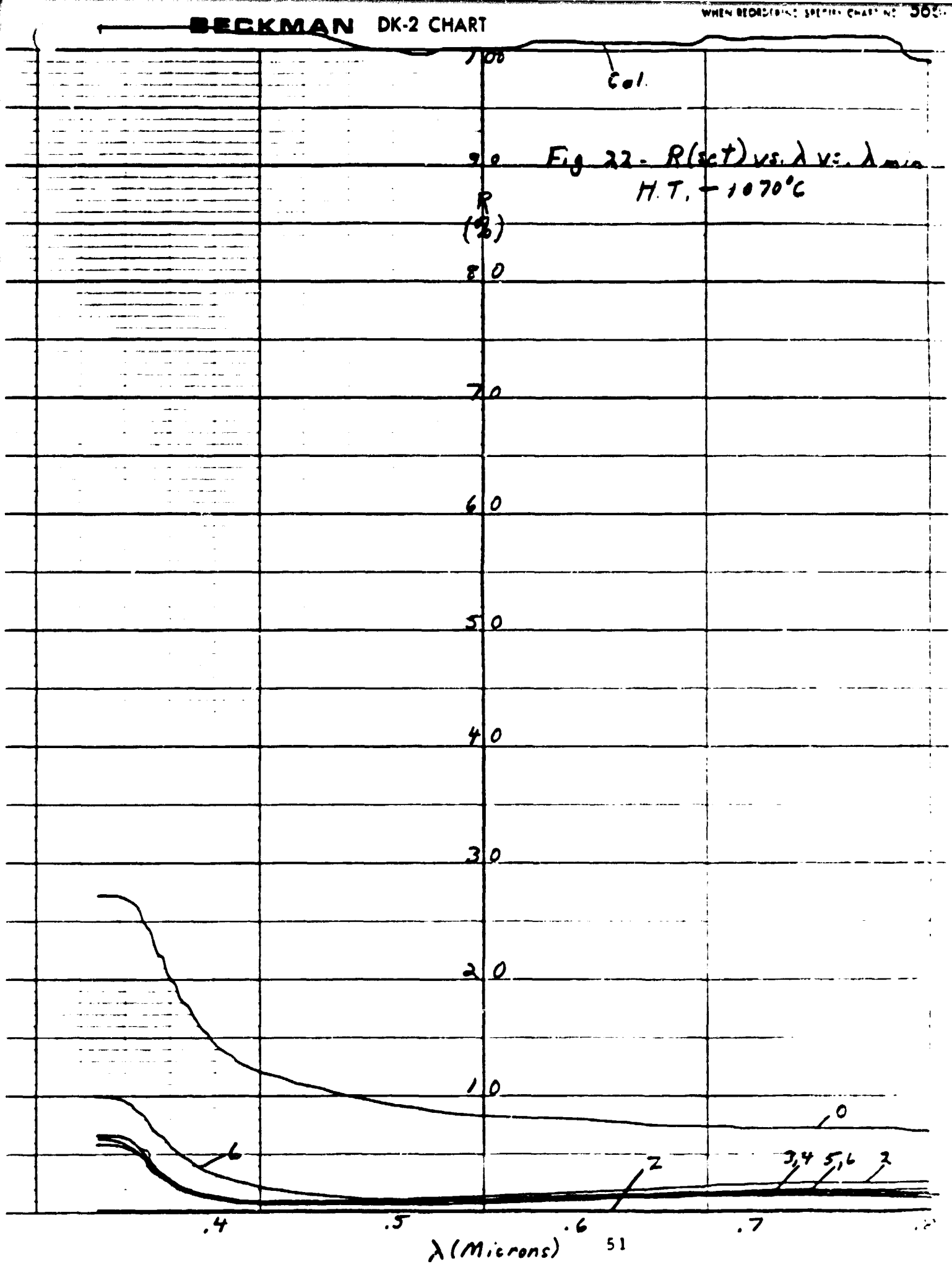
BECKMAN DK-2 CHART
Col.
Fig 22 - R(sct) vs. λ vs. λ min
H.T. - 1070°C
R (%)
100
90
80
70
60
50
40
30
20
10
0
6
2
3,4
5,6
7
.4
.5
.6
.7
λ (Microns)

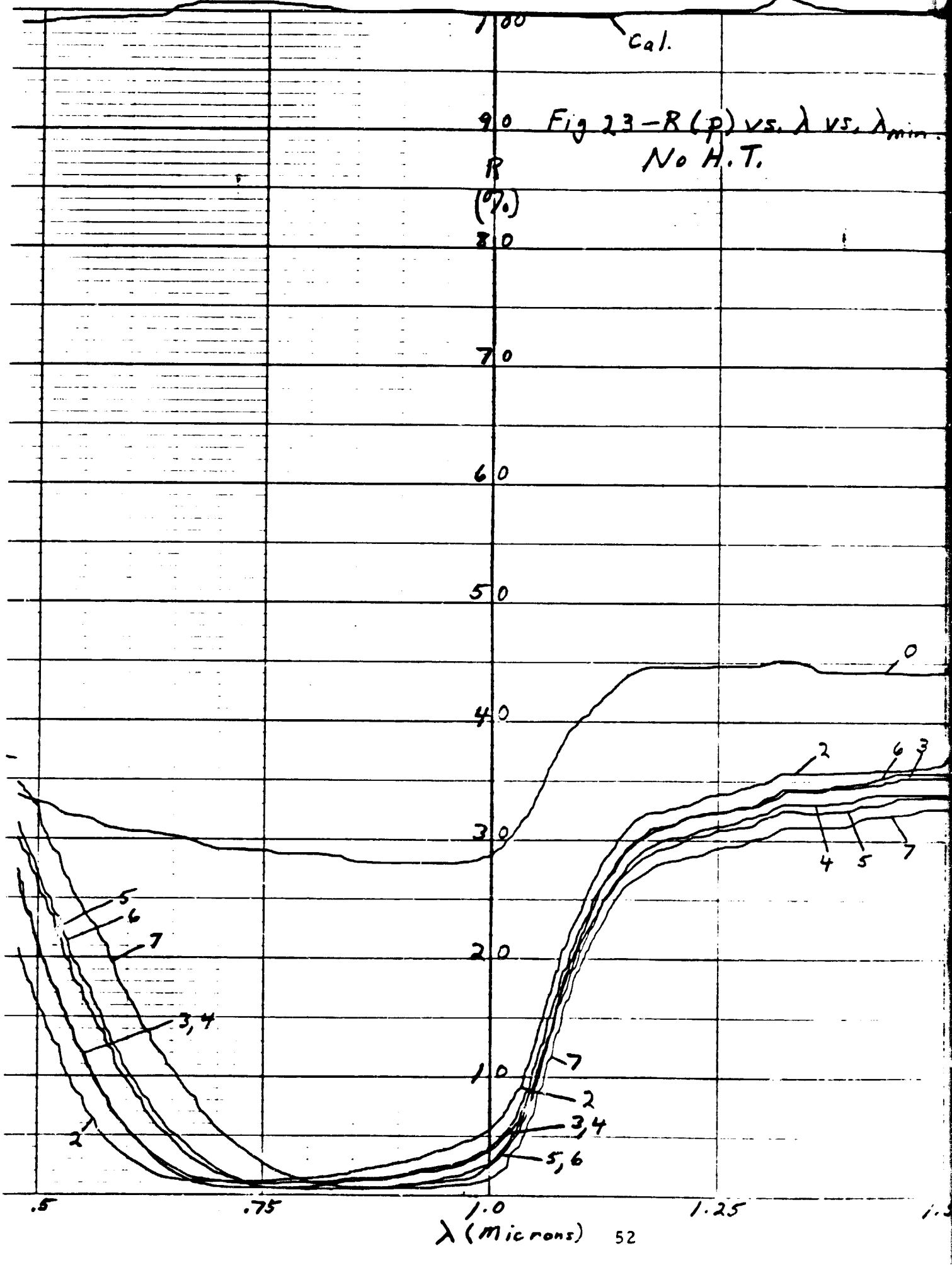
BECKMAN DK-2 CHART
Cal.
Fig 23 – R (p) vs. λ vs. λmin.
No H.T.
R
(%)
100
90
80
70
60
50
40
30
20
10
.5
.75
1.0
1.25
λ (Microns)
0
2
6
3
4
5
7
5
6
7
3, 4
2
7
2
3, 4
5, 6

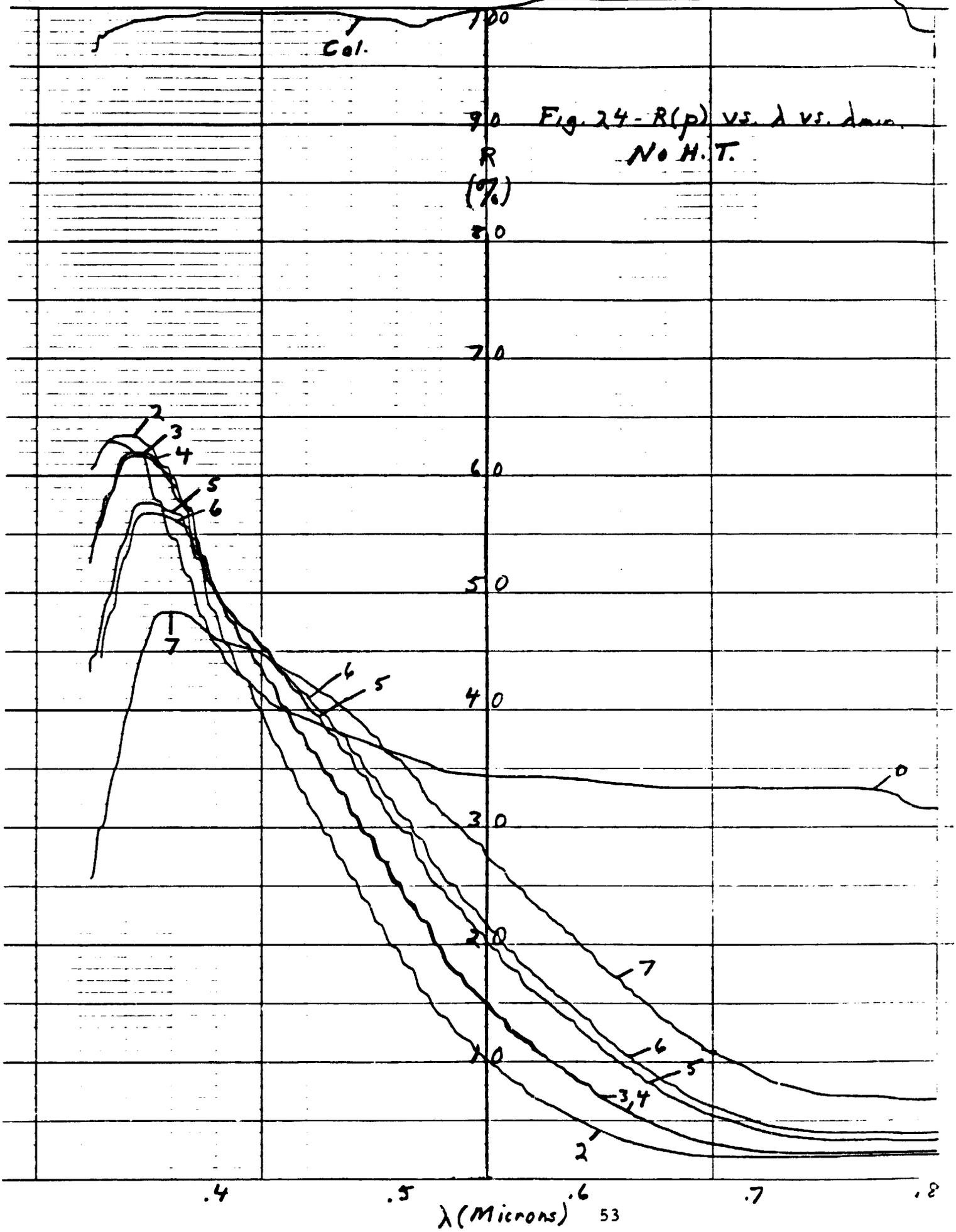
BECKMAN DK-2 CHART
WHEN REORDERING SPECIFY CHART NO. 566
Fig. 24 - R(p) vs. λ vs. λmin.
No H.T.
R (%)
100
90
80
70
60
50
40
30
20
10
Col.
0
2
3
4
5
6
7
3,4
.4
.5
.6
.7
.8
λ (Microns)

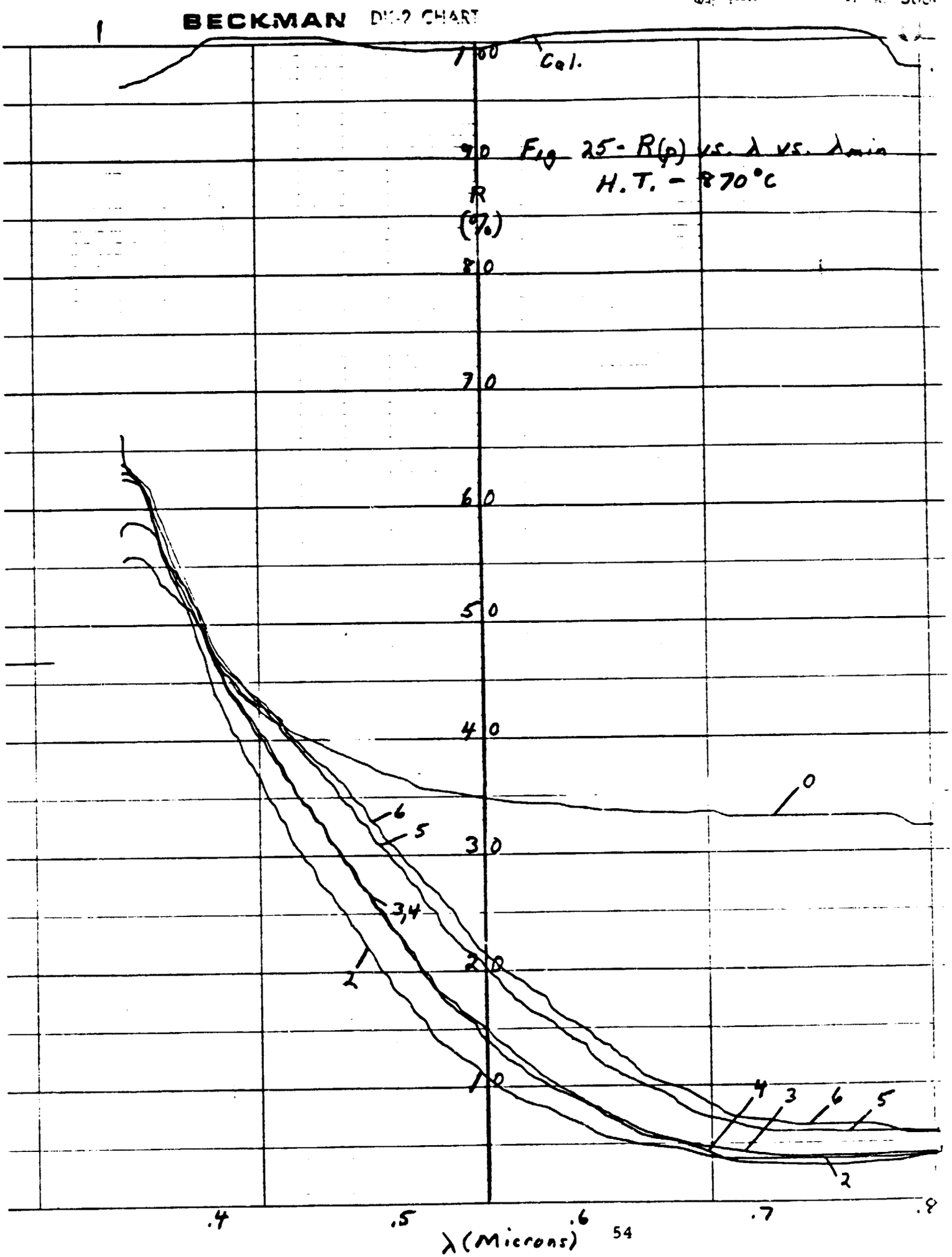
BECKMAN DK-2 CHART
Cal.
Fig 25 - R(ρ) vs. λ vs. λmin
H.T. - 870°C
R
(%)
100
90
80
70
60
50
40
30
20
10
0
6
5
3,4
2
4
3
6
5
2
.4
.5
.6
.7
.8
λ (Microns)

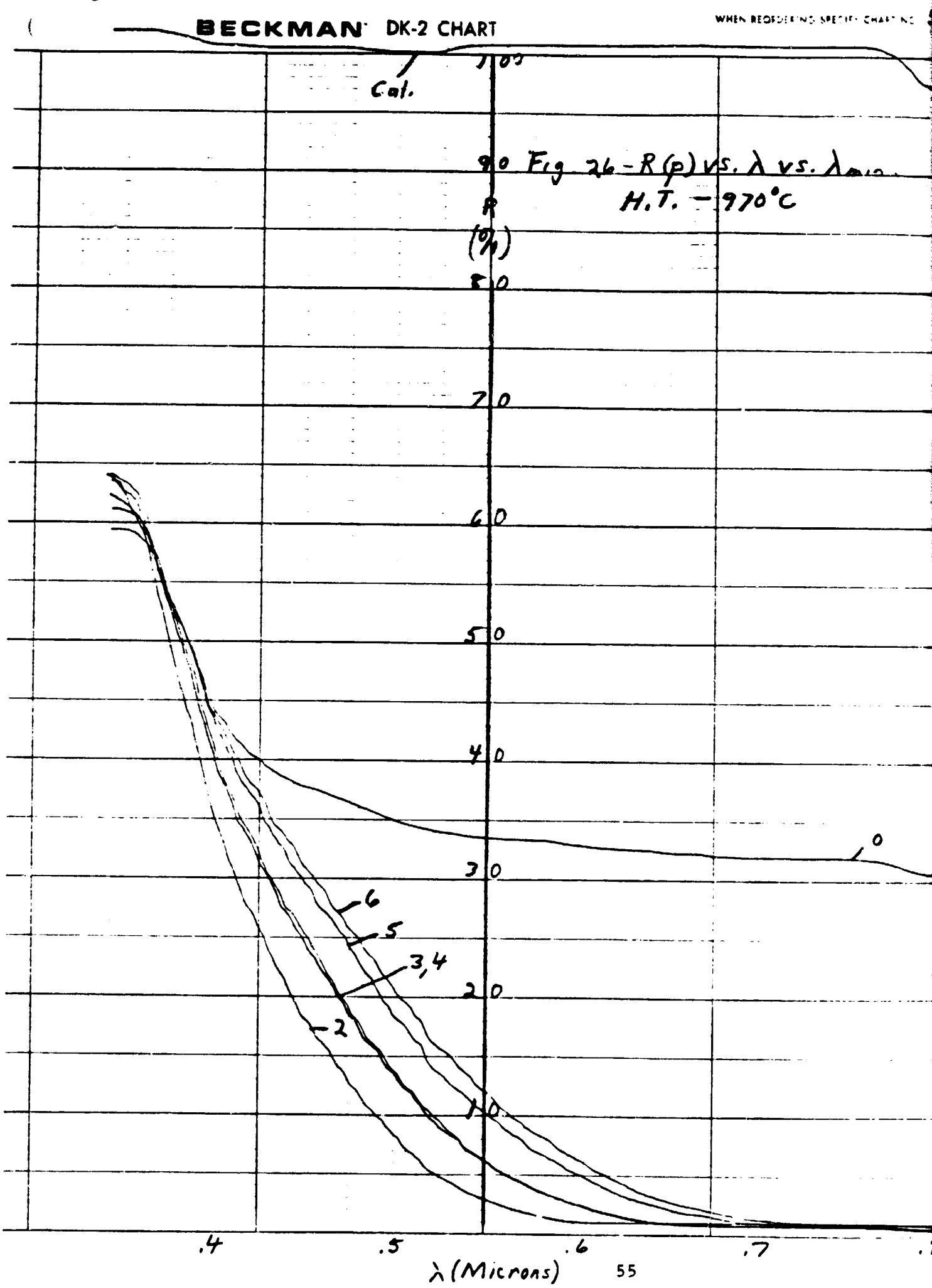
BECKMAN DK-2 CHART
Cal.
Fig 26 - R(p) vs. λ vs. λ
H.T. - 970°C
R (%)
100
90
80
70
60
50
40
30
20
10
0
6
5
3,4
2
.4
.5
.6
.7
λ (Microns)

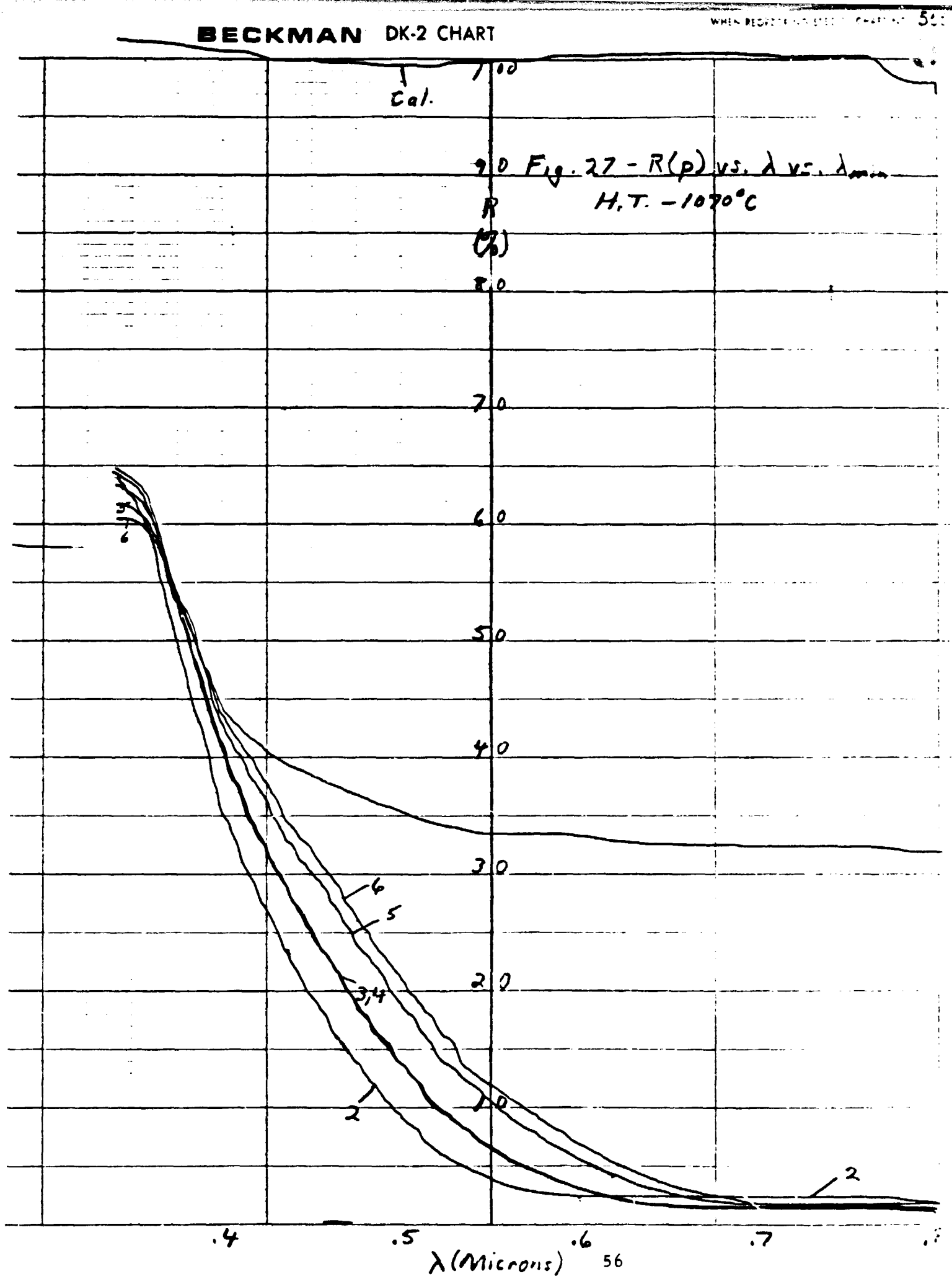
BECKMAN DK-2 CHART
Cal.
Fig. 27 - R(p) vs. λ vs. λmin
H.T. - 1070°C
R (%)
100
90
80
70
60
50
40
30
20
10
6
5
3,4
2
.4
.5
.6
.7
λ (Microns)

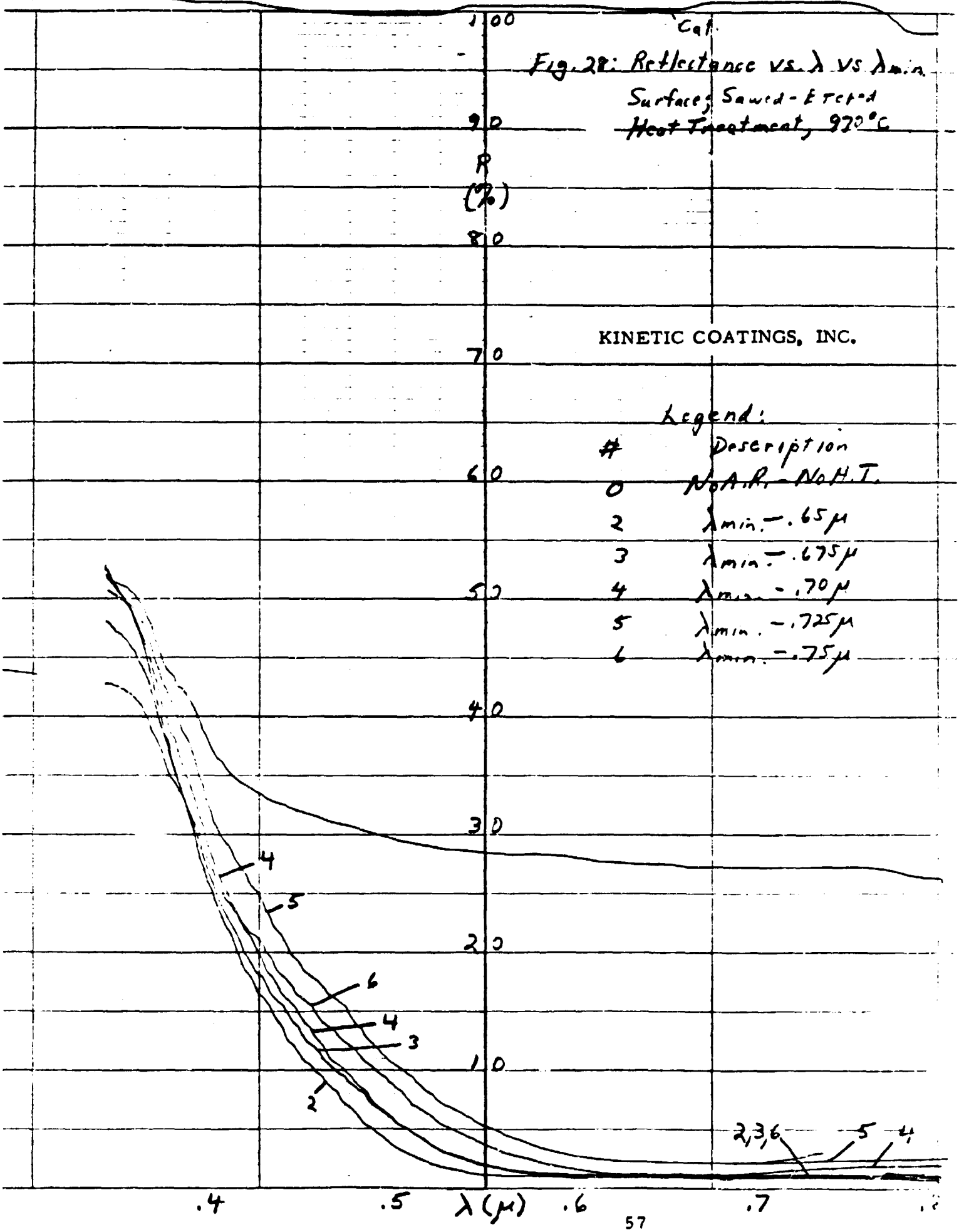
Cat.
Fig. 28: Reflectance vs. λ vs λmin.
Surface: Sawed-Etched
Heat Treatment, 970°C
KINETIC COATINGS, INC.
Legend:
Description
0 No A.R. - No H.T.
2 λmin. - .65μ
3 λmin. - .675μ
4 λmin. - .70μ
5 λmin. - .725μ
6 λmin. - .75μ
R (%)
100
90
80
70
60
50
40
30
20
10
.4
.5
λ (μ)
.6
.7
4
5
6
4
3
2
2,3,6
5
4

slight increase in R values at 1070°C, the temperature for H. T. is also obviously not critical. These results are extremely important for a production process since they mean that control of the Al_2O_3 thickness and the H. T. can be very loose as far as the AR coating performance is concerned.

Similar data is given for the set case in Figs. 21 and 22. Unfortunately, data for this case was not taken at 970°C but presumably would show lower R values as in the pt case. The values are, however, sufficiently low that the need for polish-etching before texturizing as opposed to a sawed-etched surface can safely be eliminated for production as far as AR performance in concerned.

Figs. 23-27 clearly show the shift of the reflectivity curve to higher λ's as the Al_2O_3 thickness in increased. Since there is more current to be gained at the blue end, this data indicates that the thinner coating (92.3 mμ for λ_{min} of 650 mμ) would be desirable for p surfaces. In fact, even thinner coatings might be desirable for an optimized polished surface cell. Fig. 28 which gives R vs. λ vs. λ_{min} for an se surface after 970°C H. T. shows considerably improved performance at the blue end over the p surface after 970°C H. T. (see Fig. 26). Again it is obvious that the se surface is superior to the p surface for AR performance and would be preferred for economy in production, all other factors being equal.

Based on the above data, the decision was made to make the process verification samples with an initial Al_2O_3 thickness of 99.4 mμ (λ_{min} -.70μ) and to heat treat at 970°C. To make sure that the reflectance results were temperature dependent, rather than time at temperature dependent, the heat treatment was carried out for 970°C for 10 minutes only (i.e. there was no prior H. T. at 870°C). Ten minutes was the time required for the furnace to reach equilibrium after the boat was inserted. An example of the R curves for a random process verification sample set (J9-4)is given in Fig. 29. Results for these samples were essentially the same, within experimental variations, as those obtained for the sequentially treated samples.

Transmission characteristics of the deposited Al_2O_3 coatings,

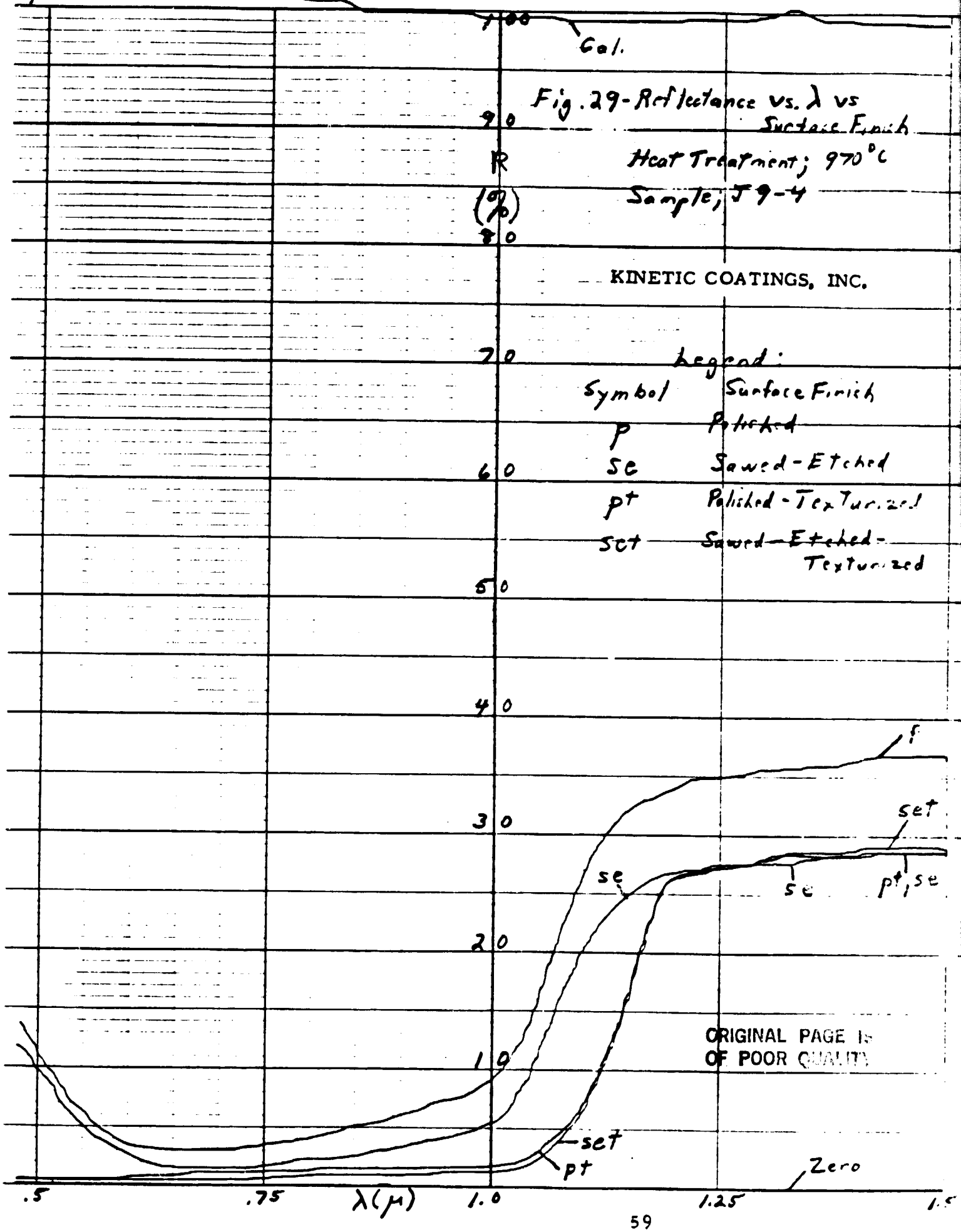

ORIGINAL PAGE IS OF POOR QUALITY

before and after H. T., may be deduced from Figs. 30-33. The latter are graphs, over the .5-1.5μ and .35-.8μ regions, of T vs. λ vs. λ_{min} for no H. T. and H. T.. Since the results for 870°C and 970°C H. T. were essentially the same as for 1070°C, only the 1070°C case is shown in Figs 31 and 33. Two standard discs, without coatings, were used to check on zero coating T values and on spectrometer stability. The first standard (S1) did not get any H. T., while the second standard (S2), received the same H. T. as the coated discs which were thermally treated with the R samples. Any changes in the bulk Al_2O_3 could thus be monitored by comparing S2 to the unheated S1. Also if there were no change in S2 due to H. T., but there were a shift in spectrometer calibration, this would appear as a shift in both the S1 and S2 transmittance curves.

From Fig. 30 it appears that T for all λ_{min} values (i. e. all AR coating thicknesses) actually increases when the coating is applied. This increase in T was still evident after the Al_2O_3 discs were heat treated at 870°C, 970°C, and 1070°C as shown by Fig. 31. Figs. 32 and 33 which give the .35-.8 μ range, without and with H. T., respectively, show that this increase in T continues down to .4μ. Since it is essentially impossible for absorption in the basic .040" thick disc to be lowered, before H. T., by application of AR coatings, the increased T value must be due to decreased reflectivity of the composite structure. This is exactly what would be expected if the n value of the deposited Al_2O_3 were lower than that of the bulk Al_2O_3 in the discs. This lowering of R is caused by grading of the index of refraction which basically causes a minor AR effect.

This mechanism was tested by measuring the reflectivity of the front surface (coating side) of the discs and comparing with S1 and S2. This data is plotted on Figs. 31 and 33 and shows that there is a direct correlation between decreased R and increased T for the coated discs. There was no change in S2 following H. T. compared to S1. When one considers that the spectrometer fluctuations are larger at the 100% end vs. the zero end of the scale, the change in R is essentially the same as the change in T.

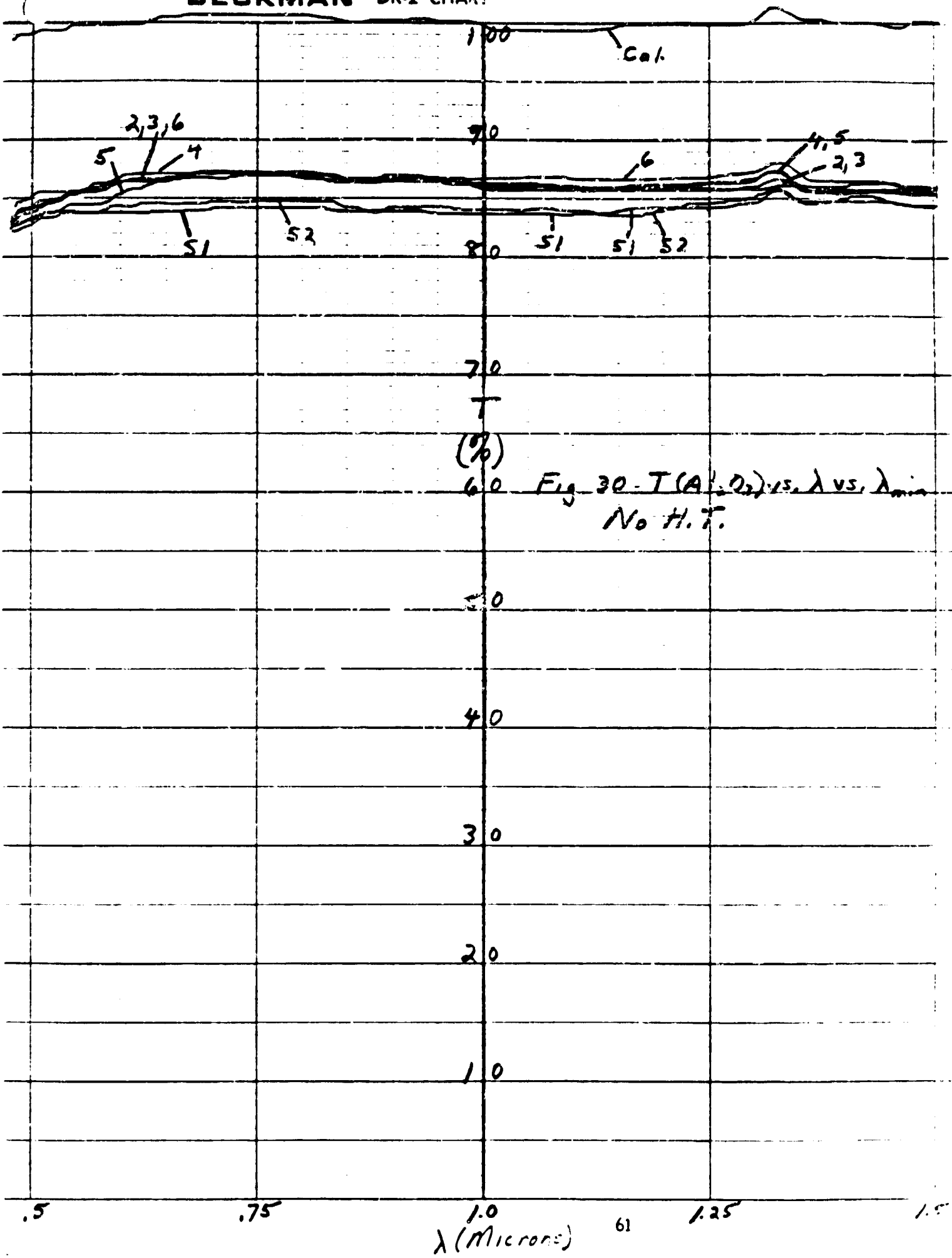

Fig 30 - T(Al_2O_3) vs. λ vs. λ_{min}
No H.T.

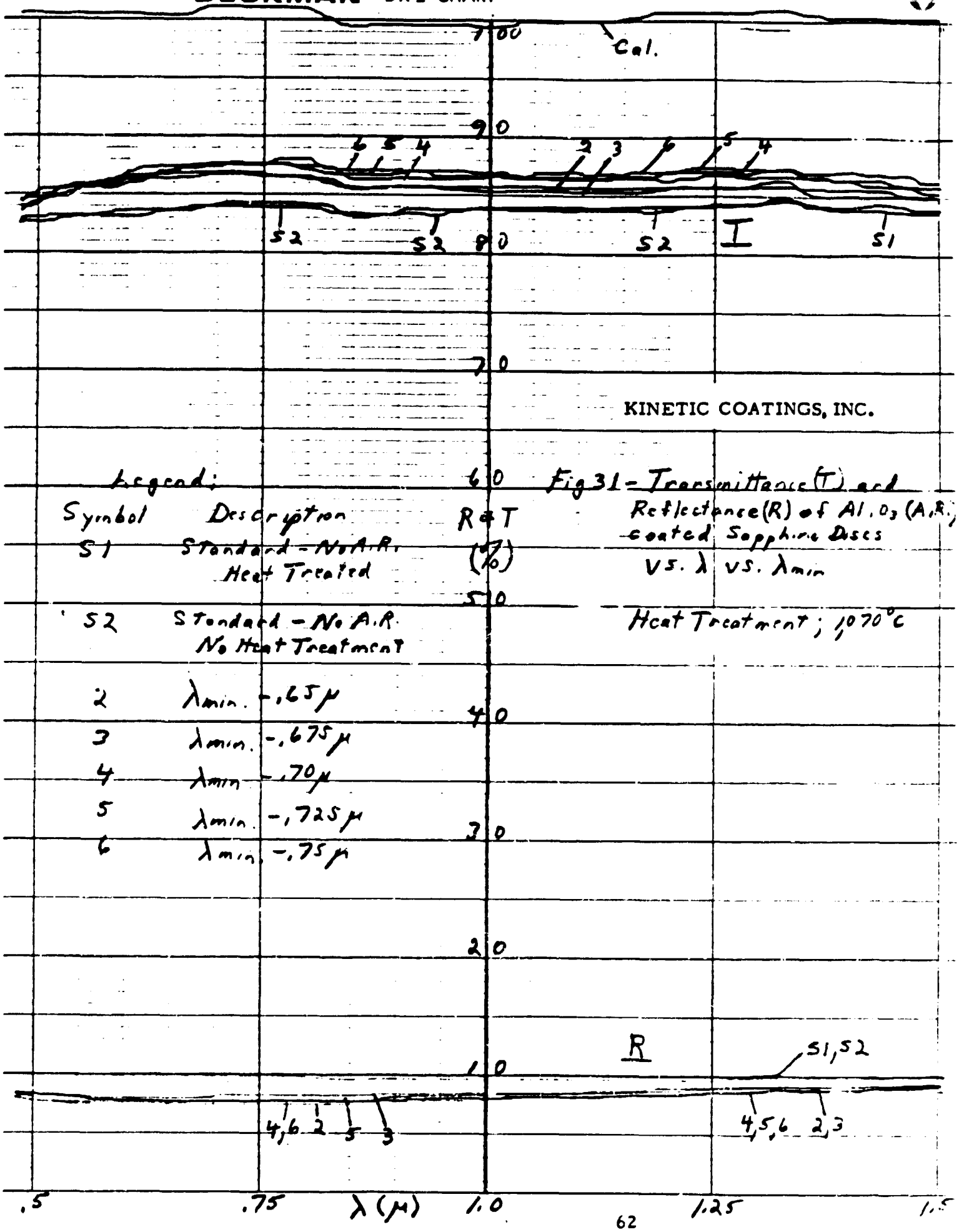

Legend:

Symbol	Description
S1	Standard - No A.R. Heat Treated
S2	Standard - No A.R. No Heat Treatment
2	$\lambda_{min.}$ - .65 μ
3	$\lambda_{min.}$ - .675 μ
4	λ_{min} - .70 μ
5	$\lambda_{min.}$ - .725 μ
6	$\lambda_{min.}$ - .75 μ

Fig 31 - Transmittance (T) and Reflectance (R) of Al_2O_3 (A.R.) coated Sapphire Discs vs. λ vs. λ_{min}

Heat Treatment; 1070°C

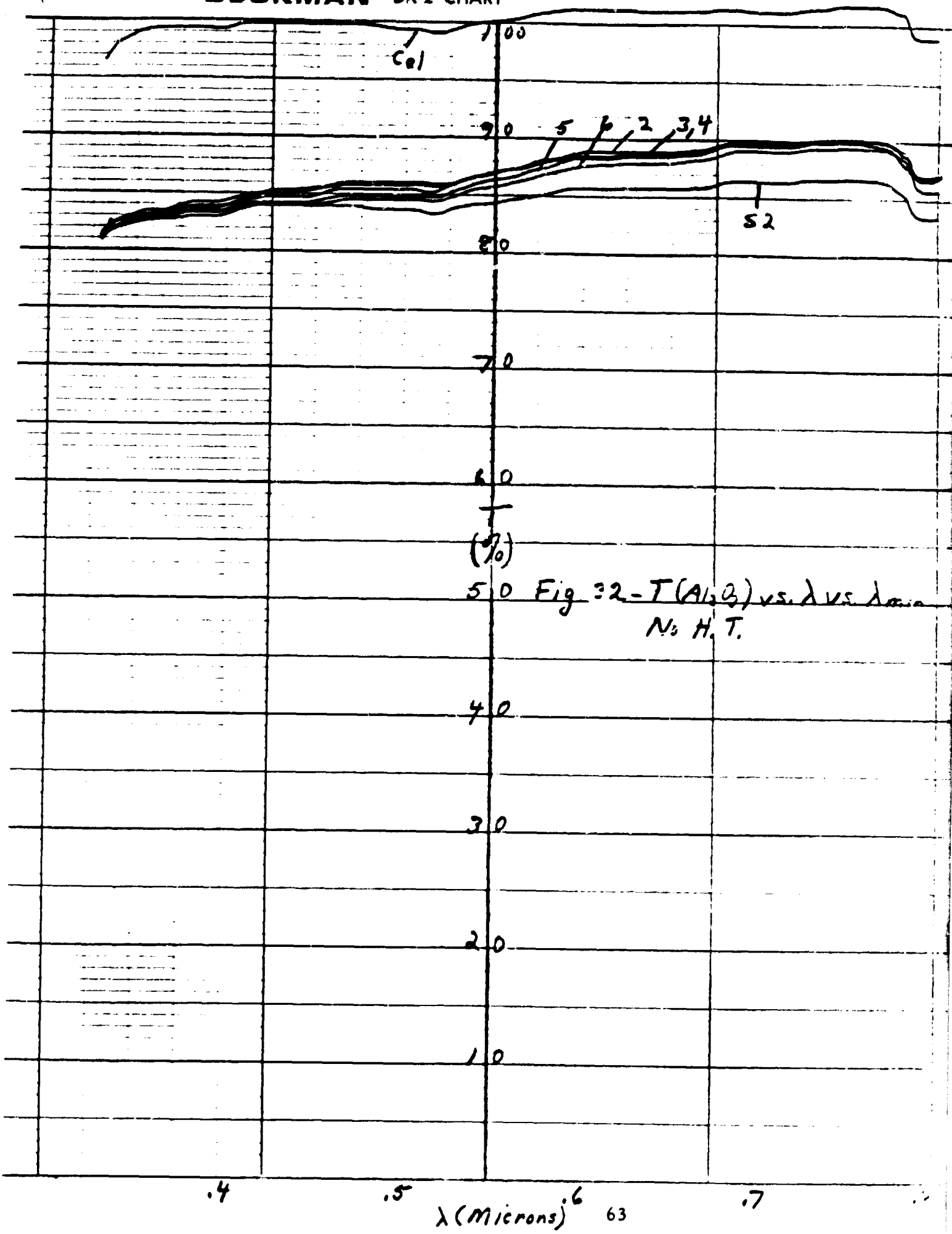

Fig 32 - T (Al_2O_3) vs. λ vs. λ_{min}
No H.T.

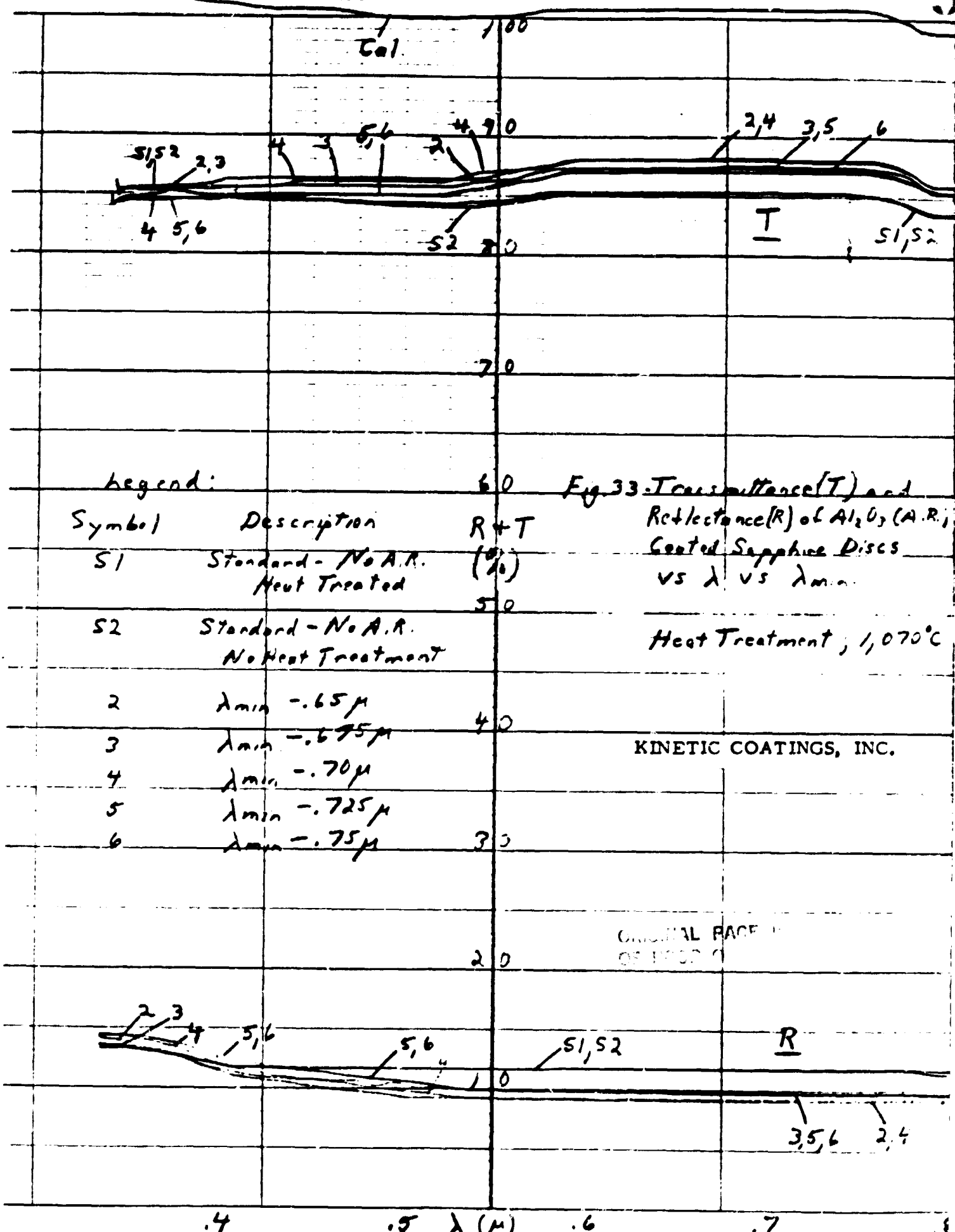

Legend:

Symbol	Description
51	Standard - No A.R. Heat Treated
52	Standard - No A.R. No Heat Treatment
2	λ_{min} -.65 μ
3	λ_{min} -.675 μ
4	λ_{min} -.70 μ
5	λ_{min} -.725 μ
6	λ_{min} -.75 μ

R + T (%)

Fig. 33. Transmittance (T) and Reflectance (R) of Al_2O_3 (A.R.) Coated Sapphire Discs vs λ vs λ_{min}

Heat Treatment, 1,070°C

KINETIC COATINGS, INC.

ORIGINAL PAGE IS OF POOR QUALITY

It may be concluded that there is negligible light absorption over the active spectrum in the thin Al_2O_3 coatings. The five coated discs were set aside and boron implanted later in the program to measure absorption losses in the AR coating due to retained boron.

From a physical point of view, all of the coatings were extremely good. The pt and set samples, in particular, are essentially carbon black in appearance after H.T. The coatings are extremely well bonded and after H.T. are essentially integral with the silicon. There were absolutely no losses due to coating delamination, inferior performance etc. in the samples used in this program.

Conclusions

The following conclusions were drawn from this phase of the program.

a) The ion beam sputtered Al_2O_3 coating is extremely effective as an AR coating when applied to texturized surfaces, with or without H. T. There is some improvement in the blue end characteristics after H. T., with 970°C being the optimum temperature of those tested. After H. T. the average reflectance loss across the spectrum is certainly less than 2% (goal 10%), with R being less than 1% over much of the active spectrum. Sawed-etched-texturized surfaces give essentially as good performance as polish-etched-texturized surfaces.

b) The ion beam sputtered Al_2O_3 coating is essentially as effective for non-texturized surfaces as more conventional materials, such as SiO, which have a better index of refraction for an AR coating between Si and air. The minimum reflectivity observed (1.6%) without H. T. agrees exactly with theory and indicates that other materials with non-optimized n values may safely be evaluated theoretically as AR coatings. After H. T. the average light loss across the active spectrum is less than 10% (goal 15%) and is considerably less than 5% from .5 to 1.1μ. Sawed-etched surfaces in general give superior performance to the polish-etched surfaces, especially at the critical blue end of the spectrum.

c) For texturized surfaces, performance of the Al_2O_3 as an AR coating after H. T. is essentially independent of Al_2O_3 thickness over the values investigated. Only minor differences are apparent without H. T. Performance after H. T. is essentially independent, for practical purposes, of the temperature used (over range 870°C-1070°C). Clearly, very rough control of Al_2O_3 thickness and temperature for thermal treatment could be used in production with negligible loss in performance.

d) For non-texturized surfaces, optimum performance after H. T. was achieved with the thinnest coating (92.3 mμ) studied. Reduced R values at the blue end could be achieved at the expense of increased R at the long λ end (cp. Figs. 23 and 26). Performance for polished surfaces improved significantly at the blue end with higher temperatures, but above 870°C decreased at the long λ end. A good compromise is reached at 970°C for a thicker cell, but for a thinner, bluer cell, 1070°C would be preferred for a polished surface. However, performance for sawed- etched surfaces was essentially the same at the blue end for 970°C and 1070°C.

e) There is no appreciable transmission loss in the deposited Al_2O_3, before or after H. T.

3.3 Back Contact

The original plan called for the use of sawed-etched Cz material only. However texturing was added to the combined coating optimization as an additional variable. Results on the texturized material were so good that it was decided to continue the program with texturized material only unless results of the other optimization programs dictated otherwise. One potential negative factor due to the texturizing was difficulty in achieving the necessary contact characteristics, but results show that a textured surface is probably as good, or better, than other surfaces for the alloying processes used.

ORIGINAL PAGE IS
OF POOR QUALITY

Optimization Procedure

The basic experiment performed involved depositing a thin layer (.1 -.3 μ) of doped Ag(3% As) overlaid with a thicker (2.0 -4.14 μ) layer of pure Nickel, on one side, or both sides, of nominal 2 ohm-cm(100) N-type Cz material blanks(5 cm x 5 cm). The depositions were carried out through a contact mask which provided a picture frame contact having a 375 μ frame around the outside edge. This frame size was chosen to conform with the frame size to be used for the implantation mask in final cells, and allowed one set of masks to be used for back contact, front contact and implantation experiments. In production a larger frame would probably be desirable for the back contact. Samples with the deposit on one side only were used for measuring sheet resistance by measuring resistance between contacts of fixed geometry(see below). Samples with deposits on both sides(same material thickness on each side) were used to measure actual contact resistance of the back contact by measuring total resistance, subtracting off bulk resistance and dividing the remainder in two.

In general the metal depositions were done by ion beam sputtering (IBS) in a small experimental system. After the optimized combination of metal layers and heat treatment was achieved, a quick experiment was done to demonstrate that electron beam evaporation(or other processes) could be used for thickening the Ni if desired. The actual metal layer thickness combinations were chosen for experimental convenience, with interpolation for other combinations possible from the values obtained experimentally. Heat treatment(H. T.) was carried out in rough vacuum(5 microns or less) with the samples inserted directly into the hot zone and held at temperature for 10 minutes. They were then removed to the end of the furnace tube(3" diffusion type), allowed to cool for 10 minutes and then vented to atmospheric pressure by backfilling with Argon. Resistance measurements were made before and after each H. T.

Originally it was planned to heat treat at successively higher temperatures of 870°C, 970°C and 1070°C to conform with the combined coating optimization. All heat treatments at 870°C were very successful. However,

when the first few samples were heat treated at 970°C, they suffered substantial electrical degradation although they were physically as good, or better, than at the lower temperatures. Consequently judicious choices were made in subsequent heat treatments on the remaining samples. After determining that a 900°C heat treatment also gave some electrical degradation, the final heat treatment experiments were reserved for successive 10 min.(or longer) heat treatments at 870°C to separate temperature and time effects. This experimental progression can be followed in the data given under Experimental Results.

The Ag and Ni combinations used were:

TABLE I

BACK CONTACT METALLIZATION

Combination #	Silver Thickness (microns)	Nickel Thickness (microns)	Total Metal Thickness (microns)
1	.1	2.28	2.38
2	.2	2.76	2.96
3	.3	2.00	2.30
4	.1	3.42	3.52
5	.2	4.14	4.34
6	.3	3.00	3.30

All thickness values are nominal and were obtained from timed runs based on calibrations made by depositing thick layers (approximately 5-10μ) on measured stainless steel shim stock and measuring the thickness increase with a dial gauge. Cumulative errors are difficult to assess exactly but are estimated at roughly ± 10%.

Resistance measurements were made on a General Radio 1608-A Impedance Bridge using the home-made apparatus shown in Figures 34 and 35. It was discovered by trial and error that soldered copper braid of the type normally used for shielding cable made excellent contact to the Ni surface.

For measuring contact resistance (Figure 34), two braid covered pads were made of a size slightly less (4.5 cm x 4.5 cm) than the samples size (5 cm x 5 cm). When covered with the braid, which was bent around the edges, they were approximately 4.8 cm x 4.8 cm. A lead weight was used to pressure the top pad against the bottom pad. Lead resistance was obtained by placing the pads in direct contact and the contact resistance measurements were made by simply inserting the samples between the pads. Since the pads were smaller than the contacts, the measured values were consistently on the safe "high" side. Since there were two contacts on the sample, the actual contact resistance was half of the difference between the measured resistance and the resistance of the bulk Si.

The sheet resistance was measured with a pair of braid covered electrodes (Figure 35), 5.7 cm long and separated by approximately 4 cm. The two electrodes were allowed to physically float with respect to each other and a lead weight was used to apply pressure. Lead resistance was obtained by shorting the two electrodes on a Ni slab.

The measurements for both the sheet resistivity and contact resistance measurements were extremely reproducible with errors estimated at less than ±.4% in most cases and never more than ± 1%. The major errors in the resulting values come from the electrode geometry which was non precise due to the inherent nature of the braid contacts used. The maximum possible error due to this source is estimated as ± 10%.

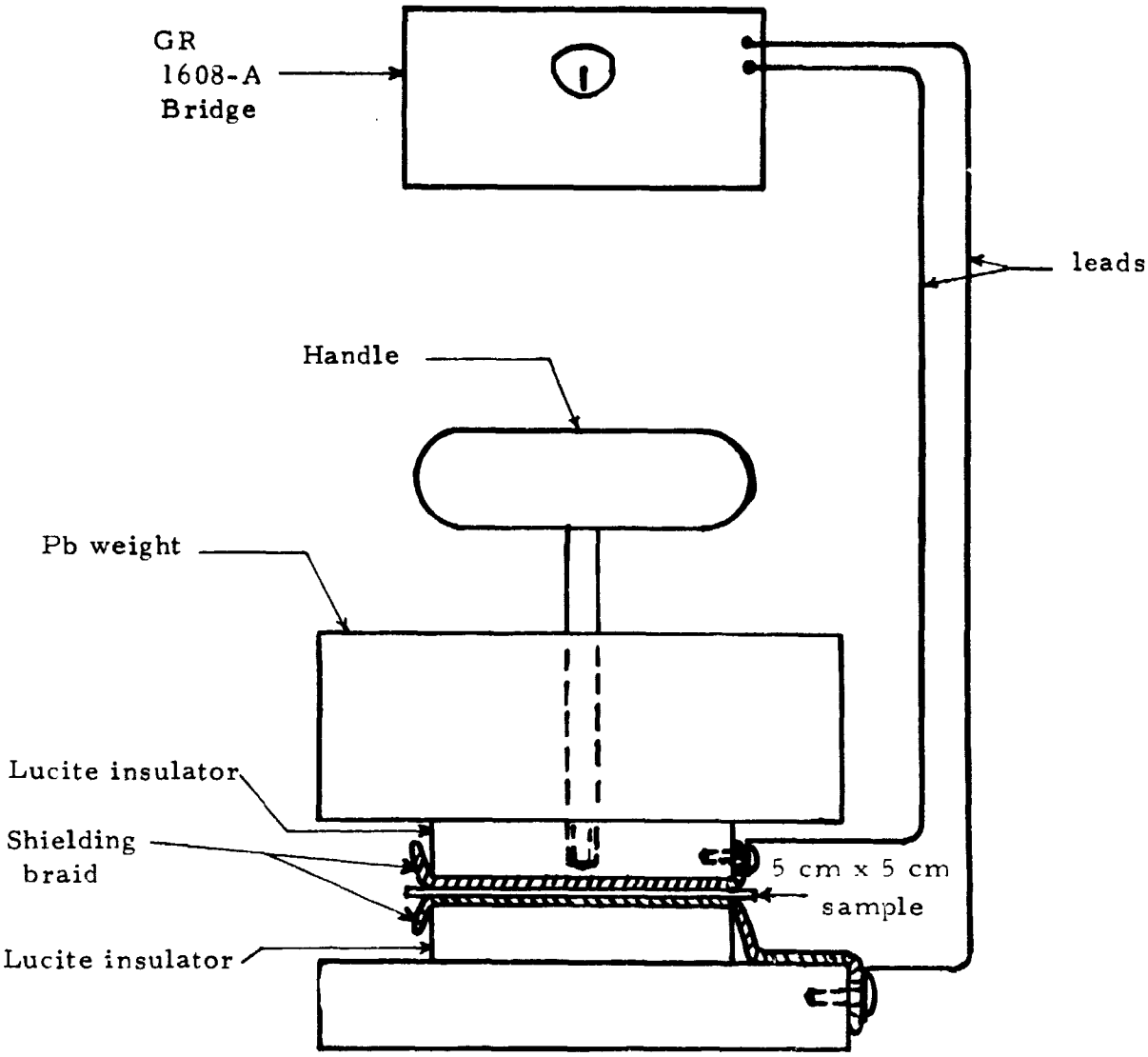

Figure 34. RESISTANCE TEST APPARATUS
(Back Contact Resistance)

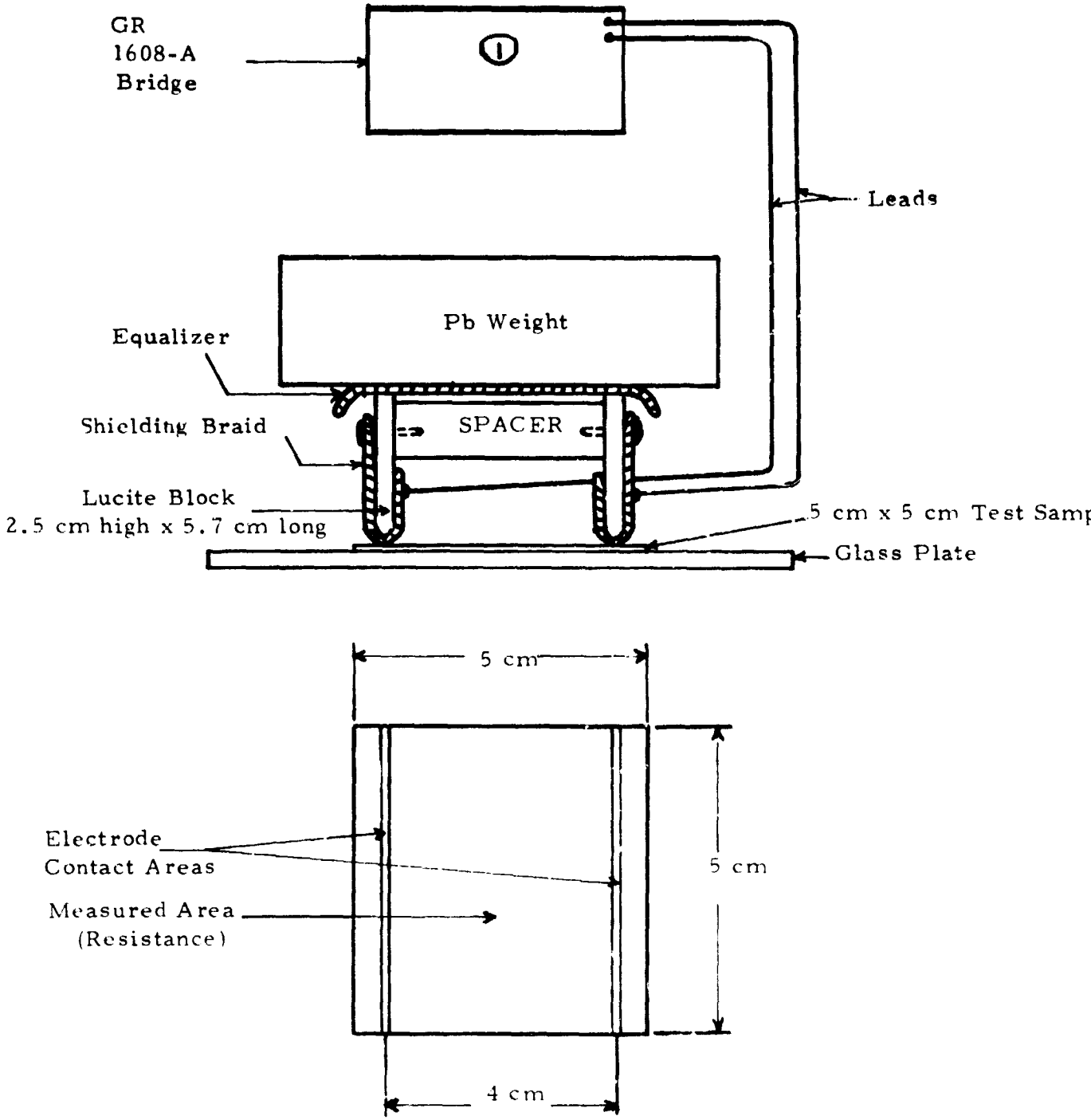

Figure 35.
RESISTANCE TEST APPARATUS
(Back Contact Sheet Resistivity)

Experimental Results

The experimental results can most easily be evaluated from Tables 2 and 3 which give the contact resistance and sheet resistivity results, respectively. The heat treatments are successive stages on the samples as shown, and, except for the exceptions noted, were for 10 minutes at each temperature. A nominal value of 3.1 mΩ was used for the resistance (front to back) of the bulk silicon (5 cm x 5 cm x 350 mμ thick) based on the average resistivity (2.1 Ω-cm: 1.7 to 2.5 Ω-cm) given by the silicon supplier. (This general value was checked on one slice using the KCI sheet resistance two electrode system described previously-the slice measured 2.02 Ω-cm). Effective resistivity values in Table 3 were determined from the sheet resistivity values by multiplying by the total metal thickness.

The most obvious point from Table 2 is that the contact resistance after one 870°C heat treatment for 10 minutes is consistently very low, of the order of 1 mΩ or less. There is a measurable increase in value after 900°C (samples J-20-21 and J-19-21) and a more significant increase after 970°C (samples J-20-11 and J-19-11). However, the increase with successive 870°C heat treatments (sample J-19-31) is slight even when the time is extended to greater than 1 hour total. The increase in value, in fact, seems to level off after the second or third 10 minute iteration. The conclusion is that, relative to contact resistance, the back contact can be heat treated at 870°C for a reasonable period of time without appreciable degradation. Higher temperatures, however, lead to relatively rapid contact degradation. There does not appear to be an "appreciable" difference in the contact resistance for the different metal combinations after 870°C heat treatment, with all of them being very acceptable.

TABLE 2

BACK CONTACT RESISTANCE

Sample #	Metal Combination #	Heat Treatment (°C)	Contact Resistance (mΩ)
J-20-11	1 (Table 1)	no H. T.	9.0
		870	.65
		970	9.1
J-20-21	2	no H. T.	8.7
		870	.6
		900	2.6
J-20-31	3	no H. T.	7.4
		870	.55
		870	1.1
J-19-11	4	no H. T.	10.5
		870	1.05
		970	39.2
J-19-21	5	no H. T.	8.8
		870	.95
		900	3.1
J-19-31	6	no H. T.	6.7
		870	1.05
		870	1.3
		870	1.4
		870	1.45
		870(30 mins.)	1.45

TABLE 3

BACK CONTACT SHEET RESISTIVITY

Sample #	Metal Combination # (Table 1)	Heat Treatment (°C)	Sheet Resistivity (mΩ/□)	Effective Metal Resistivity (x 10^{-6} Ω-cm)
J-20-12	1	no H. T.	76. 1	18. 1
		870	46. 2	11. 0
		970	1335.	318.
J-20-22	2	no H. T.	51. 9	15. 4
		870	36. 3	10. 7
		900	72. 8	21. 5
J-20-32	3	no H. T.	63. 6	14. 6
		870	38. 1	8. 8
J-19-12	4	no H. T.	51. 7	18. 2
		870	32. 7	11. 5
		970	373.	131.
J-19-22	5	no H. T.	32. 3	14. 0
		870	21. 2	9. 2
		900	41. 5	18. 0
J-19-32	6	no H. T.	38. 5	12. 7
		870	25. 4	8. 4
		870	38. 1	12. 6
		870	38. 1	12. 6
		870(30 mins.)	38. 1	12. 6

It is equally obvious from Table 3 that the sheet resistivity of the back contact is lowest after one 870°C heat treatment. Metal combinations 4, 5, and 6 all are better than the goal of 35 mΩ/□ with 2 and 3 only marginally missing and 1 being 46 mΩ/□, which might also be acceptable in a real cell case. Since combinations 2(.2 μ Ag, 2.74 μ Ni) and 3(.3 μ Ag, 2.0 μ Ni) give almost the same value, it appears that the thicker layer of the much lower resistivity Ag is quite effective in reducing the overall sheet resistivity. The effective metal resistivities for the alloyed contact material after 10 minutes at 870°C compare favorably in all cases with that of bulk Ni(7×10^{-6} Ω-cm), indicating that little improvement in deposition technique or heat treatment could be expected. (Note: shorter times could not be controlled experimentally due to furnace equilibrium conditions under load).

Again, the contact shows degradation at higher temperatures, with significant change after 900°C(samples J-20-22 and J-19-22) and catastrophic change after 970°C(samples J-20-12 and J-19-12). Additional heat treatment at 870°C(sample J-19-32) gave a significant but modest change after the second 10 minutes, but no additional change thereafter.

The overall conclusion from this data was that heat treatment for the back contact should be restricted to 870°C maximum with extended time at this temperature being acceptable. The optimum heat treatment for the combined coating(see MTR #1) was approximately 970°C. However, the loss in restricting the temperature to 870°C was expected to be relatively minor. It was known (from preprogram studies) that 870°C was acceptable for the front contact (Al) and was probably acceptable for annealing implanted boron damage.

Physical bonding of the contacts to the silicon was extremely good in all cases, with the metal and silicon being essentially integral. In order to test the capability of other deposition processes relative to the back contact configuration, combination 6(.3μ Ag, 3.0 μ Ni) was approximated by first ion beam sputtering .3 μ of Ag, followed by .1 μ of Ni. An additional 2 - 3 μ of Ni was then added using electron beam evaporation. Exact calibration of the amount of evaporated Ni could not be obtained since that much Ni would not stay on the shim stock used for thickness calibration. It did, however, bond very well to the ion beam sputtered Ni. Evaporated material was used since, of all the deposition methods, it has one of the fastest rates but least tenacious deposits. The assumption was that if it worked, any method would work as long as the initial deposit was properly made. (It should be noted here that application of the Ag layer using evaporation techniques was attempted in a preprogram study and was completly unsuccessful in forming the large area alloyed junction.)

Measured values for this sample were 1.0 mΩ for the contact resistance and 39.6 mΩ/□ for the sheet resistivity, both after 870°C for 10 minutes. The sheet resistivity compares with 25.4 mΩ/□ for sample J-19-32 after the first 10 minutes at 870°C and 38.1 after 20 minutes. Within the potential spread in evaporated Ni thickness, the value for the evaporated case is considered acceptable. Bonding for the evaporated case was also excellent.

In order to avoid the need for precise process control during remaining optimization studies, combination 6 was used for the back contact since this consistently gave acceptable values. A batch of 45 test cell blanks with this back contact was made up for use in the remaining optimization studies.

Conclusions

The following conclusions were drawn from this phase of the program:

a) The doped Ag-Ni back contact metallization heat treated at 870°C for 10 minutes provides a very effective back contact for a P on N cell. The program goal of 35 mΩ/□ sheet resistivity for the metallization is easily achieved. For all practical purposes, the contact resistance is essentially insignificant.

b) If ion beam sputtering methods, or equivalent, are used for the initial metal layers, any suitable method can be used to provide the necessary metal thickness.

c) Heat treatment for the overall cell should be restricted to 870°C maximum temperature. Periods longer than 10 minutes may be used if necessary.

d) Texturized surfaces are very acceptable for the Ag-Ni back contact in terms of physical bonding and electrical characteristics.

3.4 Front Contacts

Optimization Procedure

The basic experiments were designed to determine the following parameters:

1.) Contact resistance of the alloyed Al to P-type material.

2.) Sheet resistance of alloyed layers of different thicknesses.

3.) Contactability of alloyed Al contacts overlaid with Al_2O_3 (combined coating).

4.) Resistance of the front contact with the two contact pads (see Fig. 3) interconnected externally.

5.) Basic diode characteristics of the high temperature fired Al.

To obtain the first 4 parameters, Al depositions were made on nominal 2 ohm-cm (100) P-type slices through a picture frame contact mask having a 375 μ frame and/or a front contact mask conforming to Fig. 3. To obtain the contact resistance, a picture frame deposition (9 μ) was made on both sides of a slice. Measurements were made using the resistance test apparatus shown in Figure 34. Sheet resistances were measured on single side picture frame depositions, using the apparatus shown in Fig. 35. To determine the contactability of AR coated fired Al, a strip of Al_2O_3 was deposited over a 5 mm wide strip along one side of the Al deposited for the sheet resistance measurements. Sheet resistance after firing could therefore be measured with both legs on Al, or one on Al and the other on Al_2O_3. It was quickly determined that the values, after firing, were the same and all subsequent experiments were performed with the deposited Al completely overcoated with Al_2O_3 of the optimized combined coating thickness.

Resistance of the front contact was measured by making a picture frame deposit on one side and a front contact deposit on the other. The resistance was measured between a large area braid covered pad in contact with the picture frame side and two interconnected (zero resistance braid) braid covered pads simultaneously in contact with the front contact pads using light manual pressure. The measured values could easily be reproduced with an accuracy of better than ± 1%. Considerable difficulty was encountered, however, in achieving a suitable front contact deposit. Due to the fine line geometry(2 mils) and extended finger ~ 2.4 cm long), there was a considerable amount of undercutting (up to full bridging between fingers) using the original mask. The latter was bimetallic and consisted of a 1 mil phosphor bronze sheet used to obtain the fine lines, overlaid with 10 mils of Ni for strength. A severe undercutting problem existed which was primarily due to the extended source of material and the difficulty of keeping all fingers etc. in contact with the slice at the same time. A partial solution was achieved consisting of a second shorter, thicker(30 mils) comb-like mask which was placed over the first mask to

keep most of the area in contact by forced contact at the base and middle of each finger. Using this configuration the major part of the deposited fingers was still greater than 2 mils wide and ran to 3-4 mils in some cases. There was also some faint general undercutting in some cases, which was subsequently found (using polished slices) to cover 20-30% of the front surface. This problem could not be overcome within program funding and all cells etc. were made with this system, accepting the associated current loss.

Basic diode characteristics for the high temperature fired Al were evaluated by making very large area diodes (.9 x 1.6 cm and 5 cm x 5 cm active areas) consisting of N-type material having full area deposits of Al(9μ thick) on one side and the optimized back contact on the other. For the larger area diode the picture frame mask was used for depositions on both sides, while the smaller area diode was simply a dice out of a larger diode. The smaller area diode had approximately twice the area of the front contact and was used to give a rough measurement of the limiting effect of the alloyed junction on the overall cell characteristic. The characteristic of the front contact alloyed junction, per se, cannot readily be determined without a lot of detailed experimental work, due to the extremely long junction intercept with the surface coupled with the unfixed surface state in the non-implanted surface, even with the combined coating applied. The latter, in fact, in the absence of implantation probably confuses the issue. It was therefore decided that the measurements on large area diodes (having much shorter exposed junction lengths) were better indicators, within available experimental time, of the

alloyed junction characteristics.

In general the Al was deposited by ion beam sputterirg(IBS) in a small experimental system. Preprogram investigations had clearly demonstrated that electron beam evapoation could also be used for thickening the Al if a starting layer(~. 1 μ or more) of Al was first deposited by IBS. The actual Al thicknesses were chosen for experimental convenience with interpolations for other values possible from the values obtained experimentally.

Heat treatment(H. T.) was carried out in rough vacuum(5 microns or less) with the samples inserted directly into the hot zone and held at temperature for 10 minutes. They were then removed to the end of the furnace tube (3" diffusion type), allowed to cool for 10 minutes and then vented to atmospheric pressure by backfilling with Argon. Temperatures of 870°C and /or 970°C were used. It was originally planned to go to 1, 070°C for front contact resistance measurements, but all samples became broken in the multiple testing before this final step could be made. However, values at 970°C were essentially the same as those at 870°C and little change was expected at 1, 070°C. Since the process is limited, in any event, to less than 900°C by the back contact, there was little point in making additional samples and the experiment was terminated.

As in the back contact optimization, resistance measurements were made with a General Radio 1608-A Impedance Bridge using similar techniques. The possible errors in the measured values are small, of the order of ± 1% or less. Sheet resistance measurements are subject to possible geometry errors believed to be less than ± 10%. Front contact resistance measurements must be viewed in light of the apparent finger widening which causes discrepancies relative to calculated values. This is discussed under Experimental Results as appropriate.

Experimental Results

The resistance measured between two large area(5 cm x 5 cm) contacts(picture frame) 9μ thick and heat treated at 870°C was 2. 4 mΩ. In order to determine the contribution due to bulk resistance of the slice(350 mμ

thick; nominal 2Ω-cm) the exact value of ρ was determined by measuring the resistance between contact bars separated by 1 cm on 1.1 cm wide strips. The resulting value of 1.69 Ω-cm (average value-2 measurements) led to a value of 2.4 mΩ for the bulk resistance which, substracted from the measured value of 2.4 mΩ, left zero for the contact resistance. The exact result of zero is fortuitous but it is obvious that the contact resistance of the fired Al to P-type material is negligible for practical purposes. In particular, for measuring the front contact resistance (see below) it was therefore assumed to be zero. A notable point about this measurement is that it was made after it was determined during the sheet resistance measurements (see below) that the fired Al-Al_2O_3 (combined coating) could be contacted as easily as the fired Al alone. For confirmation, both contacts in the present case were Al_2O_3 coated before firing. It should be noted that the material was texturized so that the Al_2O_3 coating over the pyramid points might be expected to break off readily under abrasion by the braid on the test pads. This would not be expected, however, to lead to a value as low as that observed.

Results for the sheet resistance measurements are given in Table 4.

Measurements were made on the 8.6 μ sample using Al-Al contacts both at room temperature and at 870°C, with Al-Al_2O_3 measurements also made after the first and second 870°C heat treatments. The values of sheet resistance increased significantly after heat treatment, presumably due to conversion of some of the metal to a lower conductivity alloy. Values obtained with one measuring leg of the apparatus on the Al_2O_3 covered area were quite similar to values obtained with both legs on the non-covered Al. There was an additional smaller increase in sheet resistivity after a second 870°C heat treatment. Although significant, it was not of a magnitude to preclude longer term heat treatments. From these measurements it was concluded that the Al_2O_3, after firing, did not affect the contactability of the Al contact. All subsequent experiments, including the large area contact experiment described previously, were conducted on Al_2O_3 covered Al contacts.

The thicker (16.8 μ and 25.4 μ) Al layers yielded lower values of

ORIGINAL PAGE IS
OF POOR QUALITY

TABLE 4

FRONT CONTACT SHEET RESISTIVITY

Al Thickness (μ)	Measuring Condition	Heat Treatment	Sheet Resistivity (mΩ/□)	Effective Metal Resistivity (x 10^{-6} Ω-cm)
8.6	Al-Al	No H. T.	9.1	7.8
	Al-Al	870°C	16.9	14.5
	Al-Al_2O_3	870°C	16.6	14.3
	Al-Al	2nd 870°C	17.8	15.3
	Al-Al_2O_3	2nd 870°C	17.8	15.3
16.8	Al-Al	no H. T.	5.6	9.4
	Al_2O_3-Al_2O_3	870°C	9.5	16.0
25.4	Al-Al	no H. T.	4.6	11.7
	Al_2O_3-Al_2O_3	870°C	7.5	19.1

sheet resistivity as expected, but somewhat higher values of effective metal resistivity. The latter was not as anticipated since one might expect a larger proportion of higher conductivity non-alloyed metal for the thicker Al layers. The effective metal resistivities before firing were in the range of 2.8-4.2 times the resistivity of pure Al. This is believed to be primarily due to non-allowance in the calculations for the extra distance between the measuring contact bars due to the pyramid structures rather than a straight path (bulk values have been measured on flat surfaces). There may also be some error due to thickness calibration which was very rough for this experiment.

From the effective metal resistivity values, it was anticipated that front contact thicknesses in the 10-20 μ range would be needed to achieve the desired goal of 46 m Ω for the front contact resistance. For experimental convenience, and to give a suitable spread in values, nominal thicknesses of 9, 17 and 23 μ were chosen for use with the front contact finger masks. A back contact of 9μ Al was first applied to the P-type test cells using the picture frame masks. Front contacts of the nominal thickness values were then applied to the other side of the samples which were subsequently coated with the Al_2O_3 combined coating. Front to back resistance (front tabs interconnected externally) was then measured before and after heat treatment at 870°C and 970°C. For comparison the resistance was also measured between the back and only one contact tab. Since production cells would certainly be much bigger and of a different contact geometry, the intent of this dual measurement was to obtain some insight into the losses associated with single point contacts at the different contact thicknesses.

As discussed previously, considerable experimental effort was expended on the problem of preventing undercutting of the mechanical fine-line masks. Table 5 gives the results obtained with the best method developed. The values shown have the 2.4 mΩ bulk contact resistance subtracted from the measured values. From the large area experiment it was known that the Al back contact contributed zero to the measured values.

TABLE 5

FRONT CONTACT RESISTANCE

Front Contact Al Thickness (u)	Heat Treatment	Resistance One Contact Tab (mΩ)	Resistance Two Contact Tabs (m Ω)
9	no H.T.	1.67 (Ω)	1.56 (Ω)
	870°C	63.5	30.1
	970°C	65.4	31.0
17	no H.T.	1.72 (Ω)	1.64 (Ω)
	870°C	54.2	25.2
	970°C	55.9	26.1
23	no H.T.	1.64 (Ω)	1.57 (Ω)
	870°C	48.1	23.0
	970°C	50.0	23.7

The large values of resistance for the unfired cases are due to the presence of Al_2O_3 over the front contact, with contact being to broken points abraided by the braid on the measuring apparatus. After firing, this problem no longer existed and values approximating those expected were obtained. The value of 30 m Ω (goal 46 m Ω) obtained for the 9μ case is somewhat less than expected and is probably due to widening of the fingers to 3 or more mils vs. the design 2 mils. Values at the higher thickness values are surprisingly close to the 9μ value and indicate only a small advantage in going to the much thicker layers for these fully alloyed contacts. On the assumption that the finger widening (to 3 from 2 mils) will continue, the 9 μ thickness was used in initial cell fabrication.

The resistance values with only one tab contacted were roughly twice as high. Obviously if there were only a single front contact point on these cells there would be a significant efficiency loss vs. two or more contact points. This loss could be compensated by increasing the metal thickness but the relative values obtained at the larger thicknesses indicate that it would be difficult to retrieve all of the loss in this manner. Multiple pads with external interconnects is the preferred route and gives the added benefit of redundancy.

Characteristics for a 1.5 cm^2 (0.9 x 1.6 cm) and a 25 cm^2 (5 cm x 5 cm) diode are given in Fig. 36. These diodes were fabricated in the standard 2Ω-cm texturized material and had Ag-Ni backs and the Al front. Firing was done at 870°C using the standard procedure. The 1.5 cm^2 diode, having an area roughly 1.5 - 2 times the front contact finger area, has a very sharp junction characteristic and high shunt resistance. The characteristic for the larger diode, although apparently softer, is comparable since for direct comparison it should be shown on a current scale of roughly 3 A/div. (to account for relative area). From these characteristics it was concluded that the large area alloyed junction characteristic does not present a fundamental

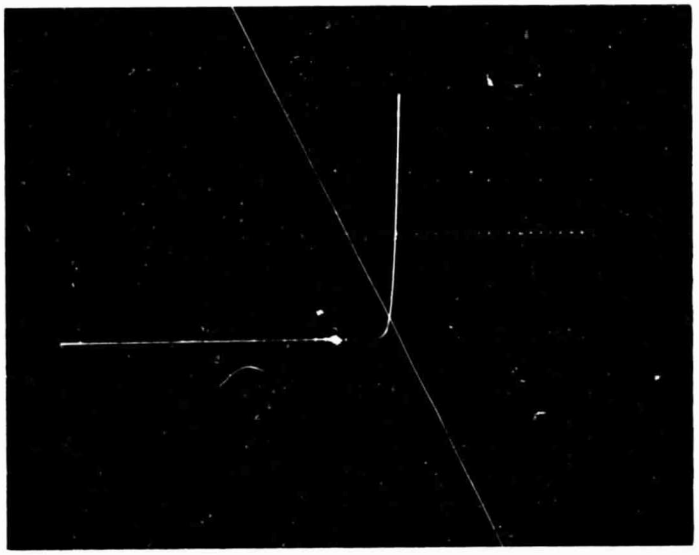

200 mA/div. -vertical
0. 5 V/div. -horizontal

36 (a) 0. 9 x 1. 6 cm Diode

KINETIC COATINGS, INC.

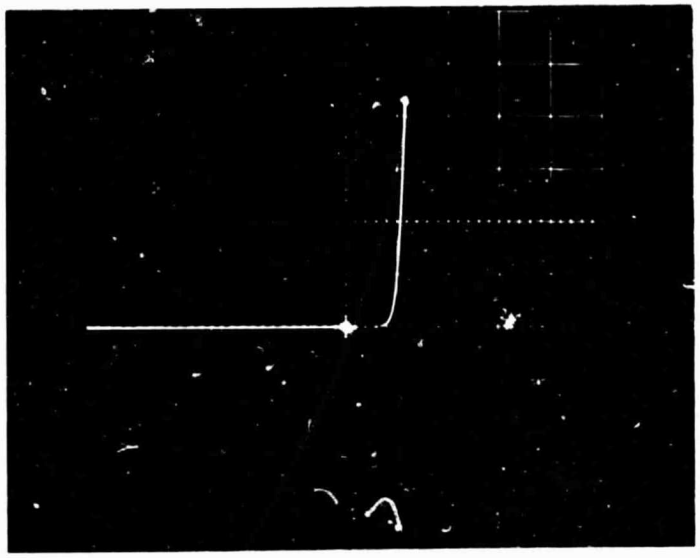

200 mA/div. -vertical
0. 5 V/div. -horizontal

36 (b) 5 cm x 5 cm Diode

FIGURE 36. LARGE AREA ALLOYED DIODE CHARACTERISTICS

block to good cell efficiencies using the program fabrication method.

It was also obvious from these results that the "large area" Al alloy needed for the back surface field on an N on P cell could be obtained by going to the high temperature (versus normal 660°C) alloy method. This procedure was incorporated in many N on P programs.

Conclusions

The following conclusions were drawn from this phase of the program:

a) The front contact optimization goal of 46 mΩ can be met with 9 μ of Al and 2 mil lines (30 mΩ measured with 3 mil lines).

b) Contact can be made to fired Al_2O_3 coated (AR thickness) Al contact as readily as to fired Al contacts.

c) Interface contact resistance of the high temperature (870°C) fired Al to 2 Ω-cm P-type material is essentially zero.

d) Junction characteristics of large area, high temperature (870°C) fired, Al alloyed diodes in a 2 Ω-cm N-type material are adequate for fabrication of good to excellent solar cells of the type being investigated in this program.

3.5 Implantation and Heat Treatment

Optimization Procedures

The basic experiments were designed to determine the following parameters:

1.) Sheet resistance of the implanted layer vs. doping level and annealing procedure (ion energy was a secondary parameter - see experimental results).

2.) Relative contact resistance to Al_2O_3 covered and non-covered Al front contacts after anneal.

3.) Optical absorption of the implanted Al_2O_3 combined coating over the critical operating region(.35 - 1.1 μm).

To obtain the first three parameters, the basic test wafer shown in Fig. 37 was used. It consisted of two pairs of parallel ion beam sputtered(IBS) Al contact pads 3 mm x 12 mm separated by 10 mm. After the contact bars were applied, 2 mm x 10 mm areas were masked(tape) on one set of bars and the entire front surface was then coated with approximately .1 μ (middle of acceptable thickness) of Al_2O_3. The areas between the bars were then implanted, using masks at "incident" implanted doses levels of 7.5×10^{14}, 10^{15}, 2.5×10^{15}, 5×10^{15}, 10^{16} and 2×10^{16} ions/cm^2. Since some of the incident ions(nominally 1/2) are stopped in the combined coating, the actual doping level achieved in the silicon corresponds to implanted levels, with no combined coating, of approximately 1/2 these values. An energy of 65 keV was sufficient to place the peak of the implanted distribution roughly at the Al_2O_3-Si interface and a value of 75 keV was chosen to ensure that the peak was at the interface, or in the Si, rather than in the Al_2O_3.

All implanations on these test wafers were performed by Spire, with those at levels up to 5×10^{15} ions/cm^2 being carried out on their own equipment. Unfortunately, for the higher dose levels (10^{16} and 2×10^{16} ions/cm^2) the time required per implant on this facility was prohibitive. Permission was therefore requested from JPL, and granted, for Spire to use the high current JPL owned machine(Extrion manufacture) housed at Spire for the higher dose implants.

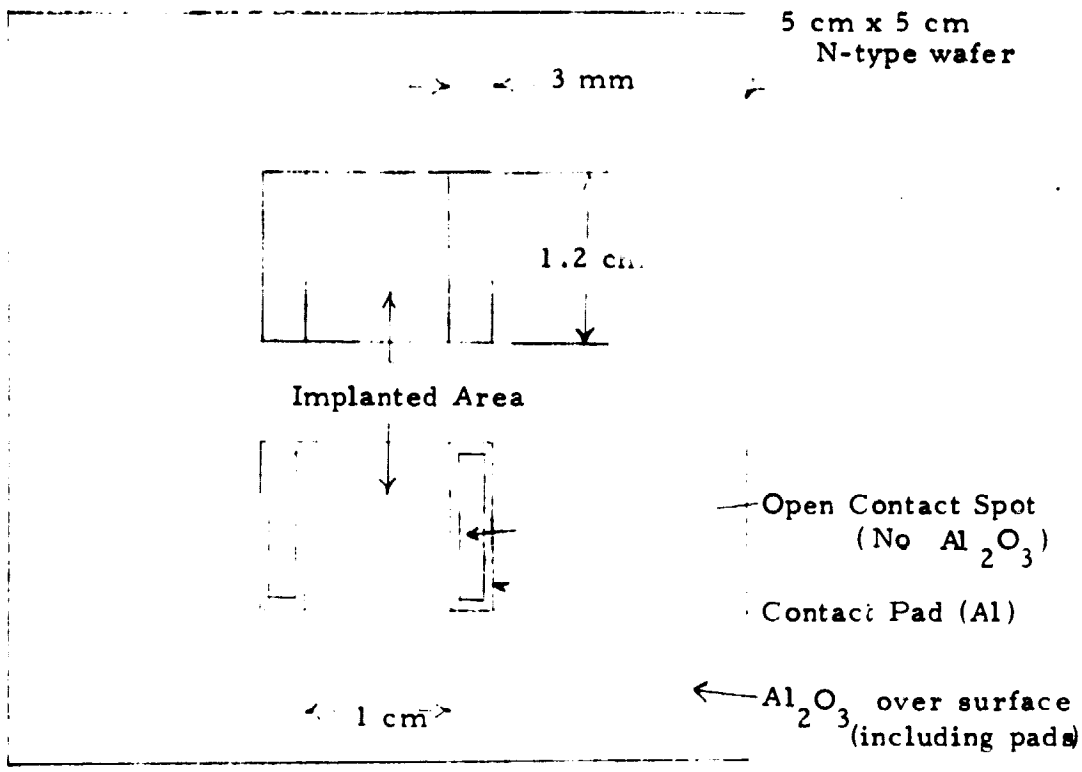

Figure 37 - Implantation Optimization Test Wafer

OF POOR

The upper energy limit on this machine for boron is 50 keV and this was the value used with the projected result of a smaller percentage of the implanted boron in the silicon. Actual data (see Experimental Results) showed that this change made it difficult to draw definitive conclusions on the achievable sheet resistance.

After implantation, the samples were heat treated in vacuum at 870°C using the standard 10 minute cycle. Some samples were subjected to additional 10 mins. or longer anneals at the same temperature to determine the effect of additional time at temperature.

After anneal, the actual resistance between the contact bars was measured using two 2 mm x 10 mm pads covered with shielding braid and separated by 13 mm(center to center) so they effectively bridged the implanted area(contact to contact) without contacting it. Since both the implanted area and the alloyed Al contacts formed P on N junctions with the N-type substrate, after anneal there was no effect on the measured resistance due to conduction in the substrate between the contact pads. A multiplication factor of 1.2(length of contact bars) was used to convert the measured resistance to sheet resistance. It was quickly determined that there was no difference in values between the measurements made using Al_2O_3 covered contacts and those using non-covered contacts. This was expected since previous results in the front contact optimization showed no measureable differences to exist, even when the values being measured were in the milliohm range. In the present case the values measured were in the 100Ω and up range.

As in the front and back contact optimizations, resistance measurements were made with a General Radio 1608-A Impedance Bridge. Since the contact resistance of the probes was very small, the possible errors in the measured values, per se, were small, of the order of ±1% or less. Errors due to geometry variations were less than ±2% while those due to implant dose level were approximately ± 10%. Some additional error is also present in the relative values at different doping levels because of the three energies used, making it difficult to project achievable sheet resistance values.

Light absorption due to the implanted boron in the Al_2O_3 combined

coating layer was measured by implanting 1 inch diameter Al_2O_3 discs(.040" thick), coated with the .1 μ thick IBS deposited Al_2O_3 layer, at levels comparable to those used in the implantation study and under idential conditions. The discs used were the same ones as those used to measure light absorption in the Al_2O_3 layer, per se, in the combined coating optimization study (Section 3.2). In the latter case, a net gain in transmitted light was observed due to a small decrease in reflectivity. In the present case it was necessary to use the same disc for the 7.5×10^{14} and 2×10^{16} ions/cm^2 implants with optical measurements being made after the lower level implant, before subsequent implant at the higher level. Because of the factor of 26 difference in the two doping levels, the effect of the lower implant on the higher level result is negligible. Although results were taken before and after heat treatment(standard 10 min. 870°C anneal), for simplicity only the heat treated results are presented.

Experimental Results

1.) Implanted Layer Sheet Resistance

Table 6 gives the results for ρs as a function of surface preparation, implant dose and anneal conditions, while Figure 38 gives the same information under standard anneal conditions only. The values plotted in the latter(and presented in brackets in Table 6) for texturized surfaces at incident implant levels of 10^{16} and 2×10^{16} ions/cm^2 are the averages for the JPL deliverable samples rather than those from the optimization experiment. These averages were for 9 or 10 samples whereas the optimization experiment involved only one sample. From the graphical representation it appeared that the initial 10^{16} ions/cm^2 sample may have inadvertently been implanted at 2×10^{16} ions/cm^2. The values from the JPL samples were relatively consistent(± 10%) and gave a smooth curve.

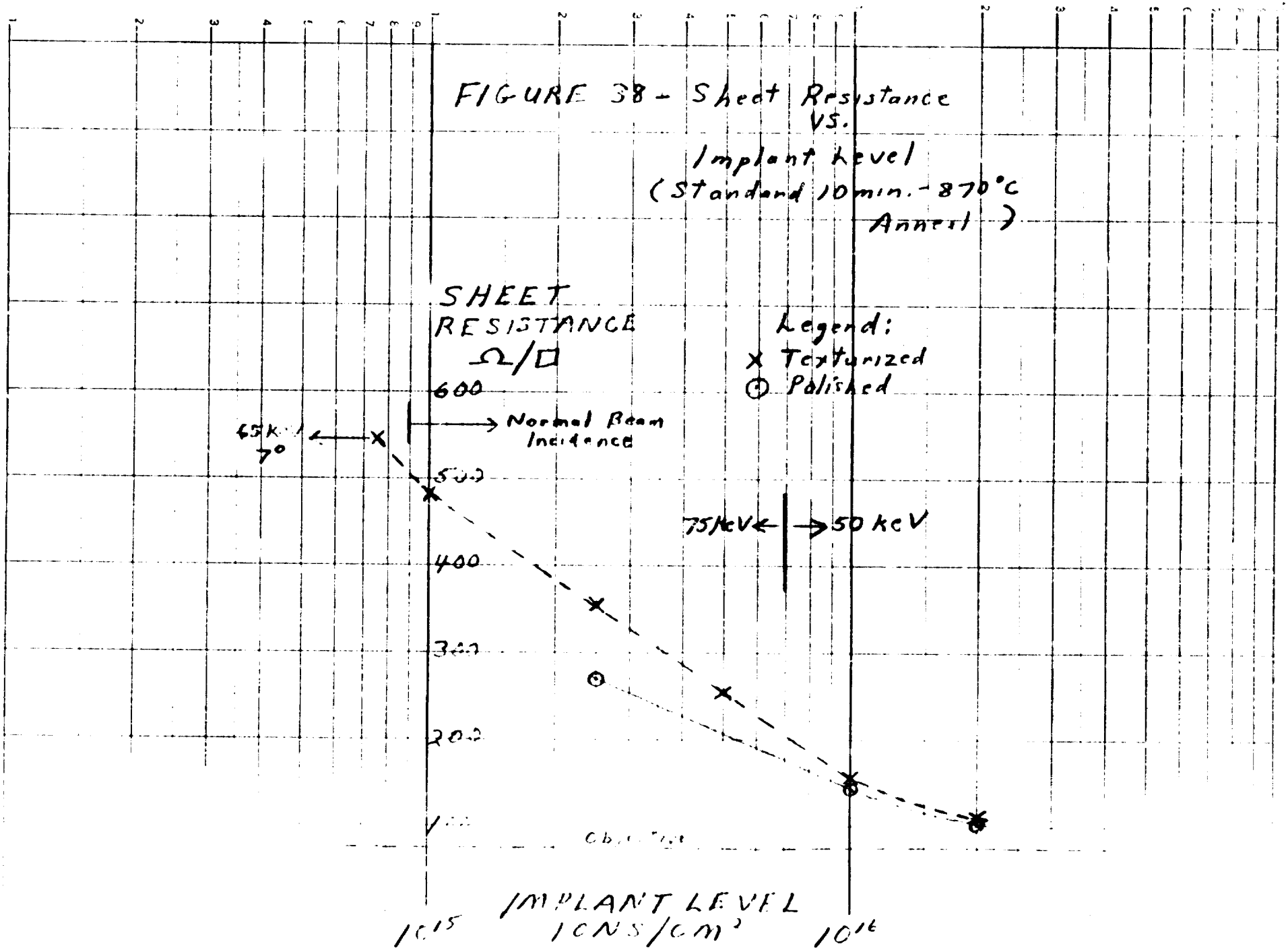

FIGURE 38 - Sheet Resistance VS. Implant Level (Standard 10 min. - 870°C Anneal)

TABLE 6

SHEET RESISTANCE

IMPLANTED LAYERS

Sample No.	Surface Condition	Incident Implant Level (ions/cm^2) (Energy-keV)	Anneal Condition (see legend below)	ρ Al_2O_3 Covered ($\Omega/\square$)	ρ Bare Al Contacts ($\Omega/\square$)
J-31-2	Texturized(T)	7.5×10^{14} (65)	S	546	545
J-31-3	T	10^{15} (75)	S	484	484
J-31-6	T	2.5×10^{15} (75)	S E	354 227	359 227
J-33-4	Polished(P)	2.5×10^{15} (75)	S EE	269 130	265 131
J-31-5	T	5×10^{15} (75)	S EE	255 138	255 137
J-31-1	T	10^{16} (50)	S E	124(158)* 101	129 104
946-1	P	10^{16} (50)	S EE	145 119	All contacts Al_2O_3 covered
J-33-6	T	2×10^{16} (50)	S EE	116(112)* 105	117 106
J-45-6	P	2×10^{16} (50)	S EE	102 88	Broken

Legend:

S - Standard 10 min. Anneal Cycle
E - Extended Anneal Cycle - Additional 10 min. at temperature
EE- Extended Anneal Cycle - Additional 15 min. at temperature

* Values from JPL Samples

C-2

An noted above, the values for the texturized surface samples in Table 6 gave a smooth curve, with the exception of the 10^{16} ions/cm^2 point, under standard anneal conditions. The normal 10 min. anneal cycle was previously chosen on the basis of the previous optimization studies and was used to avoid degradation of the back contact with longer anneals. Also the shortest possible anneal cycle is desired for most economical production in an ultimate automatic machine. From Figure 38, it appears that the 77 Ω/□ objective would require an incident implant level of more than 5×10^{16} ions/cm^2 at 50 keV on texturized surfaces using the standard anneal. However, from the demonstration cell studies (Section 3.7) it appears that a value this low is not required for medium efficiency cells. Also such high dose levels are at present relatively prohibitive using analyzed-beam implantation machines. It was for this reason that KCI initiated its program on non-analyzed-beam implanted cells.

The relative value for the polished surface samples at the lowest dose level (2.5×10^{15} ions/cm^2) is comparatively low, obviously due to the smaller effective area to be implanted and the resulting higher level of implanted boron in the silicon for a given incident implant level. All samples, with the exception of J-31-2 (7.5×10^{14} ions/cm^2) were implanted at normal incidence to the cell surface. The effective range in the polished surface samples is therefore higher than in the texturized samples where the beam enters at an angle. This is partially (almost exactly) compensated for by the thinner combined coating on the texturized surfaces due to the fact that the same amount of Al_2O_3 was distributed over the larger effective area. In any event, the measurements are sheet resistance measurements which are relatively independent of layer depth for the penetrations involved.

However, as the implant level increases, the values for the polished and texturized surfaces get significantly closer, indicating a possible saturation

effect is beginning to occur under the standard anneal conditions. To test this further, some of the samples were annealed a second time for an additional 10 minutes or 15 minutes at temperature. The choice of times was arbitrary in an attempt to get the maximum information from the available samples. From Table 6, it appears that the effect of additional time at temperature gets significantly less as the implant level increases. Comparing J-31-6 and J-33-6 shows the latter to have changed relatively much less than the former even though the additional anneal time was 5 min. longer. J-31-1, at(?) 10^{16} ions/cm^2 as discussed before is suspect but still indicates a much lower relative change than J-31-6. J-31-5 at 5×10^{15} ions/cm^2, in view of the 5 min. longer anneal time, shows a relative change of the same order as J-31-6. The switch to possible saturation appears to start at approximately $1\text{-}2 \times 10^{16}$ ions/cm^2.

The polished samples J-33-4, 946-1 and J-45-6 also show a decrease in effectiveness for the additional anneal time as the implant level increases, again starting to approach saturation at approximately 2×10^{16} ions/cm^2 or less. In this case, all extended anneals were for an additional 15 mins. at temperature so the transition is relatively smooth. It should be noted that the relatively small change for texturized sample J-31-1 at 10^{16} ions/cm^2 is probably due to an improper dose level. The best indication of this is the fact that polished surface sample J-33-4, implanted during the same experimental sequence, and also having a nominal implant level of 10^{16} ions/cm^2, actually had a higher ρs value, which is highly unlikely.

Although much longer anneal cycles might be more effective in reducing the sheet resistance values, they were not considered for the overall technique being developed. It should be noted that the actual doses implanted in the silicon were only approximately half of the stated values with the maximum therefore being 10^{16} ions/cm^2. Rather than increasing the incident dose, a more effective method of decreasing ρs would be to increase the energy to place more of the incident ions within the silicon and spread them over a greater depth to decrease saturation effects. (The apparent saturation at the higher dose levels may, in fact, simply be an artifact of the lower energy. Note that sample J-31-2 (7.5×10^{14} ions/cm^2) which was implanted at 65 keV appears to give a value above that expected from the 75 keV points. Also the lower energy would have a greater adverse

effect on the polished samples with their thicker Al_2O_3 layers.) Although there could be a minor reverse drift effect due to the fall-off of dopant at the silicon surface (peak below interface), this should have only a very minor effect on efficiency due to the broadness of the peak and to the cell configuration. Program and implant machine limitations did not allow this approach to be followed. In fact, the 50keV limit on the high current machine actually forced the program in the opposite direction. A direct extrapolation of the 75 keV points yields a value of 77 Ω/□ (objective) at less than 2×10^{16} ions/cm^2.

2.) Light Absorption in Combined Coating

Transmittance(T) and reflectance(R) curves (Beckman DK-2A spectrometer) for the implanted, Al_2O_3 coated(ion beam sputtered), Al_2O_3 discs (1" diameter x .040" thick - sapphire) are given in Figures 39 and 40 covering the spectral ranges of .5 - 1.5 μ and .35 - .8 μ, respectively. The curves shown were taken after heat tratement using the standard anneal cycle. Discs 2, 3, 4 and 5 are the same ones as those used(same numbers) in the combined coating optimization study. Number 2 was reused for the 2×10^{16} ions/cm^2 measurement(number 6) since the original number 6 disc was used in another experiment. Numbers 2 →5 were implanted on the smaller Spire machine at 65 or 75 keV while number 6 was implanted on the larger machine at 50 keV. Discs were not available to do all doping levels and implantation time was limited so it was decided to jump to the worst condition(2×10^{16} ions/cm^2) for the last disc rather than to the 10^{16} ions/cm^2 point. A simple interpolation between curves 5 and 6 would give a reasonably accurate estimate of the 10^{16} ions/cm^2 curve.

After heat treatment, all of the discs 2 through 5 continued to show greater light transmission in the .5 - 1.5 μ region(Fig. 4) due to decreased reflectance, than the standard uncoated and non-implanted disc(1). Because of a switch in standards from MgO to $BaSO_2$ during the course of this experiment (between first and second set of implantations) the curves for disc 6 could not be put on the same graph. However, on the separate curves taken for each disc, number 6 was also higher than the standard throughout the range. This change in standards affects primarily the 1 - 1.5 μ range where $BaSO_2$ has a much higher reflectance than MgO.

The difference in standards in the .35 - .8 μ range is essentially

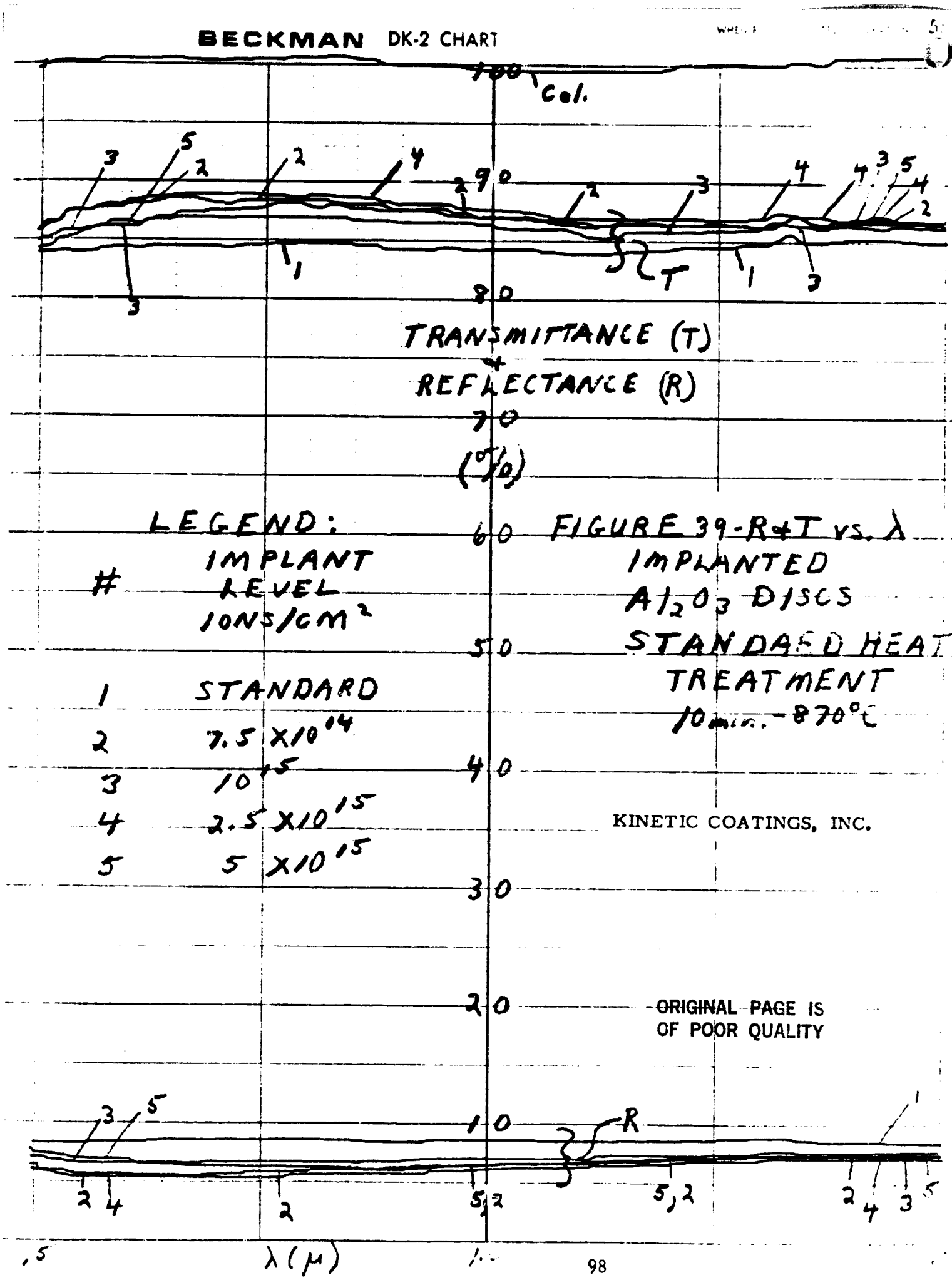
BECKMAN DK-2 CHART
100
Col.
90
80
70
60
50
40
30
20
10
TRANSMITTANCE (T)
+
REFLECTANCE (R)
(%)
T
R
λ (μ)
.5
1.0
LEGEND:
IMPLANT LEVEL IONS/CM²
1 STANDARD
2 7.5 X10¹⁴
3 10¹⁵
4 2.5 X10¹⁵
5 5 X10¹⁵
FIGURE 39-R+T vs. λ
IMPLANTED
Al₂O₃ DISCS
STANDARD HEAT
TREATMENT
10 min.-870°C
KINETIC COATINGS, INC.
ORIGINAL PAGE IS
OF POOR QUALITY

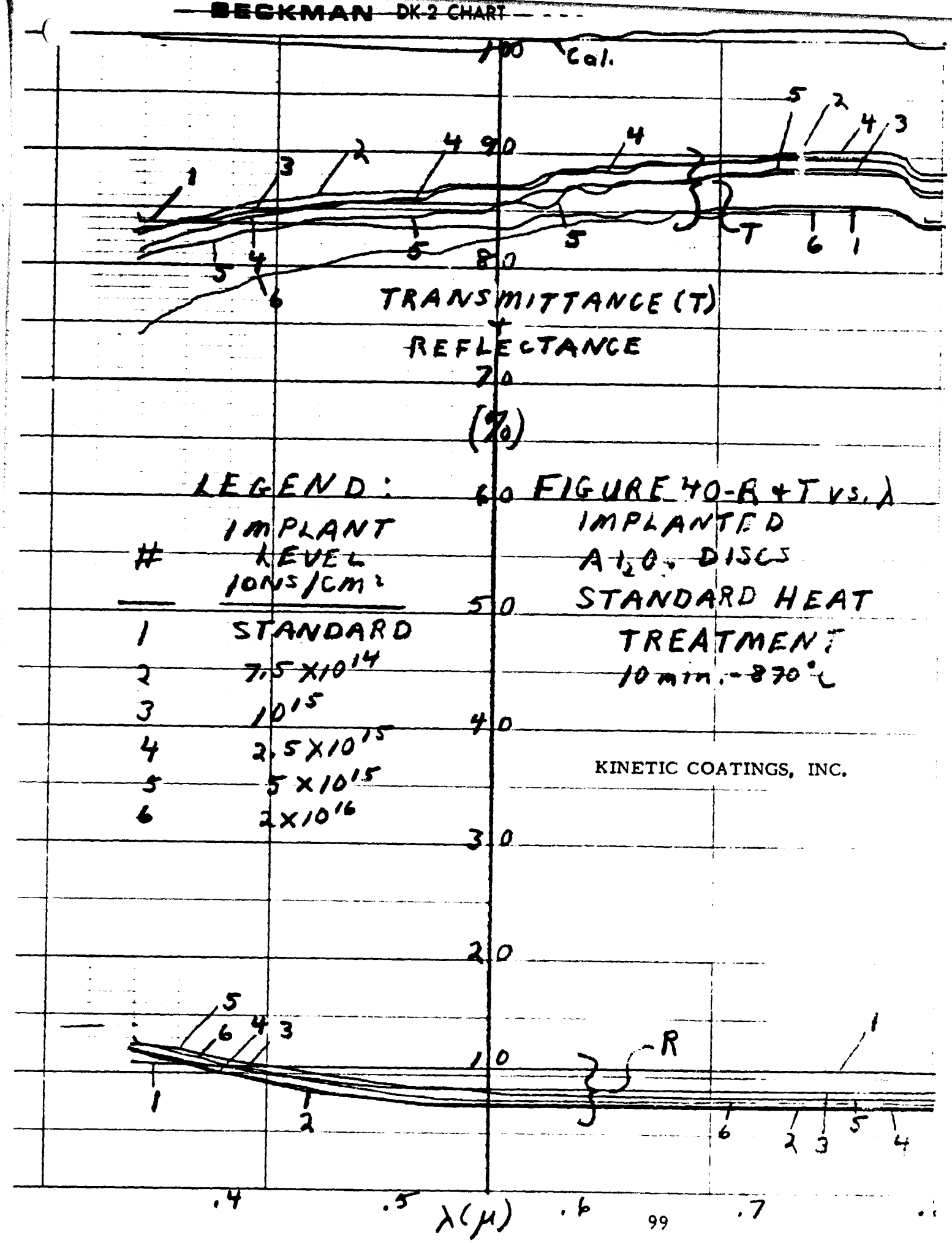
BECKMAN DK-2 CHART
100
Cal.
90
80
70
60
50
40
30
20
10
TRANSMITTANCE (T)
REFLECTANCE
(%)
T
R
.4
.5
.6
.7
λ(μ)
LEGEND:
IMPLANT LEVEL IONS/CM²
1 STANDARD
2 7.5 X10¹⁴
3 10¹⁵
4 2.5 X10¹⁵
5 5 X10¹⁵
6 2 X10¹⁶
FIGURE 40-R + T vs. λ
IMPLANTED
A₂O₃ DISCS
STANDARD HEAT
TREATMENT
10 min. - 870°C
KINETIC COATINGS, INC.

insignificant and number 6 is shown on the same curve as the others (Fig. 40). Here some slight light loss due to the implanted boron is becoming apparent at wavelengths less than .43 μ for implant levels in the 5×10^{15} ions/cm^2 range. With an increase to 2×10^{16} ions/cm^2, the light loss becomes more important, starting at approximately .7 μ and increasing to 7-8% absolute at .35 μ. The decrease in transmission was not accompanied by a corresponding change in R and indicates a true absorption due to the implanted boron. It is notable that all of the samples showed a significant absorption effect before heat treatment, perhaps indicating some surface boron boiled off during annealing, or alternately implying an outdiffusion of the boron implanted in the Al_2O_3. In any event, the results after heat treatment are those of concern in the process. The conclusion is that light absorption due to boron implanted in the Al_2O_3 does not present a prohibitive problem to cell manufacture by the present technique. As a corollary to the comments in the previous section on the fact that only half of the incident ions end up in the silicon, that half is necessary to dope the silicon and will not act as non-useful light absorbers.

Some preliminary cells made at this point by KCI in an extra-contract program clearly indicated the viability of the process for achieving the contact goals. The efficiencies were in the 10% AMI range and indicated that the 50 keV energy limit might be acceptable although limiting for the demonstration

cells. It was decided to make the first set of 50 cells using the 50 keV machine to determine the extent of the limitation.

Conclusions

The following conclusions were drawn from the implantation results on this phase of program.

1. The implanted layer optimization objective of 77 Ω/□ cannot readily be met with practical incident implant levels and 50 keV implanting ions. It appears that the objective could be achieved at implant levels of roughly 2×10^{16} ions/cm^2 if the available energy were 75 keV or more. Preliminary cell results indicate that sheet resistances (158 Ω/□) achieved with incident implant levels in the 10^{16} ions/cm^2 (50 keV) range should be adequate to achieve reasonably efficient cells.

2. No light absorption problems are evident after heat treatment with implanted boron levels up to 5×10^{15} ions/cm^2. Levels in the order of 2×10^{16} ions/cm^2 or more may cause sufficient absorption to more than compensate for gains in efficiency due to lower sheet resistance. Higher energy implants reduce this light absorption while decreasing sheet resistance and is a preferred means of improvement. Levels in the 10^{16} ions/cm^2 range are in the gray area and represent the best estimate for use in the present program.

3.6 Interconnects

Because of funding limitations only a small contractual effort was applied to cell interconnect techniques. In general, the cells were designed with contact materials and physical configurations which would lend themselves to environmentally resistant methods such as ultrasonic bonding or parallel gap welding; i.e. physical integration methods rather than surface methods.

Optimization Procedures

Conditions for real cells were duplicated by using blank wafers which were coated on one or both sides with metals (heat treated) to cell specifications (> 9 μ Al on front; .3-.5 μ Ag + 3-1.5 μ Ni on back). Polished and texturized surfaces were tried and the front interconnect tests were tried on Al_2O_3 coated contacts as well as non-coated contacts.

Interconnect strips of the desired material (1/8" wide; .003" thick) were attached using the particular system (i.e. method, electrode material etc.) being studied and break strength of an "individual" weld or bond was determined.

For the latter, a 90° pull test was used in which a polyfoam basket supported by balanced wires was attached to the bent interconnect material (i. e. tab 90° to surface) by an alligator clip. The basket and attaching system weighed 5 grams. With the wafer supported in a clamp on both sides of the welded interconnect, the basket was left hanging straight down and 5 gm weights were successively added until the interconnect spot broke. The weights were then added to determine the pull strength.

Initially, various electrode configurations were tried but it was quickly determined that tips approximately 1/16" in diameter, either rounded or flat, in general gave the optimum results for the equipment used. The latter consisted of a Sonoweld Model W-260-A ultrasonic welder and a modified Hughes Model VTW-30C stored energy (1-100 watt-seconds) welder. For parallel gap welding, special electrodes were fabricated for the Hughes system to allow the two welding tips to be simultaneously brought into contact with the contact material and interconnect material. One tip floated under tension to adjust for height differences and the spacing between electrodes was 1/8-1/4".

The following electrodes were tested for ultrasonic welding.

1. Stainless steel
2. Copper
3. Copper-tungsten
4. Brass
5. Aluminum
6. Ceramic
7. RWMA-1 (Resistance Welders Manufacturer's Association; Copper-Cadmium)
8. RWMA-3 (Copper-Cobalt-Berylium)

Best results were obtained with a rounded tip using the RWMA-3 alloy.

The electrodes used for the parallel gap welding tests were:

1. Stainless steel
2. Copper-Tungsten
3. RWMA-1 and 3
4. Copper

Copper tips with one flat and the other rounded on the end gave the best results.

Various interconnect materials were tried for both the front and back contacts including:

1. Aluminum(primarily for front)
2. Nickel(primarily for back)
3. Copper(for either)
4. Titanium(for back)

Aluminum was best on the front and titanium on the back.

Experimental Results

Results varied strongly for the many materials used for the interconnect strips and the welding electrodes. The results presented here are for the optimum or potentially useful combinations. Other combinations studied, in general gave inferior results, or were less suitable in the long run than those discussed.

a.) Front Contacts

Interconnect strips were quickly reduced to the Al case which was investigated on polished and texturized surfaces. Tests were done on texturized surfaces only for optimized polished surface cases. Multiple tests were made for each condition with the actual number depending on the results obtained. Total spread in results is given below with the normal range also indicated where necessary. The latter is somewhat operator dependent so that the full range of values might be expected to occur under production conditions. Tables 7 and 8 give the operating conditions and pull strengths for selected combinations.

In general, the parallel gap welding technique gave inconsistent results and a high incidence of wafer breakage. It was therefore discarded in favor of the ultrasonic method which gave consistent results for the optimized conditions with very low breakage.

The important case for the present program is the texturized-AR case since the final lot of cells were made with this surface. Pull strengths

TABLE 7

Ultrasonic Welding of Front Contacts

Surface	Electrode	Power (watts)	Time (sec.)	Weight (gms)	90° Pull Strength (single weld-gms)
P(no AR)	Bs(F)	6	.5	10	115-285;usual>170
P(no AR)	Bs(F)	6	.5	5	185-330;usual>230
P(AR)	Bs(F)	6	.5	5	Electrode sticks
P(AR)	SS(F)	6	.25	5	Electrode sticks
P(AR)	Bs(F)	.8	.5	5	100-225;usual>100
P(AR)	Bs(F)	.5	.5	5	80-195;usual>80
P(no AR)	RWMA-3(R)	6	.25	5	>200
P(AR)	RWMA-3(R)	6	.25	5	140-210
T(AR)	RWMA-3(R)	6	.25	5	100-190

Legend:
P = Polished
AR = Al_2O_3 coating
T = Texturized
SS = Stainless Steel
Bs = Brass
RWMA-3 = Cu-Co-Be
(F) = Flat End
(R) = Rounded End

TABLE 8

Parallel Gap Welding-Front Contacts

Surface	Energy (watt-seconds)	90° Pull Strength (single weld-gms)
P (AR)	25	45-115
T (AR)	25	10-110
P (AR)	30	20-110
T (AR)	30	50-150
P (AR)	35	70-125
T (AR)	35	15-60

using an RWMA-3 electrode were consistently in the 100-190 gm range for the ultrasonic technique. This was not unexpected since this method had been demonstrated by KCI in 1976, long before the present program started. The values are considered adequate for multiple weld conditions. It should be noted that failure of the weld for a cell case is at the Al contact-interconnect interface and has no effect on the underlying cell due to the depth of the alloyed contact. Also pull strengths, in general, were significantly higher for no AR cases and for polished surfaces.

b.) Back Contacts

Ultrasonic welding of the back contact was essentially unsuccessful for any of the combinations investigated and was discarded. Results for the parallel-gap method were somewhat more ambiguous but, in general, were also unsuccessful. Nickel, copper, aluminum, tungsten, aluminum mesh, tungsten mesh, silver and titanium interconnects were investigated. Only titanium strips gave welds of any significance. The best welds were obtained with a wide electrode on the contact material and a small electrode on the interconnect strip. The only results of interest are given in Table 9.

TABLE 9

Parallel Welding-Back Contacts

Surface	Electrode	Interconnect Material	Energy (watt-seconds)	90° Pull Strength (single weld-gm.^{2})
P, T	Cu-W	Ti	50	0-65
P, T	Cu	Ti	50	0-25

Although the welds could be made, the low strength appeared to be due to the thinness of the "brittle" Ag-Si alloy region, in contrast to the much thicker alloy region on the front. A possible solution would be a much thicker Ag layer but the cost for this would be prohibitive.

KCI solved the problem by developing a completely new back contact

and interconnect technique under an in-house program. This method works extremely well in vacuum and is specifically suited for incorporation into the cell manufacturing machine for low cost cell production. Alternately, KCI has also developed a solder reflow method that works very well with the heat treated and alloyed back contact.

c.) Cell Performance

A quick check of the ultrasonic welding method for Al strips to the Al-Si(AR) alloy was made on some of the broken or bad bar (Section 3.7) cells from the first 50 cell lot.

To check the effect of welding on the strips, narrow strips (Al-.003") were welded along the entire length of the main contact bar, rather than just at the tabs. Welds were made every 2 mm. Cells with bad bars gave slightly improved performance, presumably due to lower series resistance, but in general gave weaker welds than observed for the test wafers. Cells with good bars have improved performance and weld strengths similar to test wafers.

Figure 41 shows the characteristic of a cell with a good bar but a full length break across the fingers on one side of the bar. After welding (approximately 20 welds along the strip) the characteristic improved slightly. A couple of the welds were then broken at one end of the strip which was then rewelded. There was no change in the improved characteristic, demonstrating that the welds have no effect on cell performance and are repairable and tolerant to production errors. Lack of funding precluded further tests on good cells during this contract.

ORIGINAL PAGE IS
OF POOR QUALITY

Fig. 41 I-V Curves - Ultrasonic Bonding Interconnect
(Cell J-51-1)

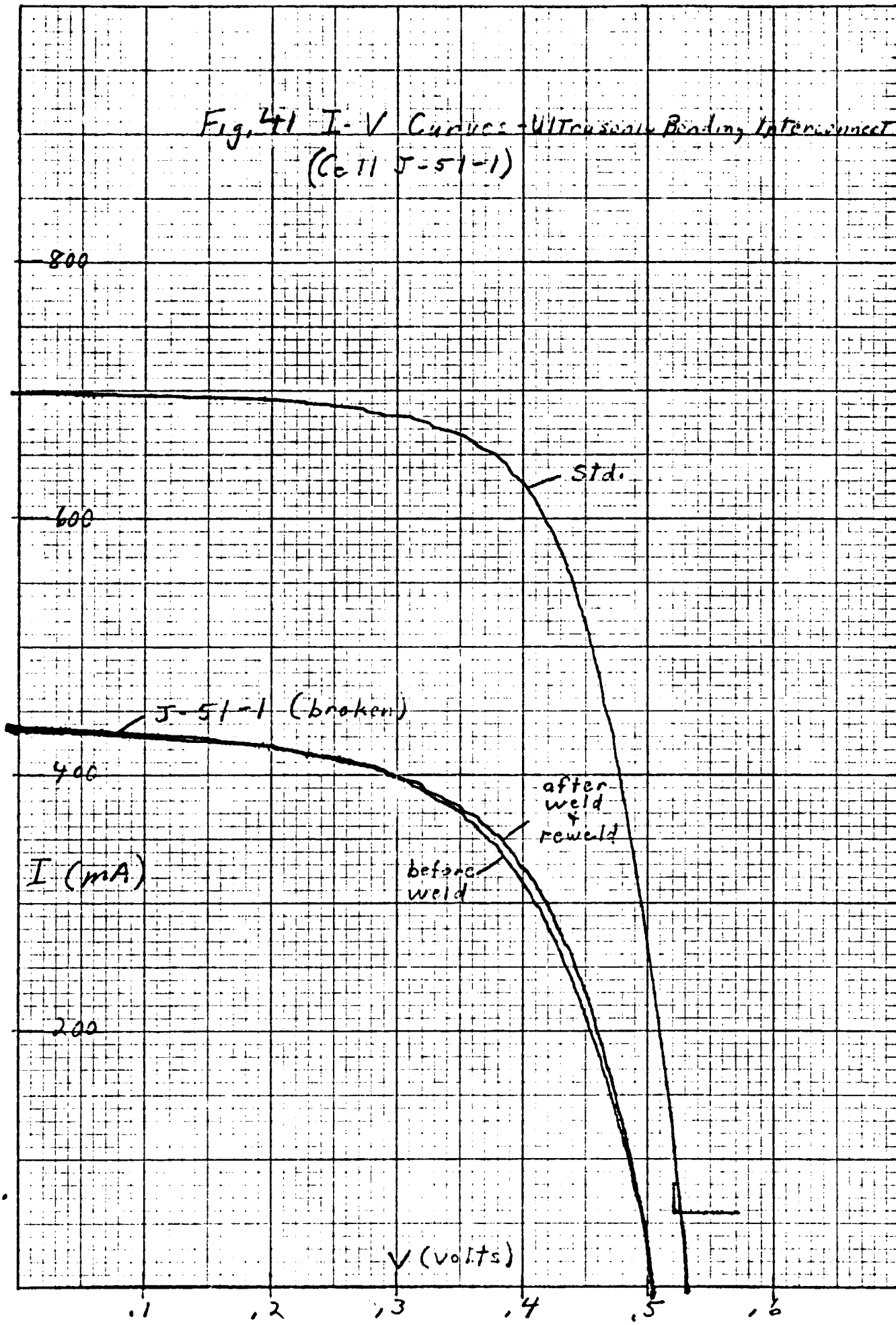

K+E 10 X 10 TO THE INCH 46 0780
7 X 10 INCHES
KEUFFEL & ESSER CO.

Conclusions

The following conclusions were drawn from this phase of the program:

1. Al interconnect strips can be ultrasonically bonded to the Al-Si alloy of the front bar, with or without the Al_2O_3 coating, with no cell degradation. Pull strength at 90° for a single weld is more than adequate for a strip multi-welded to the front contact. Ultrasonic bonding is superior to parallel gap welding.
2. Neither ultrasonic bonding nor parallel gap welding provides a suitable welding technique for attaching interconnect strips to the back contact, however an in-house effort successfully demonstrated good interconnect techniques.

3.7 Demonstration Cells

Two 50 cell lots of demonstration cells were planned for the program, a test lot and a final demonstration lot. In addition, some preliminary cells were made in an in-house program in order to anticipate potential problems, but more importantly to demonstrate the viability of non-mass-analyzed ion beams for the KCI basic process. The latter was done before any of the program demonstration cells were made and represented a strictly proprietary development.

The first 50 cell test lot included many variations in cell surface, contact thickness etc. and was implanted on a service basis at Spire on the large Extrion production machine. Many problems occurred because of this implant procedure, including inadequate energy as discussed previously, non-uniform or improperly dosed implants, and front bar stripping on polished surface cells. The latter was apparently due to thermal effects which could not be avoided with the machine implant procedure. Results from the KCI non-mass-analyzed study led KCI to establish an in-house program to place into operation an implant machine based on a semi-analyzed beam and having higher energy (up to 150 keV) capability. This machine was used to make the final 50 cell demonstration lot.

Fifty Cell Test Lot

Using 60 standard starting blanks as received from the manufacturer, it was planned to vary parameters as shown in Table 10 to give a matrix of different cells.

Some additional cells were added by KCI to supplement the above in case of any serious cell losses. In particular, a few additional cells with polish-etched front surfaces and 18 μ thick front contacts were processed up to the implantation stage and kept in reserve. This turned out to be a fortunate choice since an unusual problem arose during the implant step. All cells (with one exception)

TABLE 10

Cell Variables - Test Lot

Group No.	Number of Cells	Front Surface Finish	Back Surface Finish	Front Contact Thickness(μ)	Incident Doping Ion Density (ions/cm^2)
1	6	Polish-etched	Sawed-etched	9	5×10^{15}
2	6	"	"	9	10^{16}
3	6	"	"	18	5×10^{15}
4	6	"	"	18	10^{16}
5	3	Sawed-etched	Polish-etched	9	5×10^{15}
6	3	"	"	9	10^{16}
7	3	"	"	18	5×10^{15}
8	3	"	"	18	10^{16}
9	6	Texturized	Texturized	9	5×10^{15}
10	6	"	"	9	10^{16}
11	6	"	"	18	5×10^{15}
12	6	"	"	18	10^{16}

were processed in the sequence of texturizing (if needed), front contacting, application of combined coating, back contacting and finally heat treating. The back contact was inserted after implantation rather than before to avoid possible handling problems during transfer for implantation. This change is irrelevant to the overall processing procedure.

Boron implantations for junction formation were carried out by Spire using the high current Extrion implanter. The cells were to be divided into three sets of 20 with uniform distribution of the available samples and implantations were to be done at three different times to avoid any catastrophes. It was necessary to use makeshift holders to adapt the cells to the implanter.

After implantation (and before heat treatment) of the first set it was observed that some front contact tabs and/or bars were fractured out of the silicon as shown in Fig. 42. This was not a delamination but an actual "cratering" effect with the silicon from the substrate still attached to the back of the stripped Al.

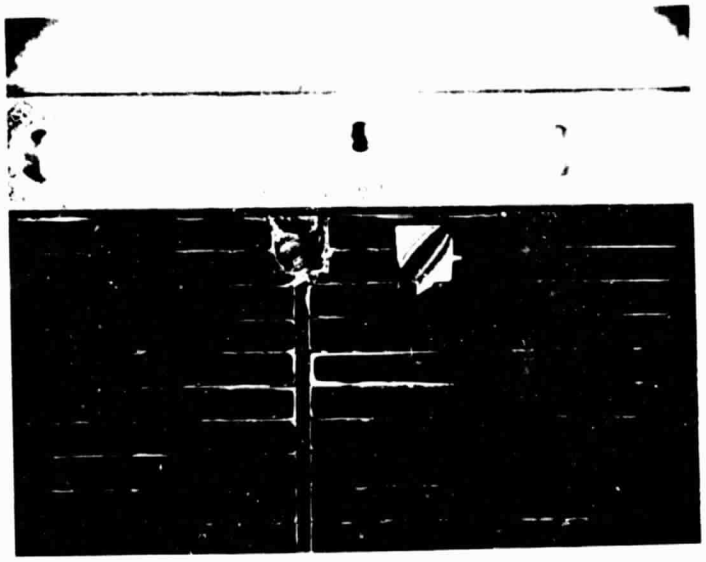

42(a) Stripped Contact Pad
(Al side of pad up)

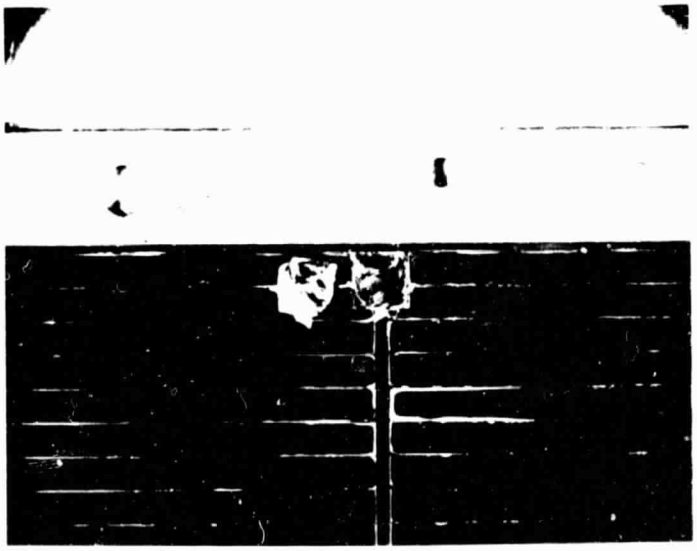

42(b) Stripped Contact Pad
(Si side of pad up)

ORIGINAL PAGE IS
OF POOR QUALITY

Fig 42 Stripped Front Contact Pad

This effect had not been observed on cells implanted previously on the smaller Spire implanter or on one polished cell implanted on the larger machine. Also it has never been observed in heat treated cells or in cells made with a non-analyzed ion beam at much higher incident power densities . It is clearly an artifact of implantations on the Extrion machine using the makeshift holders and apparently is connected with sudden cooling (by contact with room temperature valve) on removal from the machine. Various attempts, including lower current and holder changes, were made to alleviate the problem but, if anything, it seemed to get worse in the last two runs. In addition, many of the implants seemed very non-uniform (observation of boron coloring in combined coating), much too heavy (e.g. 5×10^{15} ions/cm^2 implants with very heavy boron coloring) or too low an energy, or inconsistent or too light (e.g. other 5×10^{15} ions/cm^2 implants with no observable boron coloring; some 10^{16} ions/cm^2 had no observable coloring as opposed to 5×10^{15} ions/cm^2 implants with heavy coloring). In general the character of the implants indicated some difficulties in operating the machine with boron at the maximum energy level (50 keV) and current (250-500 μ A).

More importantly, the proper design energy level was 75 keV which meant that, in general, too little of the boron ended up in silicon and too much in the combined coating. The result of this is too low doping and additional light absorption in the combined oxide. Since the cells could not be implanted with heavier doses, this meant lower efficiencies in general than would be obtained with the correct parameters.

During application of the back contact, another problem was observed on the cells with sawed-etched or polish-etched back surfaces. After a group of 12 cells was contacted in the normal way, stress patterns and delaminations were observed on these surfaces but not on the texturized samples. These cells were processed directly as they came back from the sizing step (sawed from 3" round to 5 cm square) which was carried out before any of the KCI process steps (i.e. front contact etc.). The sizing step was performed by waxing the 3" round slices together and sawing the whole stack to size and then separating and cleaning the slices with hot trico.

As returned to KCI these slices were supposed to be free of wax but

apparently were not. The texuturized cells which had been etched, and therefore were free of wax, did not show the problems. Light rubbing of the back of the cells (after implant) with a swab dipped in 6-1-1 etch removed an obvious layer and eliminated most of the problem and this was done with the remaining cells. This etching procedure was not required on contact test cells made on material as received directly from the original supplier (Wacker). The problem is an artifact of the sizing step and would not occur on the as-grown materials (e.g. EFG or dendritic) which are the ultimate objective of this program. However, the above procedure was used to complete the cells and obtain the necessary data. Also the metal thicknesses on the back were changed to 0.5 μ Ag and 1.5 μ Ni to reduce stress in the film tending to cause delamination at residual wax areas. Conductivity of this combination was tested as comparable to the original 0.3 μ Ag plus 3 μ of Ni. A third major problem occurred during application of the combined coating (Al_2O_3) to a run of 12 cells. Two of the cells fell off the substrate holder onto the target during the run and silicon sputtered from these cells badly contaminated the deposited Al_2O_3 resulting in a brownish color. Since most of these cells were sawed-etched and no others were available, it was necessary to continue processing them per schedule. As discussed below, this contamination clearly reduced current and fill factor. The two cells which fell off and were sputtered were subsequently Al_2O_3 coated and gave reasonable results.

Although far from adequate for obtaining the desired data, the above procedures were followed out of necessity. Heat treatment was carried out using the standard 870°C ten minute anneal cycle or multiples thereof. The above stated problems seriously restricted the number of extra cells available for heat treatment studies which, in general, were carried out on broken or tab deficient (cratering) cells.

Because of the problems (tab cratering, residual wax, bad Al_2O_3), most of the polish-etched and sawed-etched cells suffered some major deficiency. Some texturized cells were lost to breaking during implant or in handling, but in general the texturized cells were in relatively good shape. The one problem which affected all three cell surfaces was severe undercutting of the machanical front contact mask by the energetic depositing material. This led to wide fingers and general coverage of large front surface areas by Al with consequent loss of current. Various methods were tried to circumvent this problem but with the limitations of the available masks it could not be avoided. Loss of current due to light absorption in the resulting thin Al layer was estimated (by visual observation of cells at sharp angle before heat treatment) to be as much as 25-30%. The solution to this problem would appear to be magnetic hold-down of the masks. Funding was not available to the program to implement this solution.

A few of the premininary cells were made with wider fingers (10 mils-fingers opened to supporting mask width) to observe the effect on cell series resistance. This resulted in lower series resistance but also caused a loss of current due to additional covered surface while not avoiding the general undercutting problem.

Figures 43 and 44 give data on a few of the cells which were given multiple heat treatments to determine the effect of additional annealing. The cell numbers (not including S or 38-3) are the assigned numbers of the delivered samples (see Table 11) and the numbers in brackets refer to the first, second, or third heat treatment. This data was taken before KCI received a secondary standard having characteristics similar to the cells being tested. Such a standard was subsequently obtained from JPL from the delivered cells as tested by ASEC. This was used in testing the final 50 cell demonstration lot, and the ASEC data on the first lot has been used in Table 11 since it is more accurate than the original KCI data. The latter, which was based on a non-similar diffused cell (JPL terrestrial standard TSS030; Isc - 113.3mA, Voc - .5665 V at 100 mW/cm^2) gave consistently lower efficiencies than the true values. The

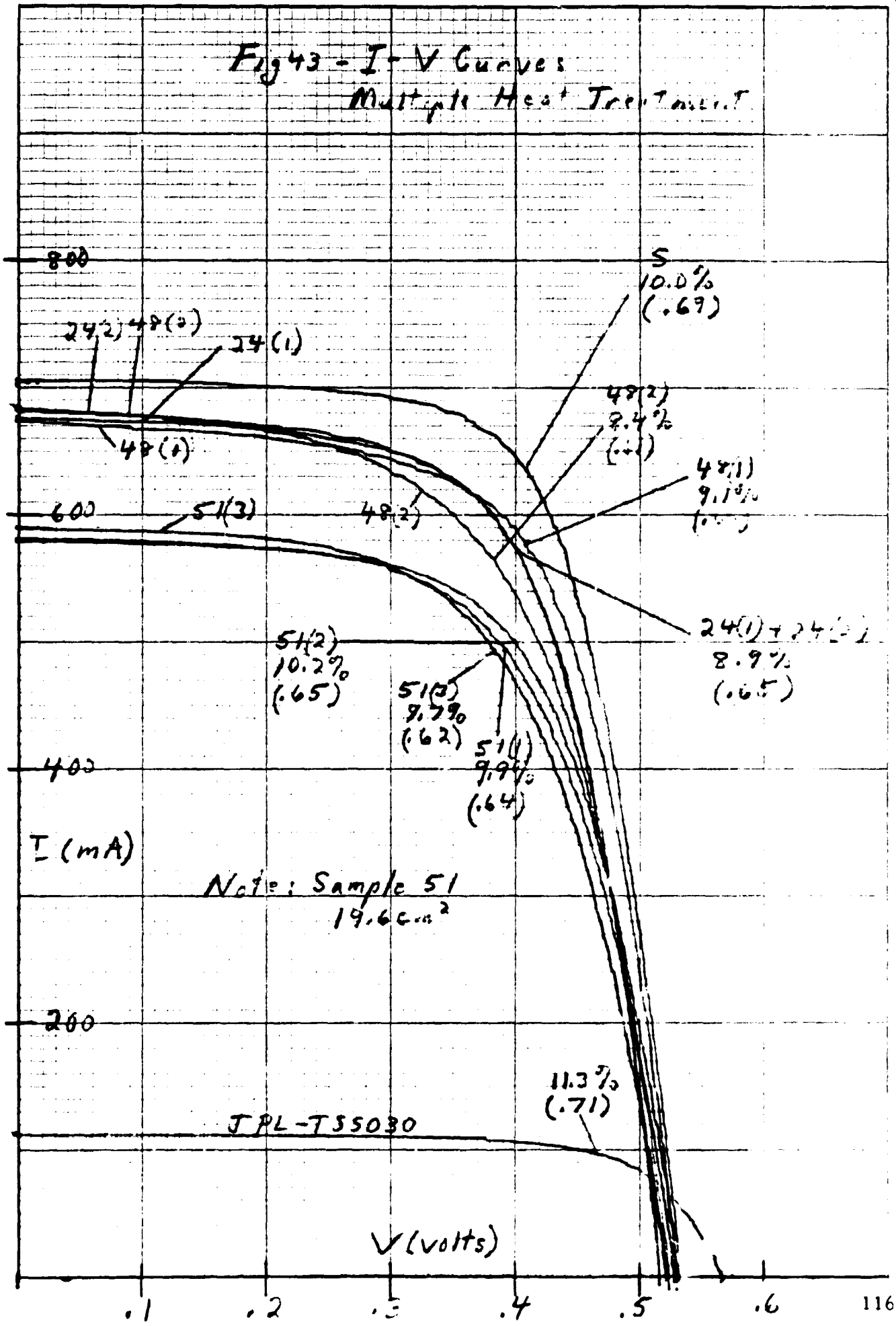
Fig 43 - I-V Curves
Multiple Heat Treatment
800
600
400
200
I (mA)
V (volts)
.1
.2
.3
.4
.5
.6
S
10.0%
(.69)
48(2)
8.4%
(.61)
48(1)
9.1%
24(2)
48(2)
24(1)
48(1)
51(3)
48(2)
24(1) + 24(2)
8.9%
(.65)
51(2)
10.2%
(.65)
51(3)
9.79%
(.62)
51(1)
9.9%
(.64)
Note: Sample 51
19.6 cm²
11.3%
(.71)
JPL-TS5030

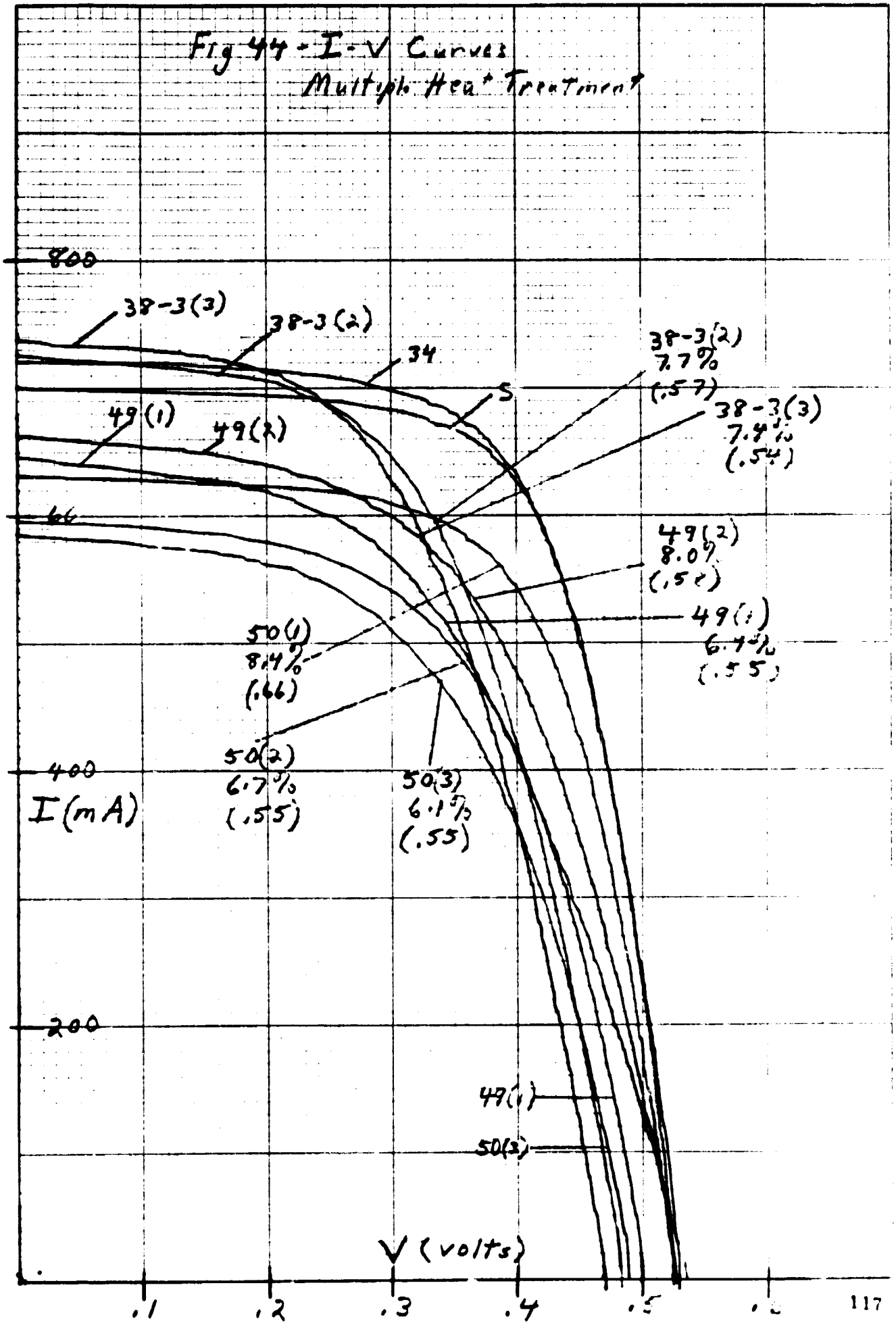
Fig 44 - I-V Curves
Multiple Heat Treatment
800
600
400
200
I (mA)
V (volts)
.1
.2
.3
.4
.5
38-3(3)
38-3(2)
34
5
49(1)
49(2)
38-3(2)
7.7%
(.57)
38-3(3)
7.4%
(.54)
49(2)
8.0%
(.52)
49(1)
6.7%
(.55)
50(1)
8.4%
(.66)
50(2)
6.7%
(.55)
50(3)
6.1%
(.55)
49(1)
50(3)

values in Figs. 43 and 44 based on the original values are therefore low but the trends with heat treatment are valid.

The standard (S) shown is one of the preliminary cells which was initially calibrated vs. the JPL cell and used to set the light to keep all relative values correct. The JPL cell would not fit into the simulator which had an unusual cell holder which was a Pb weighted copper square with a 5.7 cm square opening in the center and two small braid covered pads which contacted the cell contact pads (see Figure 3). The back contact was pressured against a temperature controlled (nominal 28°C) gold plated block by the pressure from the weighted front contact. The temperature variation was confined to the 28 ± 1°C range. A 300 watt ELH lamp was used for illumination and the curves were taken by electronic biasing methods.

From Figure 43 it is seen that cell 24 showed a very slight increase in Isc but no change in efficiency with a second heat treatment. This cell was a texturized cell with the special 10 mil wide fingers and had the silicon-contaminated Al_2O_3 coating. The wider fingers apparently decreased the light generated current but improved the F.F. over other cells with the contaminated Al_2O_3 (see sawed-etched cells). Cell 51 (texturized) went up slightly

ORIGINAL PAGE IS
OF POOR QUALITY

in F.F. and efficiency after a second heat treatment (H. T.) with little Isc change and then went up slightly in Isc and down in F.F. with a third H. T. This cell was interesting in that it had a clean break across all 28 fingers on one side and still fired on the combined H. T. with no appreciable problems. Cell 48 (polish-etched), which went up slightly in Isc and clearly down in F.F. with a second H. T., has very significant Al undercutting along the cell edge. This was typical of most of the polish-etched (p) cells, and although not as readily observable, was almost certainly the case for the other surface types.

Cell 49 (Fig. 44) is an example of a cell (p) with both bad front contact pads (from implant) and a very bad back (residual wax). Paradoxically, this cell went up in both Isc and F.F. with a second H. T., perhaps due to additional areas of the back firing through the residual wax. Cell 50 (sawed-etched) had bulging contact pads and a very bad back but gave surprisingly good performance under the circumstances. This was one of the few sawed-etched (se) cells with good Al_2O_3. Subsequent firings gave significantly poorer performance. Cell 38-3 was a special cell heat treated before and after implant. The performance after the second H.T. was significantly poorer than for cells heat treated only after implant. A third H.T. raised Isc slightly but decreased the F.F. For comparison, cell 34 was a texturized (t) cell with a bad contact tab after one H. T.

From this and similar data, it was concluded that a single H. T. was desirable and longer heat treatments were unnecessary for achieving near-optimium cell output. Bad tabs caused some lowering of shunt resistance and F.F. in some cases but did not cause full cell failure; nor did a contaminated Al_2O_3 coating, residual wax on the back or breaks in the cell before H. T. In general it appears that operational cells are produced in spite of major problems and that highly consistent output should be achieved for a fully developed production process

The delivered cells included many which were broken, had bad tabs or bad implants, or which had other manufacturing deficiencies. They did serve, however, to point out potential problems. Table 11 gives the cell numbers, groupings, digital data etc. The symbols under comments are defined at the end of the table.

TABLE 11

DELIVERED CELL CHARACTERISTICS(AMI-28°C)

Cell #	Front Surface Finish	Front Contact Thickness (μ)	Implant Level (Ions/cm^2)	I_{sc} (mA)	V_{oc} (mV)	F.F.	η (%)	Comments
1	p	9	5×10^{15}	686	532	.65	9.5	
2	p	"	"	670	530	.63	8.9	NI, HI
3	p	"	"	638	513	.54	7.0	NI, HI
4	p	9	10^{16}	668	538	.67	9.6	BT, BU
5	p	18	5×10^{15}	688	535	.65	9.6	BT
6	p	"	"	685	531	.68	9.9	BU, BT
7	p	"	"	709	538	.68	10.4	BT
8	p	"	"	642	532	.74	10.2	BT, BU, NI
9	p	18	10^{16}	680	537	.73	10.6	BT
10	p	"	"	688	525	.68	9.8	BT
11	se	9	5×10^{15}	682	530	.59	8.5	BAR
12	se	"	"	641	530	.60	8.1	BAR
13	se	"	"	699	480	.63	9.3	AR redone
14	se	"	"	619	533	.44	5.2	BAR, BT
15	se	"	"	619	532	.65	9.7	BB
16	se	9	10^{16}	711	530	.67	10.0	AR redone
17	se	"	"	590		.72	9.0	WF
18	se	18	5×10^{15}	630	530	.65	8.7	BT, BAR
19	se	"	"	475	533	,63	7.9	BT, B

TABLE 1 (Continued)

Cell #	Front Surface Finish	Front Contact Thickness (μ)	Implant Level (Ions/cm^2)	I_{sc} (mA)	V_{oc} (mV)	F.F.	η (%)	Comments
20	se	18	10^{16}	640	530	.70	9.5	BU, BB
21	se	"	"	645	532	.63	8.6	BT
22	t	9	5×10^{15}	739	519	.60	9.2	
23	t	"	"	731	521	.67	10.2	
24	t	9	10^{16}	682	522	.68	9.7	M, WF, BAR
25	t	"	"	749	529	.69	11.0	
26	t	"	"	740	521	.66	10.1	
27	t	"	"	730	520	.64	9.7	
28	t	"	"	732	525	.67	10.3	
29	t	18	5×10^{15}	632	510	.70	9.0	WF
30	t	"	"	735	520	.70	10.7	
31	t	"	"	740	515	.63	9.6	BU
32	t	"	"	740	521	.67	10.3	
33	t	18	10^{16}	745	525	.69	10.8	
34	t	"	"	725	532	.70	10.8	BT
35	t	"	"	720	528	.67	10.1	
36	[illegible]	"	"	740	525	.69	10.8	
37	t	"	"	655	510	.70	9.4	B
38	p	9	5×10^{15}	675	538	.59	8.5	BT
39	p	"	"	685	540	.66	9.8	BT, NI
40	p	"	"	710	549	.62	9.6	BT
41	p	"	10^{16}	672	540	.54	7.9	BT, BB, M
42	p	18	5×10^{15}	650	541	.63	8.9	BT, HI
43	p	"	10^{16}	641	520	.62	8.5	BT, M, BU
44	p	"	5×10^{15}	675	525	.67	9.7	BT, BU
45	p	"	"	680	530	.70	10.4	BT

TABLE 11(Continued)

Cell #	Front Surface Finish	Front Contact Thickness (μ)	Implant Level (Ions/cm^2)	I_{sc} (mA)	V_{oc} (mV)	F.F.	η (%)	Comments
46	p	18	5×10^{15}	671	520	.58	9.1	BT
47	p	"	"	668	525	.65	9.1	BT
48	p	18	5×10^{15}	680	530	.62	9.0	BT
49	p	9	10^{16}	668	535	.58	8.2	BT, NI, VBB
50	se	18	5×10^{15}	585	500	.58	6.8	BT, VBB
51	t	9	10^{16}	585	530	.65	10.2	B

Legend:

BT	: Bar tabs or bar strain	VBB	: Very bad back
BU	: Bar undercutting	B	: Broken
BAR	: Bad AR	NI	: Non-uniform implant
WF	: Wide Fingers	HI	: Heavy implant
BB	: Bad back	M	: Multiple heat treatment

In addition to the above legend, BT sometimes included "bulging" tabs after firing or bar pull back from original area. In these cases, the bar usually looked lifted or above the surface before H. T. and is probably the result of residual wax rather than implant since none of the polish-etched surfaces were cleaned before deposition of the front contact. Heavy implant appearance could also be due to low energy or a combination of both. Sample 49 was by far the worst case with the implant appearing to be doughnut shaped about the middle, indicating an apparent lack of scanning. Many of the other samples are almost as bad. Also, many of the backs had slight back strains or bubbles in very small areas due to wax not removed by the swab etching. This is not believed to have affected the cell efficiencies and is not noted where it occurred.

The results may best be interpreted on a group basis (Note underlined breaks in Table 11). The first group is the polish-etched -9μ -5×10^{15} ions/cm^2 case(designation p-9-5×10^{15}; similar system used for other groups).

ORIGINAL PAGE IS
OF POOR

Of these only No. 1 seemed to be properly implanted, with No. 2 having an apparently heavy implant with much of the boron in the oxide, and No. 3 having a very heavy implant. The explanation for the excess boron in the Al_2O_3 may be due to the use of lower incorrect energies. In this event the one that looks the heaviest would, in fact, have the lowest doping level since less boron would end up in the silicon. It would also have less light reaching the active region due to absorption in the boron in the Al_2O_3. Basically all of these cells have inadequate doping of the implanted layer resulting in high sheet resistance and poor carrier collection.

No. 4 was the only p-9-10^{16} cell to survive the implant and which was not used for multiple H. T. or the original back contact tests before the residual wax was removed. By eye the implant level in this sample looked much less than that of samples 2 or 3 although the energy was nominally the same and the dose was supposed to be twice as high. Undercutting was very bad on this sample which had overall performance slightly better than No. 1.

Although they all had bad tabs from implant, plus an assortment of other problems, the four p-18-5 x 10^{15} cells gave better performance than the previous 9 μ cells. The implants, however, were not as heavy by eye as the p-9-5 x 10^{15} cells implying, by continuation of previous argument, higher energy and a larger proportion of boron in the silicon. The improved curve factors could be due to this effect and/or to the thicker front contact. Cell 8 was notable since it had very bad undercutting and lower current but a better F. F. The latter was probably due to the thin Al layer over the surface tending to reduce Rs.

The two surviving p-18-10^{16} cells also had imperfect tabs with No. 10 being particularly bad, showing strain and pull-back along the entire bar. Again a badly undercut cell, No. 9, had a better F. F. although this could also be due to the better condition of the tabs and bar.

A variety of factors were present in all of the se cells but particularly in the se-9-5 x 10^{15} cells. Three of these cells (11, 12, and 14) had bad Al_2O_3 coatings with No. 14 being very badly contaminated and having by far the worst performance of any cell made including all of those with cratered tabs etc. Cell No. 11 was much less contaminated than No. 12 which was much less than 14.

Clearly the Si contamination of the Al_2O_3 led to lower currents through absorption and to lower fill factors. Cell No. 13 was one of the two cells that fell on the Al_2O_3 target and were sputtered on to the remaining se cells in the bad Al_2O_3 run. It therefore had a sputter cleaned front surface which had Al_2O_3 applied in a subsequent run. The performance of this cell was better than that of 11, 12, and 14 which otherwise were identical. Cell No. 15 had modest back problems only and appeased to suffer primarily from low doping and/or front contact resistance.

The se-9-10^{16} cells included the other cell (No. 16) sputtered in the bad Al_2O_3 run and subsequently Al_2O_3 coated. Cell No. 17 was a wide finger (10 mils) cell which therefore nominally had 9% less active area than the other cells and an equivalent 9.8% efficiency with a relatively good F.F. The wide fingers have partly made up for inadequate doping (edges closer to current generating region) and/or for the thinner front bar. Data from the texturized cells indicates that the former is the more important factor.

Increasing the bar thickness for the se-18-5 x 10^{15} cells (18 & 19) did not improve the F.F. over thinner bar cells, but the data is limited. Cell No. 18 had a bad Al_2O_3 and gave lower current and F.F. as in other bad Al_2O_3 cells. Cell No. 19 was rather interesting in that it was broken across all 28 fingers and had both tabs ripped out during implant. It nevertheless still had an efficiency of 7.9% with only one end of the remaining bar contacted during testing.

Both of the two se-18-10^{16} cells (20 & 21) were of special note. Cell No. 20 had bad undercutting and some back problems but had a relatively good F.F. Again the thin Al layer over the front surface due to the undercutting apparently helped to compensate for inadequate doping but also caused lower current. Cell No. 21 had two ripped out tabs, but still performed reasonably well after H.T.

The two t-9-5 x 10^{15} cells (22 & 23) were clear of major problems in fabrication except for the general undercutting problem. Cell No. 22 had rather poor performance for such a clean cell with the lack of F.F. most likely due to inadequate doping. Cell No. 23 was reasonable, especially in view of the thin bar and low doping and indicated that the 9 μ bar might be satisfactory with better

implant conditions. It should be noted that the standard was also implanted at 5×10^{15} but at 75 keV and had a much thicker front contact(23 μ).

Of the five t-9-10^{16} cells(24 - 28) available, only No. 24 which had wide fingers, a bad Al_2O_3 and a double H. T. was of special note. The latter factor is unimportant since there was no change in the cell after the second H. T. (see Fig. 43). The contaminated Al_2O_3, by analogy with previous results, probably explains the lower F. F. than cell No. 17 on an se surface. The effective relative efficiency of 10.6%(9.7% corrected for additional area loss) was, however, comparable. Of the others, cell No. 25 had the best performance and gave the best demonstration of the advantage of higher doping. By comparison, cell No. 27 was optically good and its poorer performance is believed due to lower doping.

The t-18-5×10^{15} cells (29-32) did not show any significant improvement over the t-9-5×10^{15} cells. Cell No. 29 had wide fingers and a definite sheen at low angles indicating widespread undercutting probably resulting in current loss. Its relative efficiency(area corrected) was 9.8%. Cell No. 31 had bad undercutting and unlike other similar cases, had a poorer rather than better F. F.

Results for the t-18-10^{16} cells(33 - 37) were relatively consistent. The lower current for No. 37 which had a broken corner is unexplained.

The next group (38-41) involves four p cells having 9μ front contacts and either 5×10^{15} or 10^{16} ions/cm^2. All of these cells had tab cratering etc. and still performed within 10-20% of the better cells. In general this was true also of the damaged 18 μ cells (group 42 - 47). Cell No. 43 was a multiple H. T. and had values of 9.1% and .66 before the second H. T. Cell No. 42 had very bad undercutting and a heavy or low energy implant in the Al_2O_3. A few additional cells(48 - 51) which had various processing problems and were used for multiple H. T. experiments(see Figs. 43 & 44) were included as examples in the delivered samples. The effect of very bad backs due to the original residual wax problem was evident in cells 49 and 50. Cell 49 also had a very non-uniform doughnut shaped implant.

The previous cell data indicates strongly that inadequate doping was a major factor in limiting cell performance through increased series resistance

and poor current collection. Performance of the p cells which finished processing indicates that the higher level of doping in the polished surface versus the higher area texturized surface(for same number of incident ions) made up much of the advantage of the lower reflectivity and higher current of the texturized cells. There may be a small advantage for the 18 μ thick front contacts versus the 9 μ contacts but it is not obvious that this would be true if the sheet resistance of the implanted layer were significantly reduced. A preferred approach is increased doping and/or more fingers plus a slightly wider main contact bar. The latter could be done with no loss in area using standard tapering techniques. This was considered originally and rejected for the program because of the difficulties in making the mask.

In order to evaluate further the relative importance of front contact thickness and doping level, series resistance measurements were made on selected cells (Figs 45-49) using the Handy[6] method. The major difficulty encountered in obtaining believable results with this method was that quite small shifts in temperature can shift the voltage enough to significantly affect the measured values. This was minimized by making the measurements at the two light levels for a particular cell as closely together as possible and with a minimum exposure to the light. These curves were taken with the older standard which accounts for the efficiency differences vs. Table 11. The values quoted below are therefore below the true values by .6-.8% absolute.

Fig. 45 compares two similar (t-9 μ) cells differing only in the number of implanted ions with the values of Rs being calculated at two different points on the curves. The 10^{16} ions/cm^2 cell (No. 26) shows an approximate 25-30 mΩ advantage over the 5 x 10^{15} ions/cm^2 cell (No. 25). However the efficiencies and fill factors were comparable within experimental error. A similar comparison (Fig. 46) was made for t-5 x 10^{15} ions/cm^2 having 3 different front contact values including regular 9 μ (No. 23) and 18 μ (No. 32) cases and a wide finger -18 μ case (No. 29). Values of Rs were very similar for all three cells. Efficiencies etc. were very similar for No. 23 (9 μ; 9.5%; .65 F.F.) and No. 32 (18 μ; 9.4%; .64 F.F.) indicating little advantage for the

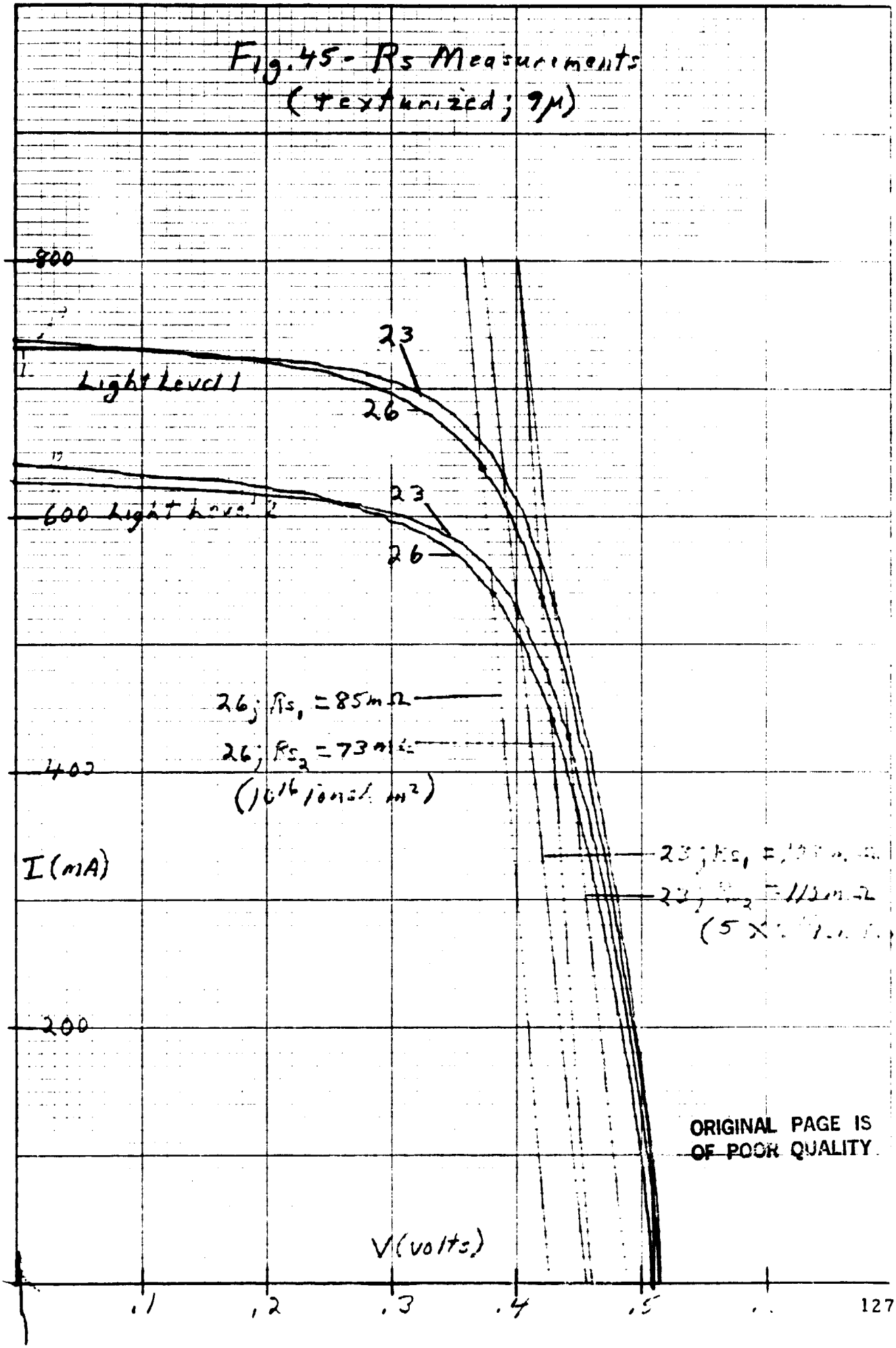

ORIGINAL PAGE IS OF POOR QUALITY

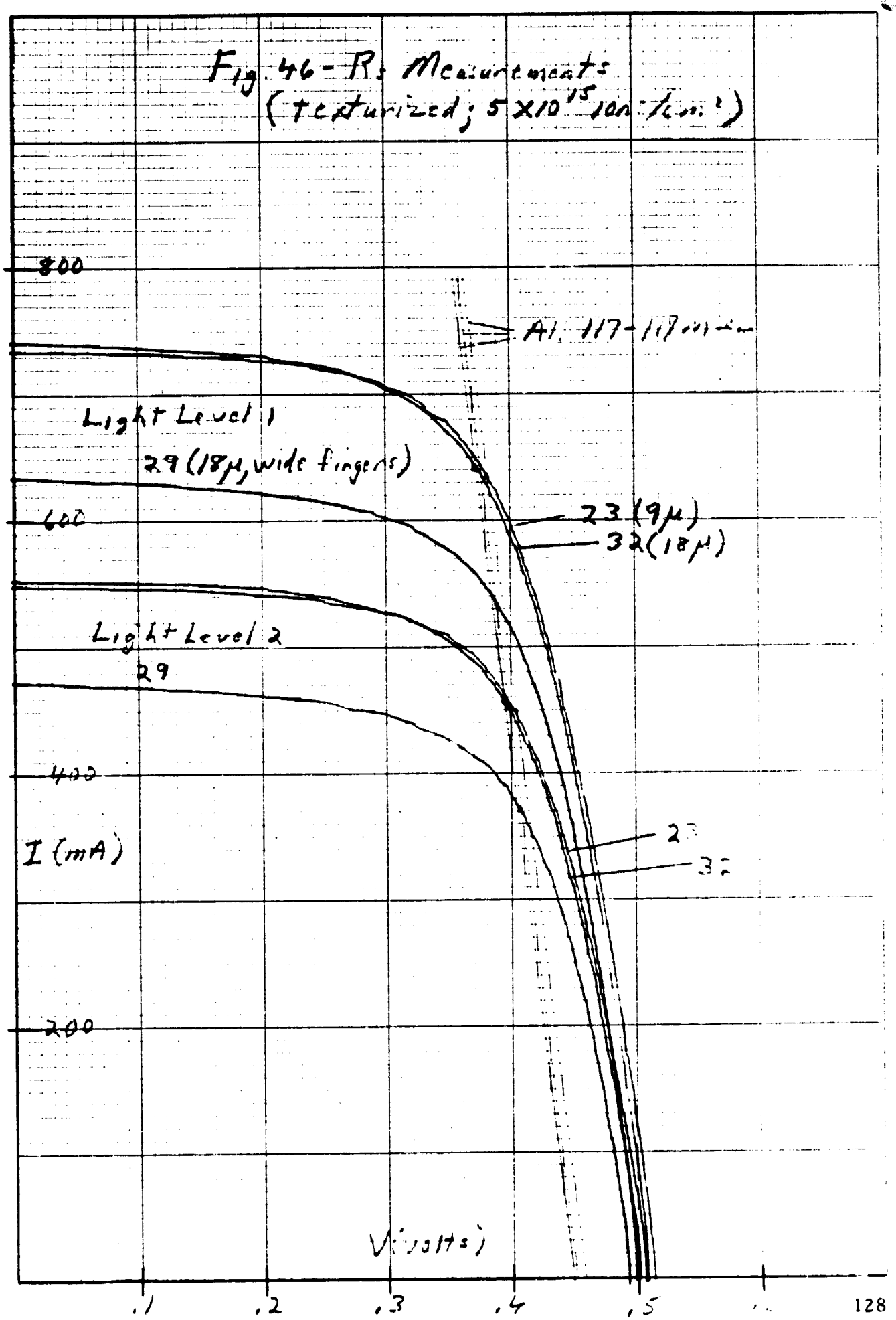
Fig. 46 - R₂ Measurements
(texturized; 5 X10^15 ion/cm²)
800
600
400
200
I (mA)
Al. 117-118 mm
Light Level 1
29 (18μ, wide fingers)
23 (9μ)
32 (18μ)
Light Level 2
29
23
32
V (volts)
.1
.2
.3
.4
.5

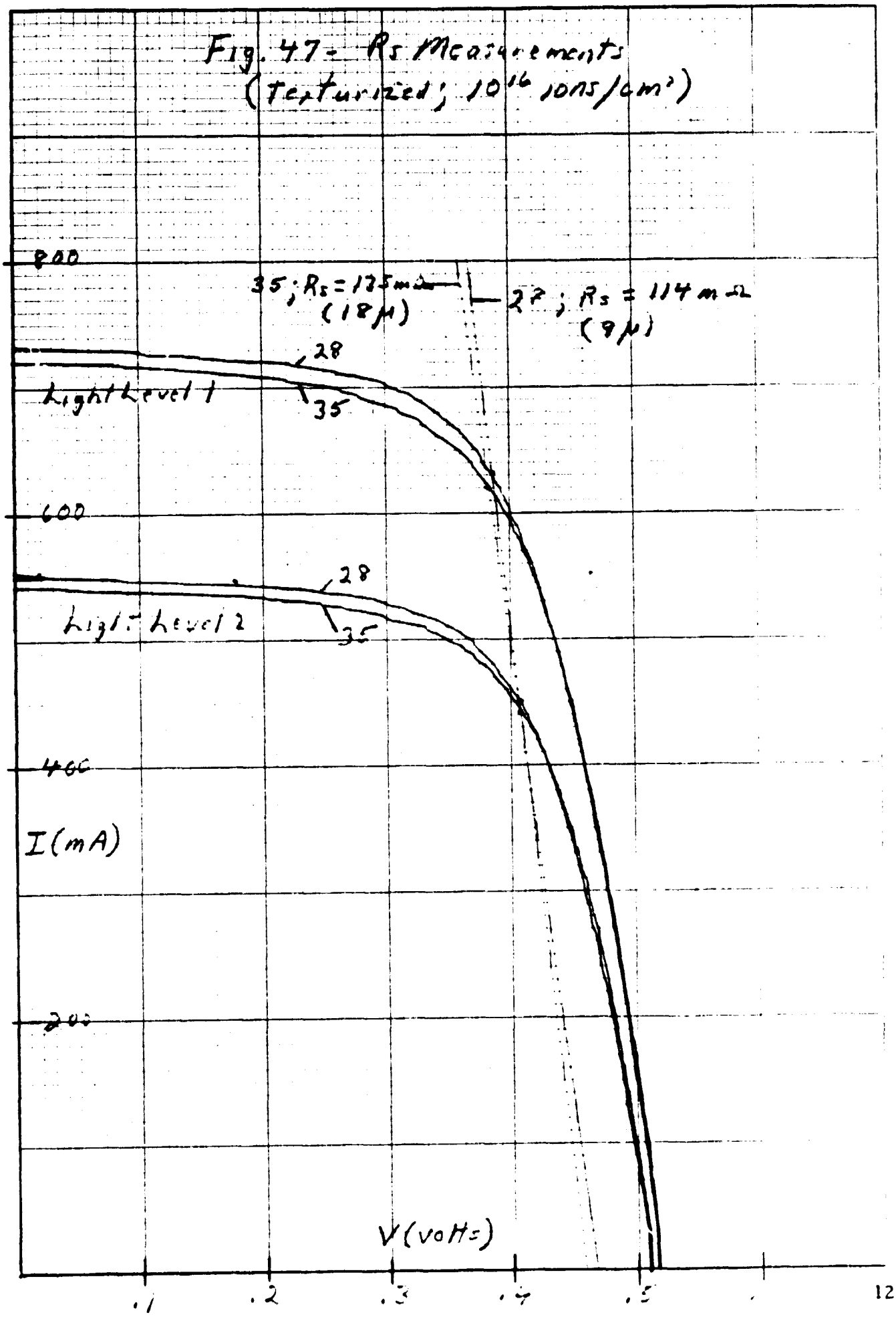
Fig. 47 - Rs Measurements
(Texturized; 10^16 ions/cm^2)
800
35; Rs = 125 mΩ
(18 μ)
22; Rs = 114 mΩ
(9 μ)
28
Light Level 1
35
600
28
Light Level 2
35
400
I (mA)
200
V (volts)
.1
.2
.3
.4
.5

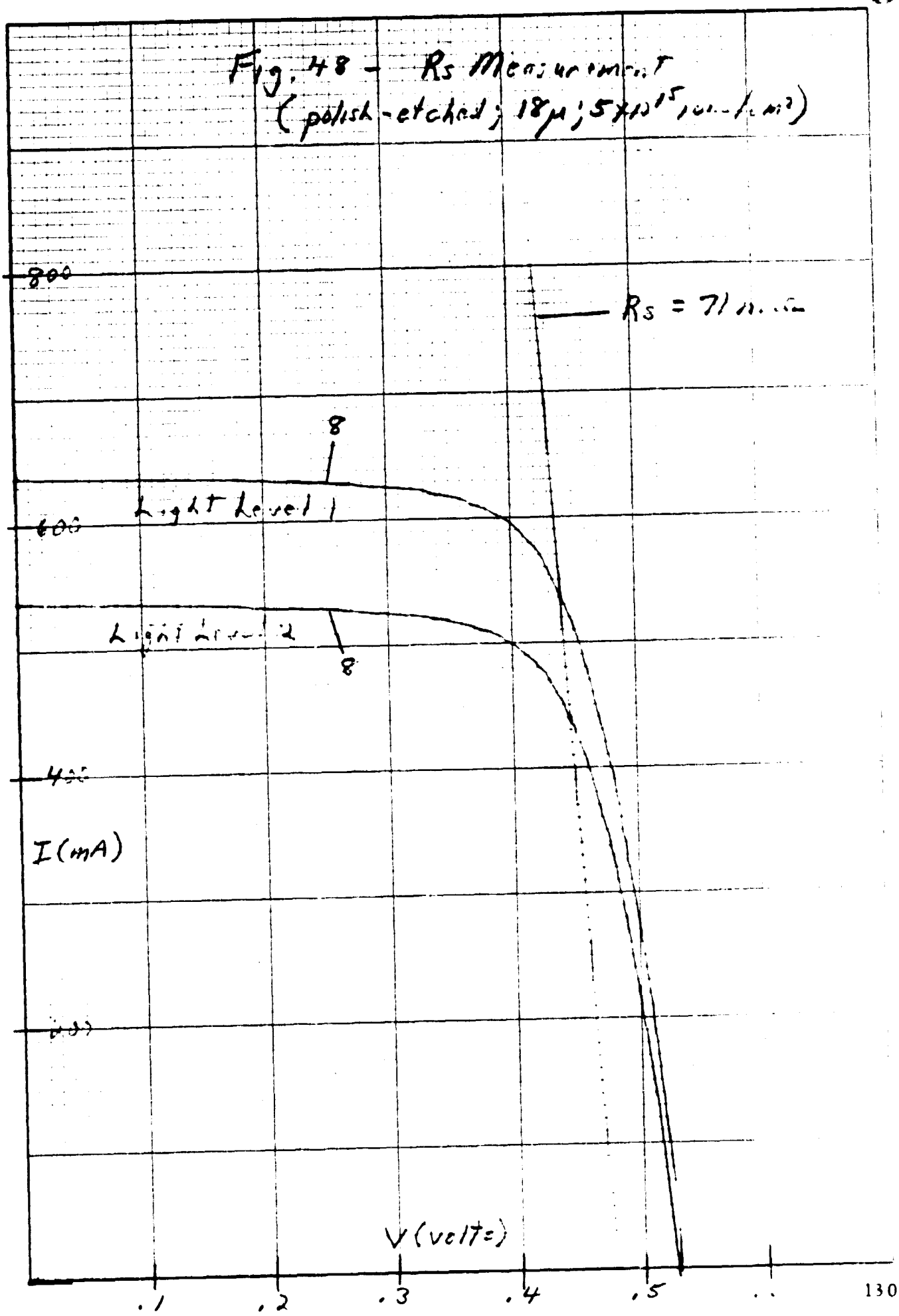
Fig. 48 - Rs Measurement
(polish-etched; 18μ; 5×10^15, [illegible])
Rs = 71 [illegible]
8
Light level 1
Light level 2
8
800
600
400
200
I (mA)
V (volts)
.1
.2
.3
.4
.5

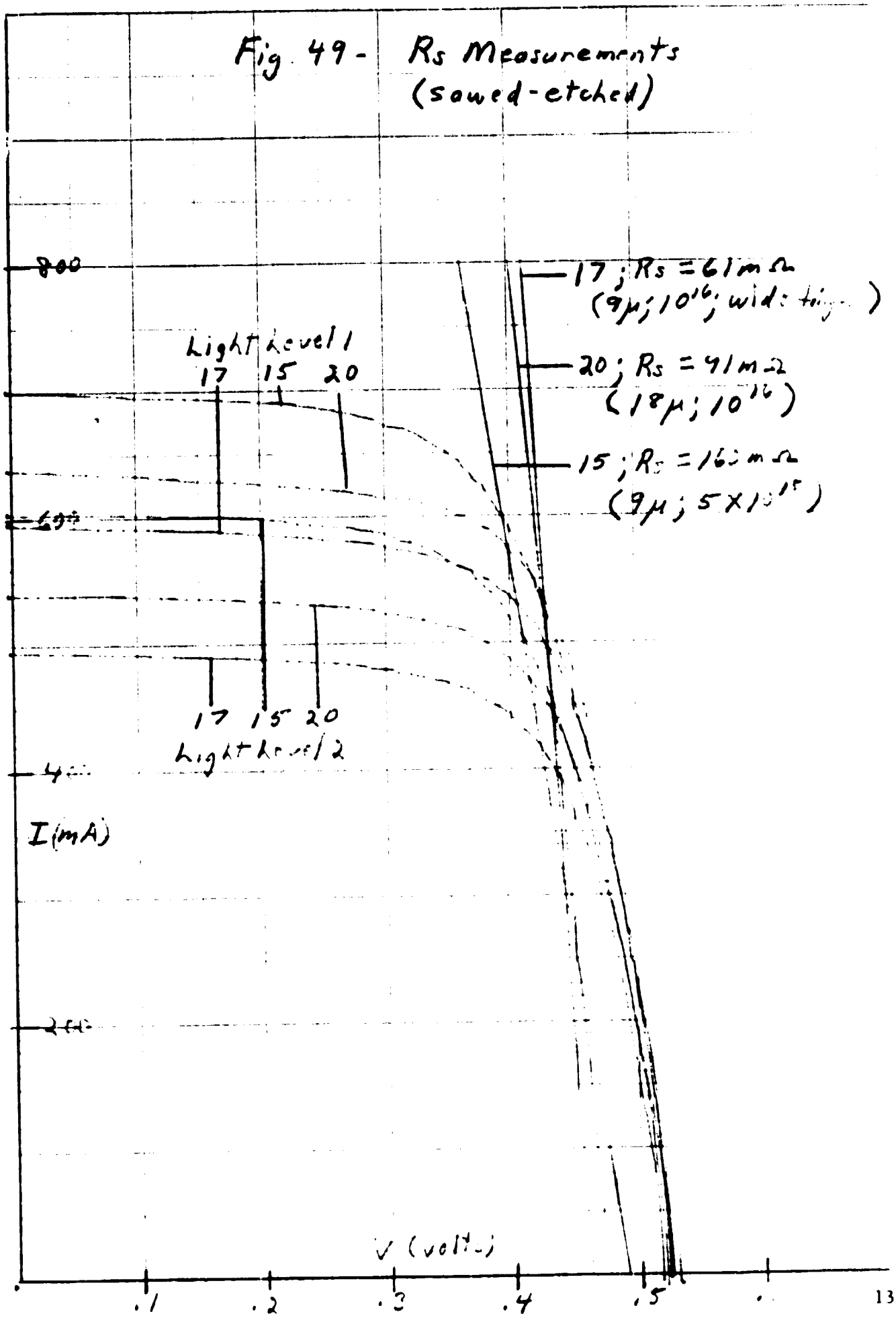
Fig. 49 - Rs Measurements
(sawed-etched)
17 ; Rs = 61 mΩ
(9μ; 10^16; wide fingers)
20 ; Rs = 91 mΩ
(18μ; 10^16)
15 ; Rs = 163 mΩ
(9μ; 5×10^15)
Light level 1
17 15 20
17 15 20
Light level 2
I (mA)
V (volts)
.1
.2
.3
.4
.5

18 μ cell. The wide finger cell (18μ) measured lower in efficiency (8.8% area corrected) but slightly better in overall F.F. (.66). The final texturized cell comparison (Fig. 47) was on two similar 10^{16} ions/cm^2 cells having different front contact thickness. Here the 18μ cell (No. 35) has an advantage over the 9μ cell but the difference is small when the experimental error (estimated at ±10%) is considered.

It was difficult to obtain similar comparisons on p cells because other factors (tabs etc.) tended to complicate the results and conclusions. Fig. 48, however, shows an interesting cell (No. 8) which had 18μ front contacts and 5×10^{15} ions/cm^2. Rs for this cell was relatively low (71 mΩ) in spite of the lower doping level as well as a bad tab and undercutting. The Al layer from the undercutting may be responsible for the lower Rs value, and much lower Isc (631 mA) in this case. The F.F. however was .72 giving a cell efficiency of 9.3%.

Comparison on se cells was also difficult. Fig. 49 shows three quite different cases including wide finger-9 μ-10^{16} (No. 17), regular 9μ-5×10^{15} (No. 15), and regular 18μ-10^{16} (No. 20). The measured Rs value on No. 17 was the lowest obtained on any cell in spite of the 9μ front contact with the 18μ-10^{16} case being acceptable and the 9μ-5×10^{15} case being a bad third.

From this and previous data it was concluded that the inadequate doping level (approximately 1/4 of design) and the finger spacing were factors which could most readily be changed to make significant improvement in cell performance. The other major factor was the undercutting problem. Additional fingers, a modified bus bar and reduction of the undercutting all required a masking change. The simplest method of raising the doping level was to get more of the incident ions into the material which required higher energies, as per the original requirements. (More incident ions require more current which in the long run is not desirable for economic reasons). Polish-etched cells have a distinct advantage for doping level in general because of the smaller surface area. Sawed-etched cells are better than texturized in this regard, but the data from the present experiment is not adequate to be sure of their relative performance. Results for se cells, however, in view of the various problems, are considered very encouraging.

Conclusions

The following conclusions were drawn from this phase of the program:

1) The processing method can be used on any of the three surfaces (t, p, se) studied. Relative importance of the three surfaces is likely to be heavily dependent on economic factors.

2) Inadequate doping of the surface layer due to too low an implant energy is a major factor reducing I_{sc} and F.F.

3) Thicker front contacts are marginally better than the 9μ design value. A better approach to improved performance would be a new front contact configuration with more fingers and a tapered bus bar, combined with higher doping.

4) The Spire implant facility (Extrion Machine) presents problems for KCI's cell structure using polished-etched material(minor problem on se) with respect to tab and bus bar cratering. This problem might be alleviated with suitable cell holders but an improved machine with higher energy is a preferred solution.

5) Undercutting of the front contact mask is seriously reducing light generated current and to a lesser extent V_{oc} (note: Voc for p is higher than se which is higher than t - reverse order to surface area doped). Improved masks and hold-down methods are the obvious solution.

6) Operational cells with less than 20% performance degradation are obtained independent of major process problems or deficiencies, with no need for normal semiconductor production precautions.

ORIGINAL PAGE IS
OF POOR QUALITY

Non-Analyzed Ion Beam Cell

In an effort to anticipate the future needs of the basic process being developed under this contract, KCI conducted a short-term experiment to demonstrate a KCI proprietary process for making ion implanted solar cells using a non-analyzed ion beam. This experiment was carried out at the same time as the preliminary solar cells, before the first 50 cell test lot. In order to optimize information flow, the results of the highly successful non-analyzed ion beam experiment were presented, along with data on the preliminary cells, at the 12th PIM (April 4-5, 1979). These results were omitted from the slide data in the JPL report of the meeting and are included here, as presented, for reference. Because of this experiment, KCI was confident that its semi-analyzed ion beam machine (see next section) could be used for the final 50 cell demonstration lot.

All fabrication conditions for the cell (938-1, see Figure 50) were similar to those used in the present program, except for the implanting ion beam which was accelerated directly into the cell from the source without intermediate mass analysis to remove undesired beam impurities. The source was a proprietary low density type operated on BF_3 and produced a beam containing B, F, F_2, BF_2, BF_3 etc. (from quadrapole spectrometer measurements). The implant level was estimated by implanting areas between bars as in the present program, and is believed to be about 10^{16} boron ions per cm^2. The back contact for this cell, which was also made from one of the old "backed" test blanks, was reasonably good with only very minor non-alloyed areas along part of the edge. The front contact, however, was made in conformance with the program defined acceptable thickness of 9μ, and therefore had relatively high bus bar and finger resistance; i.e. along metallization, not to cell.

Implantation was carried out at 50 keV for comparison with the analyzed beam cells implanted at Spire. Most of the heavier ions (F_2 up) were stopped in the implantation oxide with only F ions getting through as contaminants. Figure 50 also shows a curve for cell J-34-2, the old standard. These curves were taken before the simulator was modified for temperature control, and

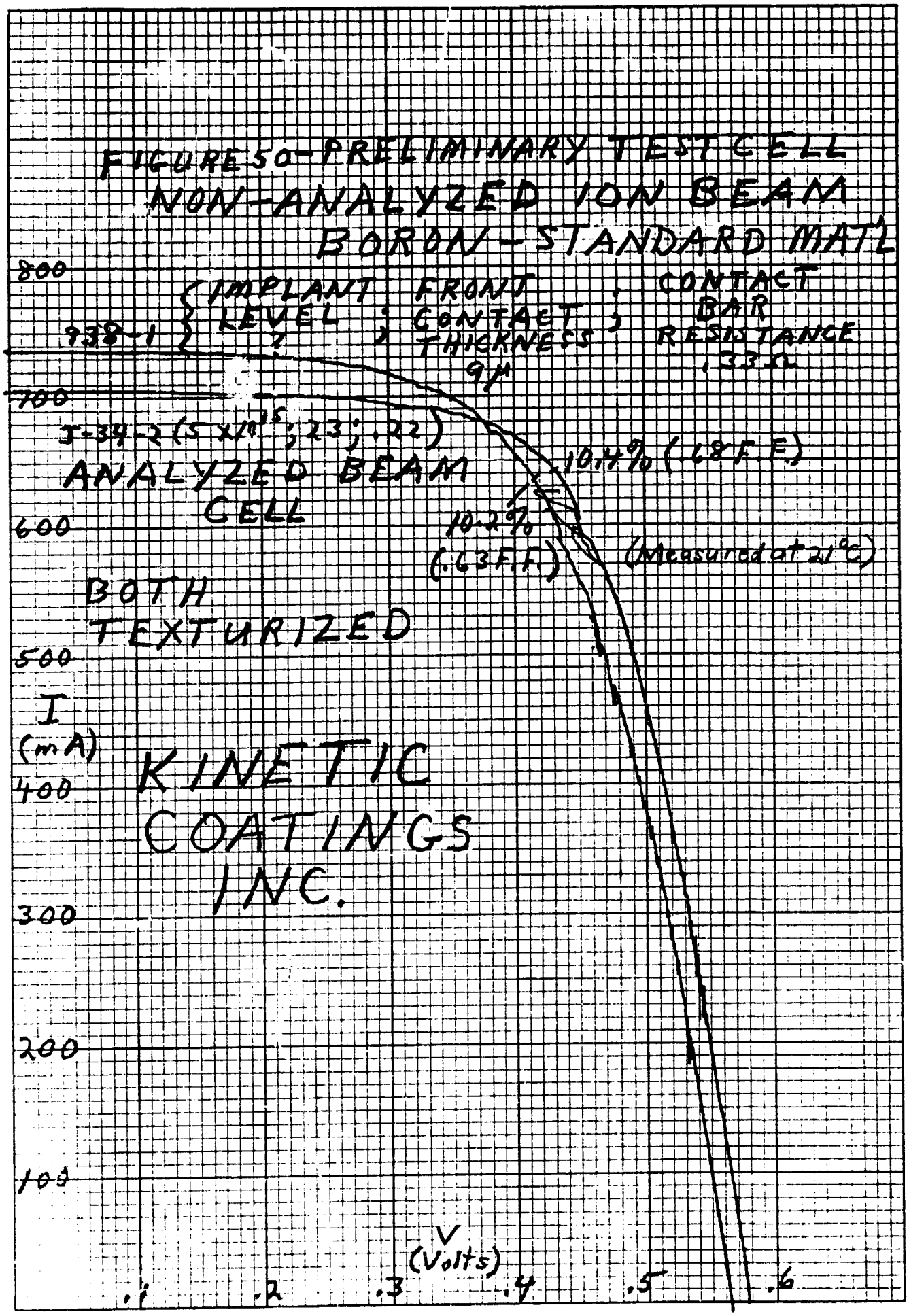
FIGURE 50 - PRELIMINARY TEST CELL
NON-ANALYZED ION BEAM
BORON - STANDARD MAT'L
938-1
IMPLANT LEVEL ?
FRONT CONTACT THICKNESS 9μ
CONTACT BAR RESISTANCE .33Ω
J-34-2 (5 x 10^15 ; 23 ; .22)
ANALYZED BEAM CELL
10.4% (.68 F.F.)
10.2% (.63 F.F.)
(Measured at 21°C)
BOTH TEXTURIZED
KINETIC COATINGS INC.
I (mA)
800
600
500
400
300
200
100
V (Volts)
.1
.2
.3
.4
.5
.6

were taken at 21°C leading to high V_{oc}. The efficiencies, however, are somewhat below the true values due to the standards problem discussed previously. Cell 938-1 was the first cell tried on the non-analyzed beam system. Other experiments by KCI confirmed the results which, for proprietary reasons, are only summarized here.

Modifications to this non-analyzed ion implanted (NAII) cell, and to the procedure for making it, for improved performance are relatively straightforward. Some severe limitations which were in force in the crude demonstration can be eliminated simple by using proper equipment. The present result is a very significant advance towards achieving the ultimate objective of a completely automated, simple and inexpensive cell manufacturing process.

Semi-Analyzed Implantation Machine

Results from the non-analyzed cell clearly indicated that a non-analyzed or partly analyzed beam could be used to make the cells under this program. KCI had access to an old solar cell production machine[3,7] used on the early Air Force ion implanted cell programs in the mid '60's. This machine (Figure 51(a)) was the first pre-acceleration analysis machine and is extremely simple in concept. The ions extracted from the source at a few keV are analyzed by a very low mass resolution magnet system and are then accelerated to the substrate which is at potential. Originally it was used for phosphorus with the source fed with PH_3. Because of the large separation of the P and H ions, poor mass resolution was adequate. PH ions were known to give the same cell characteristics as P ions.

For present purposes, the machine was modified to simplify it still further and to make it compatible with an automated process of the type being developed under this program. In essence, it delivers accelerated ions through a hole in a dome at high potential. The cells flowing through the dome are implanted to the desired dose which is a function of flow rate and ion current. The source is a proprietary low density type which gives 175-200 hours of operation before requiring maintenance. The latter is usually restricted to filament replacement and a multiple filament arrangement can

ORIGINAL PAGE IS
OF POOR QUALITY

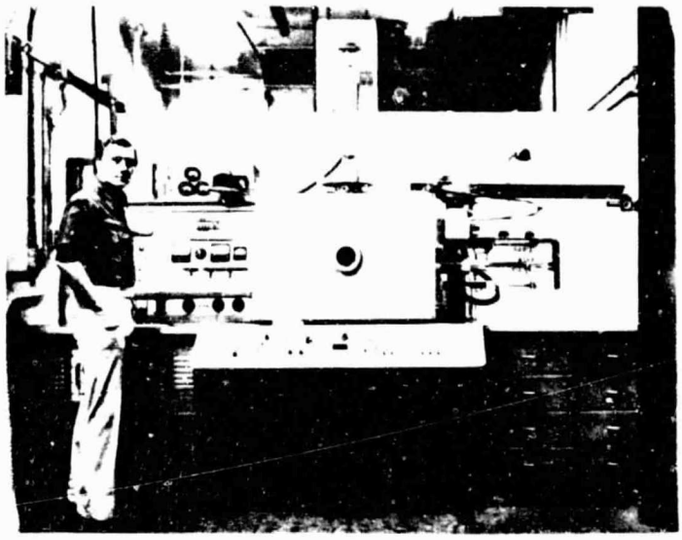

Figure 51(a) - Overall Machine

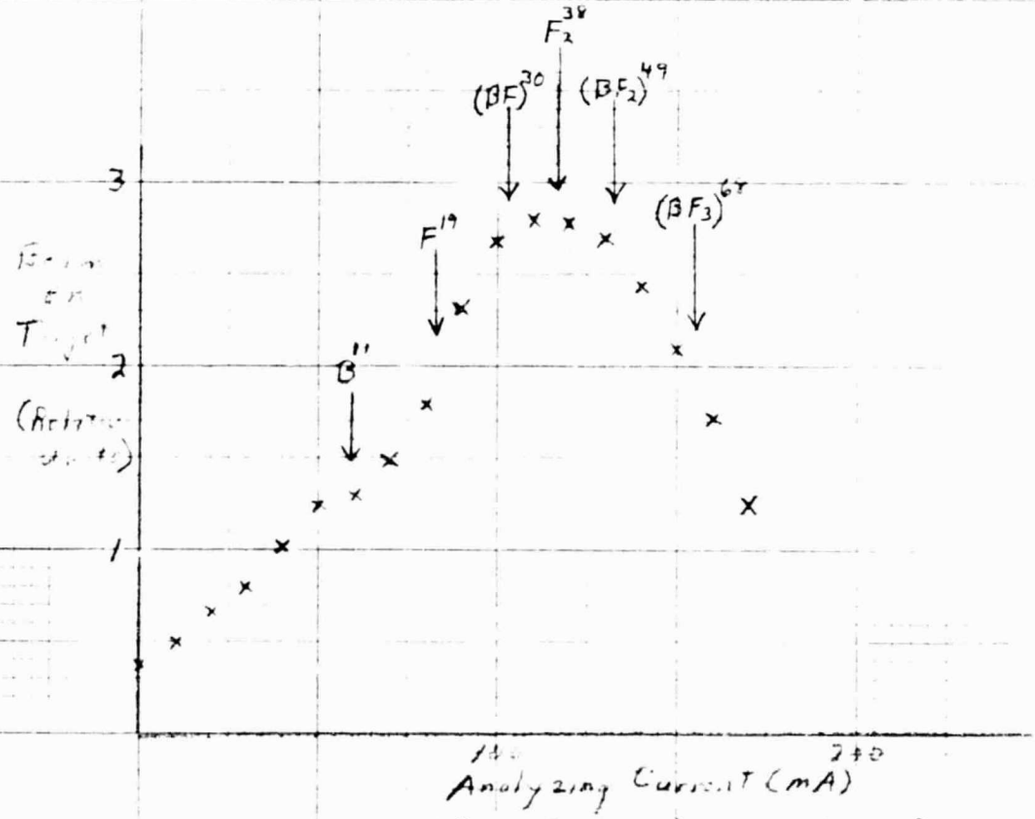

Figure 51(b) - Semi-Analyzed Beam Distribution

Figure 51 - Semi-Analyzed Implantation Machine

therefore extend up time to many hundreds of hours before maintenance is required.

For the 5 x 5 cm cells a uniform line beam 1 x 5 cm extracted from the source produced a 5.6 cm long intercept area overlapping the cell in one direction. Uniformity in the other direction was obtained by linear operation under the beam. The system used could easily be scaled to a 10 x 50 cm, or larger, beam. For KCI use on non-analyzed cells, the magnet can be removed so that the source feeds directly into the dome and on to the cells. In this configuration, an enlarged version could provide a 50 cm x 50 cm, or larger, beam.

Since the non-analyzed ion beam approach did not become incorporated into the present contract, KCI decided to restrict this program to the semi-analyzed version. This approach, although slightly more complicated, does avoid any complications due to sputtering by the heavier ions (see Fig. 51(b)) from the source. Some evidence of this was seen in the non-analyzed cell done at 50 keV. The effect is considerably lessened at 75 keV and can easily be compensated for, if necessary.

Ion energies up to 150 keV are available with this machine. The primary motivation in assembling the machine was to have enough energy available to implant near the optimum value (75 keV). A secondary motivation, or course, was to test the semi-analyzed approach on a batch of cells.

As viewed in Fig. 51 (a), the machine is mounted on a chem lab bench. The power supplies are to the left with the vacuum chamber in the middle , having a bushing on top to bring the accelerating voltage to the dome in the middle of the chamber. The source is in back and cells are loaded in batches through a large door in the end of the vacuum chamber. The ion source and accelerating components are very simple and can easily be expanded and incorporated into a large automatic machine.

Fig. 51 (b) gives the relative ion current as a function of the analyzing magnet current (I_A) with the prime masses of interest indicated. For implantation of the final cell lot the magnet was set at the nominal position

(I_A = 60) for B''. At this setting there is a large component of F^{19} and underlying contributions from the higher masses, in essence a semi-analyzed beam. The analyzing system to achieve this degree of separation is quite simple and inexpensive and can readily be duplicated on a large scale. with permanent magnets.

Demonstration Cells

A final lot of 50 delivered cells was made using the semi-analyzed machine and fixed parameters. The cells had the standard texturized surface and Al_2O_3 coating, a front contact 9 μ thick and a back contact composed of .5 μ Ag overlaid with 1.5 μ Ni. To allow for breakage, 55 blanks were started, five of which had backs applied 9 months previously.

Although the semi-analyzed beam had been tested on sheet resistance test samples, no solar cells had been made and it was not known whether the standard 10 minute heat treatment would be effective. It was decided to use the 5 older blanks for initial annealing tests and then to do the other 50 cells in lots of 5.

During processing, nine of the new blank cells were broken, five badly. Four of them with small to large corner breaks were included in the delivered lot. Data on the delivered 50 cells is given in Table 12. The 5 older blanks are cells 101-105 and the cells with broken corners were 110, 115, 125, and 132. All data was taken at 28 ± 1°C using an ELH 300 watt lamp in the simulator. Before each cell's I-V curve was taken, the light level was set with a secondary standard (No. 25) from the first 50 cell test lot. This cell had similar characteristics to the cells being tested and had been tested under AMI conditions by ASEC.

The standard curve obtained by ASEC and the KCI curve for the best new cell are shown in Fig. 52. With the light set at the proper value, the ASEC curve for the standard could not be exactly reproduced on the KCI simulator. The efficiency ran a few percent low while V_{oc} ran a few millivolts high. The difference in efficiency is probably due to the hold down system. In the KCI system the cells are pressured against the backing plate by weighted contacts at the contact pads only. Since the cell back contact was designed to

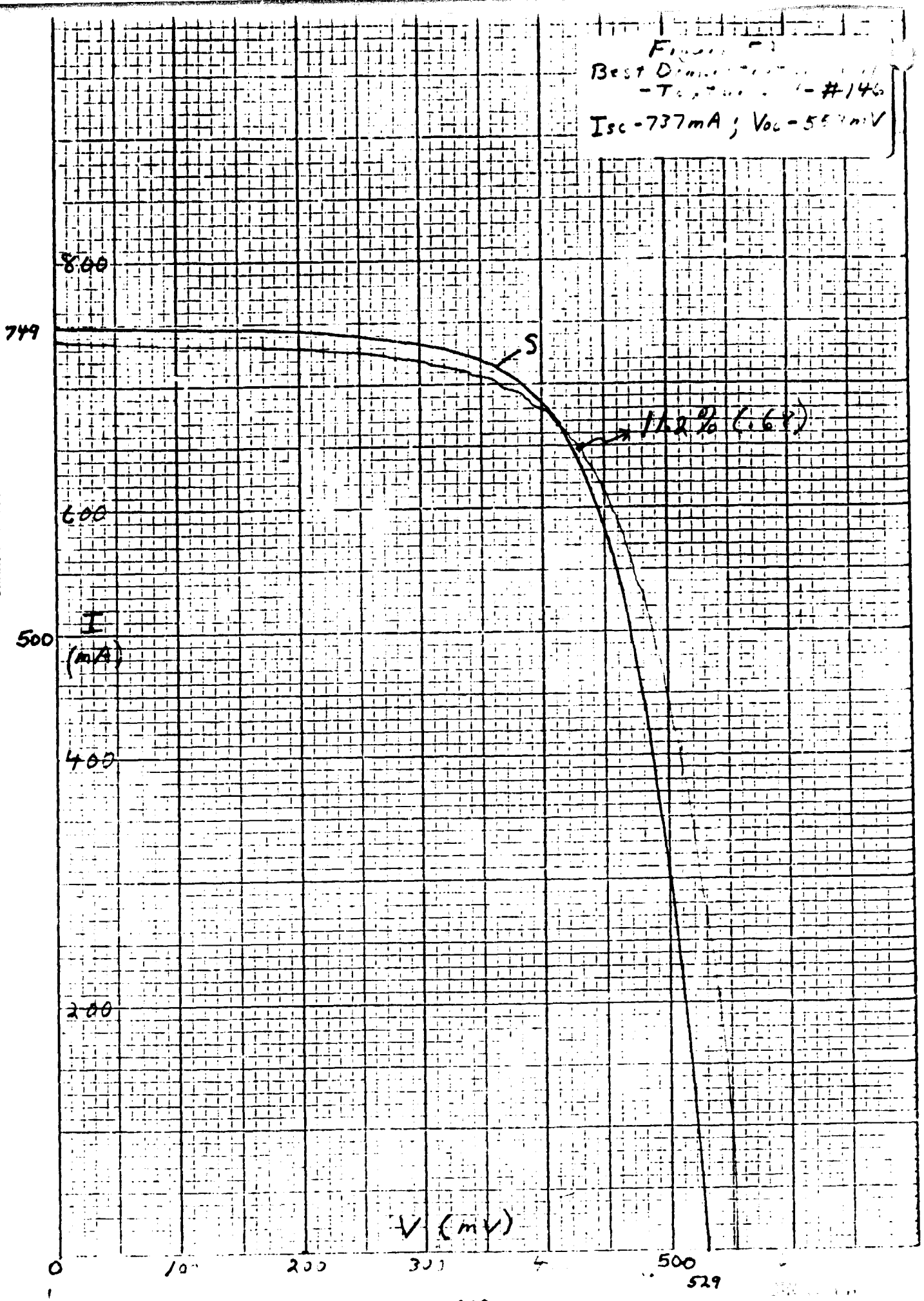

CHART NO. 16800008-001

POOR QUALITY

TABLE 12

DEMONSTRATION CELLS

Sample No.	I_{sc} mA	V_{oc} mV	Eff. %	Fill Factor
101	724	549	10.4	.66
102	776	544	10.7	.63
103	741	545	9.9	.61
104	721	554	11.2	.70
105	748	548	10.9	.67
106	665	534	9.5	.67
107	720	540	10.1	.65
108	720	548	10.6	.67
109	688	537	9.9	.67
110*	696	538	9.9	.66
111	731	537	9.7	.62
112	719	533	10.1	.66
113	705	528	9.5	.64
114	747	549	10.6	.65
115*	744	544	10.6	.65
116	705	540	10.0	.66
117	706	545	10.3	.67
118	744	545	10.8	.67
119	720	537	10.0	.65
120	751	546	10.7	.65
121	757	542	10.5	.64
122	746	547	10.7	.65
123	691	531	9.4	.64
124	731	540	10.4	.66
125*	725	543	10.3	.66
126	729	545	10.5	.66
127	696	532	9.5	.64
128	726	541	10.3	.66

TABLE 12 (continued)

Sample No.	I_{sc} mA	V_{oc} mV	Eff %	Fill Factor
129	686	529	9.4	.65
130	744	549	11.0	.67
131	718	530	9.4	.62
132*	695	540	10.0	.66
133	695	537	9.9	.66
134	723	547	9.6	.61
135	748	551	10.5	.64
136	725	541	10.4	.66
137	713	540	10.0	.65
138	740	550	11.0	.68
139	732	545	10.7	.67
140	740	550	11.1	.68
141	747	548	10.5	.64
142	766	547	10.9	.65
143	749	551	11.1	.67
144	725	545	10.6	.67
145	727	551	11.0	.68
146	737	553	11.2	.68
147	725	549	11.0	.69
148	725	545	10.6	.67
149	748	554	11.0	.66
150	693	541	10.2	.68
AVERAGE	725	543	10.36	.65

* Broken Corner.

be contacted at multiple points, with the sheet resistance adjusted accordingly, this two point hold down can intoduce a series resistance relative to a vacuum hold down. The latter would be a better approximation to an interconnected cell. In any event, the simulator was always set such that the standard curve on the KCI simulator was inside the ASEC curve around the maximum power point. The KCI efficiency values are therefore believed to be close to the real values but slightly on the low side.

Because of the limited number of cell blanks remaining from the initial crystal, it was necessary to do annealing studies for the semi-analyzed ion beam cells on the cells to be delivered. These studies were therefore done carefully on successive batches of 5 cells. The first batch of 5, which consisted of the older blanks (samples 101-105), gave efficiencies of 9.9-11.2% (average 10.6%) and indicated no problems with the semi-analyzed beam. Succeeding batches , however, appeared to give somewhat lower efficiencies and V_{oc} values.

Many variables were checked including beam energy and composition, possible furnace contamination and possible edge shorting effects. The latter effect is possible because of the use of the same mask for the implant and the back contact. Because of slop in the mask it was possible for the back contact to get near one or two of the edges. In addition, undercutting of the front contact mask brought the front contact near the edge. It was believed that the two effects on one edge at the same time could lead to some slight edge shorting since the cells were presized. The solution for this potential problem is a proper back mask with sufficient edge clearance. However, no real data to show that this was a real problem was found.

Also no data of any kind was found to indicate that furnace contamination was a problem. In fact, from studies to date, it is apparent that the furnace condition has essentially no effect on the cell performance. This is obviously due to the passivated front surface and back contact, which during the short anneal prevent the intrusion of contaminants into the cell interior. The material used in this program was tested by ASEC (through JPL) to have a diffusion length of 200 μ before and after annealing.

The factor causing the lower efficiencies was finally traced to an accidental misalignment of the high voltage dome. Interception of the ion beam on the edge of the dome was sputtering stainless steel on to the front and sides of the cells causing some slight decrease in available light and in shunt resistance. After this was corrected, the final 15 cells had efficiencies from 10.0 to 11.2% (average 10.75%) with higher I_{sc}, V_{oc} and F.F. values.

A few of the blanks with broken corners were processed through as cells with polished-etched (as received) front surfaces. These cells were all implanted when the dome was misaligned and inadvertently had Al_2O_3 coatings with the same deposition time as the texturized surface cells. Because of the reduced area the coatings were therefore much too thick (see Section 3.2). In addition, the front surface, as in all cells produced under this program, was 20-30% covered with a thin Al coating due to undercutting of the front contact mask. In spite of these problems, which were partly compensated for by the effectively thicker front contact, the cells were quite acceptable. Fig. 53 shows a typical characteristic for these cells which clustered around 10%. A correct Al_2O_3 coating and implantation without the sputtered stainless steel would raise the efficiencies to at least the 10.5% range.

An important point on these polished cells was that there was absolutely no indication of front contact fracturing or bulging as in the cells implanted on the Spire machine. Power density on the cells during implant was approximately the same. Visual inspection of these cells showed the implants to be uniform, and no anomalous implantation effects were observed on any of the cells produced.

Short Anneal Cycle Cells

Additional in-house experiments were conducted by KCI on broken corner cell blanks to develop a very short anneal cycle process. As part of the machine construction program, KCI investigated the effect that varying the composition of the implanting beam would have on the sheet resistance and annealing characteristics of implanted layers formed in the standard cell structure. A method of altering the beam was developed which

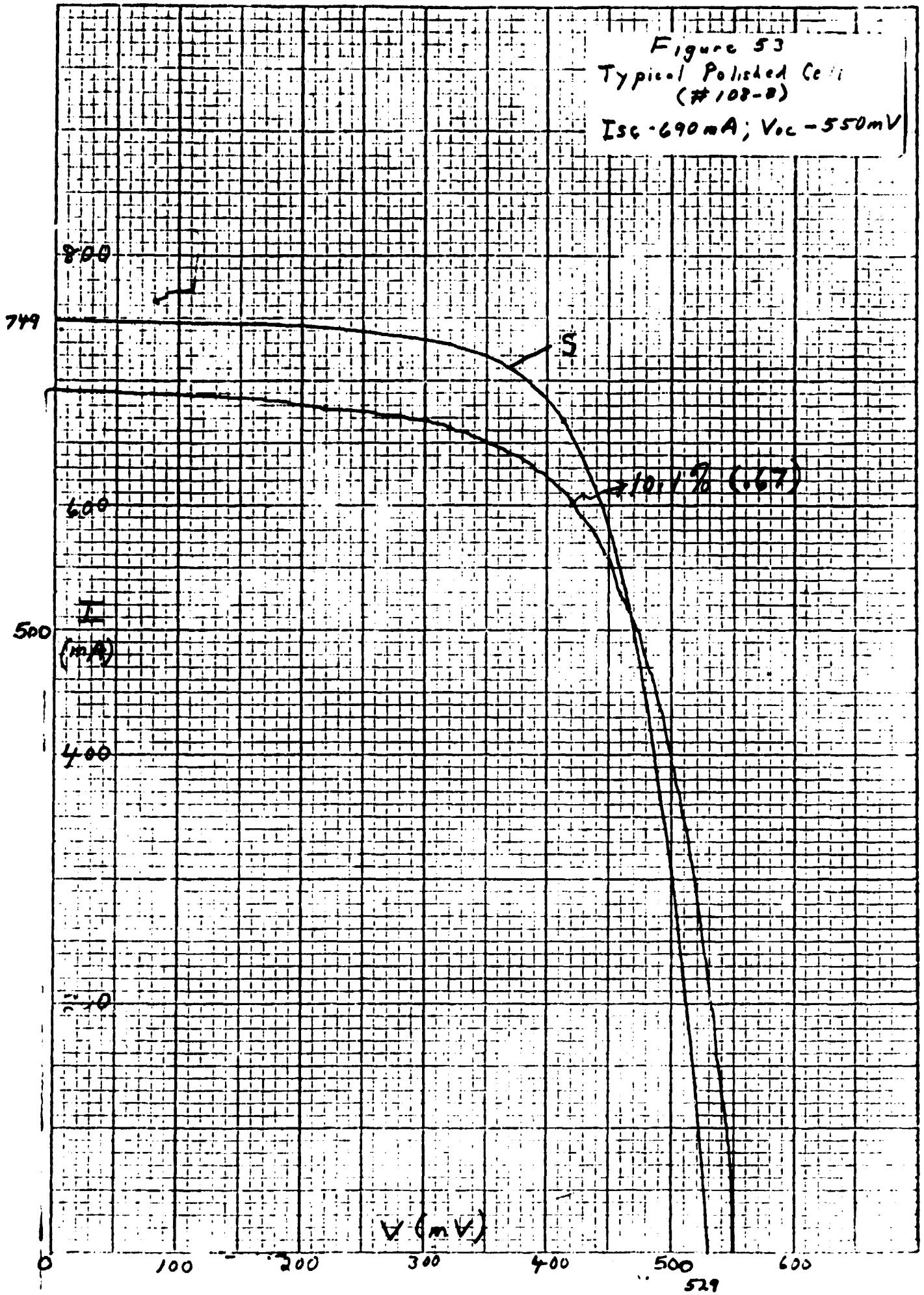

CHART NO. 16800008-001

allowed very short anneal cycles, of the order of 15-22 seconds at temperature. Shorter times could not be investigated because of the time required for the furnace to approach equilibrium after the boat was inserted.

Using this altered beam method, standard structure cells were made with the anneal cycles shortened. Fig. 54 shows the I-V curves for two of these cells (texturized). The first, No. 52-8, was annealed by directly inserting the boat to the center hot zone, leaving it there for 22 seconds and then directly removing it to the cool zone. The first cycle (curve 8-1) gave an efficiency of 10.9%. After a second cycle (curve 8-2) the efficiency dropped to 10.4%. A second cell, No. 52-7, was inserted into the central hot zone with a linear 15 second insertion time, held there for 15 seconds, and then removed with a linear 15 second removal time. The first cycle (curve 7-1) gave an efficiency of 10.5% and the second an afficiency of 10.8%.

Other texturized cells gave confirming results. In addition, one polish-etched surface cell was made with the same implantation technique. This cell was broken across one set of fingers after implant,but before annealing, with the area reduced to 19.8 cm^2. The Al_2O_3 coating for this polished cell was the correct thickness and the anneal cycle was the 15-15-15 second type. The first anneal cycle gave an efficiency of 10.0% and the second an efficiency of 9.9%, (Figure 55). This figure also shows a series of typical standard curves taken on the KCI simulator vs. the ASEC standard curve. This is typical of conditions used in testing all of the demonstration cells.

There were no failures in using the short anneal cycle technique and efficiencies were comparable to the longer cycle cells. Clearly in production the short cycle will be used. For the projected automatic machine (see Section 3.8) the material is 100 cm wide and moves through the machine at 50 cm per minute. A 15-15-15 second cycle would require a hot zone, including approach and recede zones, only 35-50 cm long. The zone for the 22 second anneal would be even shorter. The requirement for this hot zone is only for a simple resistance furnace with thermal reflectors. In vacuum this is a very efficient system and requires none of the complexity of energy beam annealing machines. The anneal cycle itself is also extremely simple,

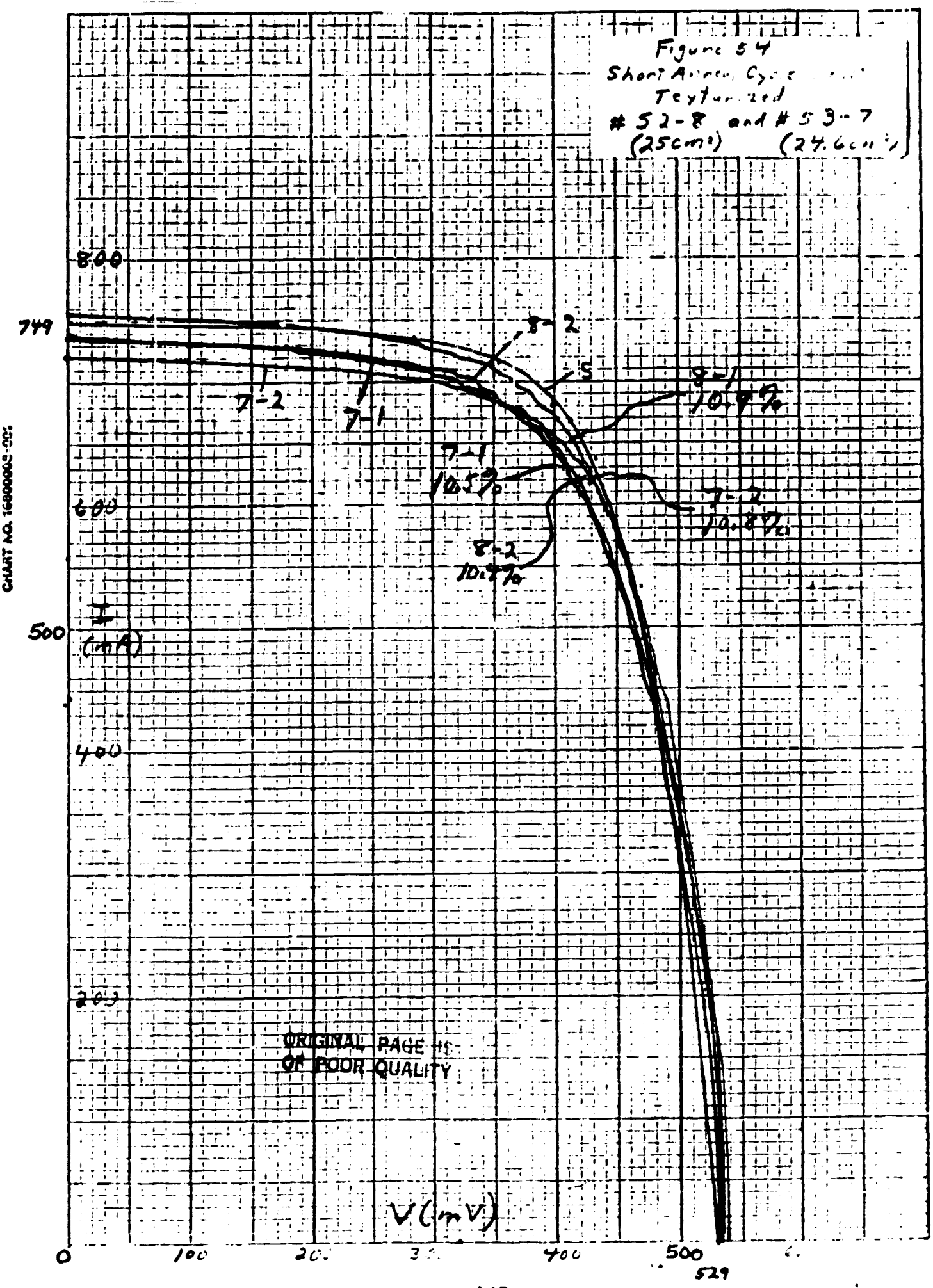
Figure 54
Short Anneal Cycle
Texturized
52-8 and # 53-7
(25cm²) (24.6cm²)
800
749
600
500
400
200
I (mA)
8-2
S
8-1
10.9%
7-2
7-1
7-1
10.5%
7-2
10.8%
8-2
10.9%
V (mV)
0
100
400
500
529
ORIGINAL PAGE IS
OF POOR QUALITY

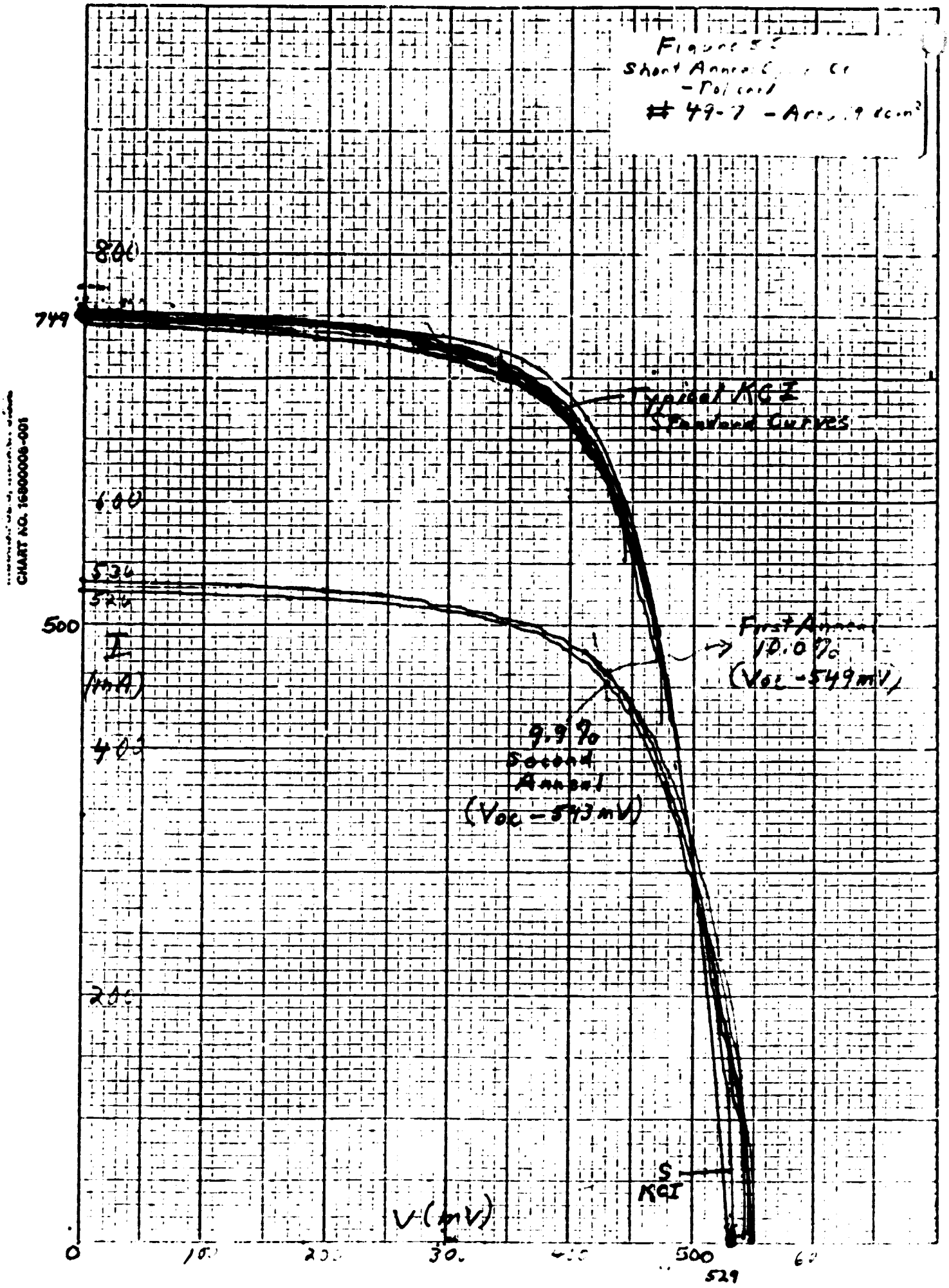

Figure 5
Short Anneal
-Polished
49-7 - Area 9 cm²
800
749
600
536
526
500
I
(mA)
400
200
0
100
200
300
400
500
529
600
V (mV)
Typical KCI
Standard Curves
First Anneal
10.0%
(Voc - 549 mV)
9.9%
Second
Anneal
(Voc - 543 mV)
S
KCI
CHART NO. 16800008-001

especially when contrasted to some of the more esoteric combinations which have been investigated in the higher efficiency cell programs.

3.8 Economic Analysis

An economic analysis (SAMICS) has been performed for projected automatic manufacturing machines capable of accepting incoming wafers at one end and converting them, in one vacuum chamber system, to completed, tested cells at the other. These machines are based on the processes and cell configuration being developed under the present program and on additional proprietary processes which KCI has developed in-house. A simple conceptual outline of the machine is shown in Fig. 56.

Basically material is batch loaded or interlock fed at one end then sequentially goes through the process steps as discussed in this report. The original concept was for linear material such that the front contact could be applied through two internal mask systems. The first consists of variable gaps between bars to apply fingers along the material. The second consists of reciprocating openings to apply main contact bars across the fingers. Alternately flip-on recyclable masks could be used and would extend the system to conventional materials or other geometries. The back mask is relatively simple, consisting of a defined opening for linear material or a flip-on mask for other geometries. In principle, with proper front masking, the back does not have to be masked at all. Strong indications that this is possible were given by cell results during the program. Further considerations on these masks and related effects were not a part of this program, but have been made by KCI.

The combined coating material is applied over the whole front surface and implantation is done through a flip-on edge mask. Annealing, as discussed previously, would be performed in a simple, short, efficient resistance heated furnace. It is possible to perform cell testing in the same chamber, using a simple ELH lamp system and laser marking of rejects. However, the program results indicate that, for a fully developed process and machine, all full sized cells would be usable and could be incorporated into modules with only minor loss in overall efficiency. As touched on briefly in Section 3.3, it is also possible

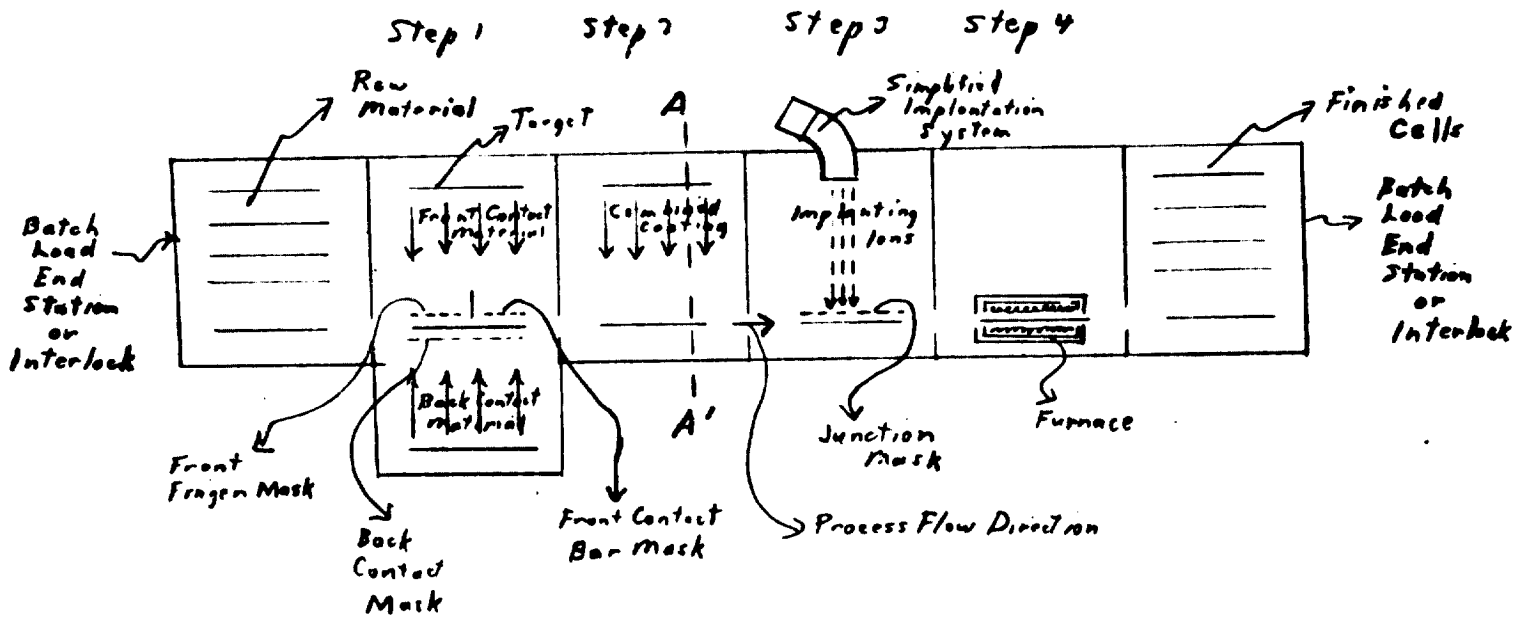

Figure 56 - Projected Large Scale Manufacturing Method

to incorporate partial module fabrication into the same machine.

It is assumed that 4 of these machines would produce 20% of the 1986 goal of 5×10^8 peak-watts/year. A yield of 95% of 10% AMI cells through the machines and a 5% loss in module fabrication are assumed. The 4 machines must therefore process 1.11×10^6 m^2 of starting material to yield 1.05×10^6 m^2 of cells and 1.0×10^6 m^2 of effective module output. The calculated capital cost of each machine was $ 7.5 M in 1979 dollars. This was arbitrarily increased to $ 10M to provide a 33% margin of error in the cost calculations. The equivalent 1975 dollar cost is $ 7.5 M. An additional safety factor was taken in the power consumption which was arbitrarily increased from the calculated 500 kW to 1 MW per machine. Since the SAMICS analysis appears to discriminate against such large automatic machines through the use of people and space multiplying factors which are geared to more labor intensive methods, the resulting cost factors are believed to be on the safe side.

The basic assumptions used in the analysis were:

<u>Machine</u>

No. of machines	:	4
Starts/4 machines	:	1.11×10^6 m^2/yr
Output/4 machines	:	1.05×10^6 m^2/yr-acceptable cells
Operating cycle	:	360 days/yr - 3 shifts
		20 hours/day processing } Average
		4 hours/day maintenance } Average
Operating personnel	:	5/machine/shift
Deposition method	:	Combination of proprietary techniques

<u>Cells</u>

Efficiency	:	10% AMI
Al	:	9 μ - front contact
Al_2O_3	:	.1 μ - combined coating
Ag	:	.5 μ } back contact
Ni	:	1.5 μ } back contact

The SAMICS analysis sheets are attached as Appendix 1. The resulting 1986 inflated price is $.87/peak-watt "through cell production" with a corresponding deflated 1975 price of $.45/peak-watt. This leaves approximately

$.05/peak-watt for module fabrication. Part of the latter can be done in the large machine at essentially no increase in cost.

It is important to note that these calculations have been made with significant safety factors and that the process steps have been clearly demonstrated. From program results, it is reasonable to expect that elimination of factors such as Al undercutting of the front mask would result in production cell efficiencies in the 11-12% AMI range and proportionately lower cost. Finally the process is relatively independent of substrate defects and can be used on more exotic silicon forms.

4 New Technology

No new technology subject to the provisions of this contract has been developed.

5 Conclusions and Recommendations

Conclusions

In addition to conclusions drawn previously as the result of optimization of individual cell elements, the following overall conclusions have been drawn from this program:

1) The basic KCI process is essentially a foolproof technique for fabricating medium efficiency cells in an extremely simple and reproducible manner.
2) The basic cell structure is resistant to catastrophic failure due to breakage, thermal treatment or other potentially destructive process variables
3) The process, as investigated under this contract, is inherently appropriate for automated production without requiring close process control.
4) Inexpensive semi-analyzed or non-analyzed ion beams can be used for fabricating the cells.
5) Thermal treatment for cell activation can be extremely simple, of very short duration, conservative of production energy, foolproof, and cheap.
6) The JPL-SAMICS analysis indicates that an automatic machine for producing KCI type cells could deliver cells at a cell cost of $.45/peak-watt in 1975 dollars. Efficiency increases are likely in production and would lead to proportionately lower costs.

Recommendations

It is recommended that a program be instituted to develop a

production level machine for producing the KCI type cells using a non-analyzed or semi-analyzed implantation approach. Proper implementation of such a program would require the use of the basic method applied during this contract combined with proprietary KCI information and techniques.

REFERENCES

1. AF 33(657)-10505, "P-N Junction Formation Techniques" (Nov. 1962-Sept. 1963).

2. AF 33(615)-1097, "P-N Junction Formation Techniques" (Oct. 1963-Aug. 1964).

3. AF 33(615)-2292, "Ion Implantation Junction Techniques" (Nov. 1964-Jan. 1965).

4. AF 33(615)-3636, "Thin Silicon Solar Cells by Ion Implantation" (Jan. 1966-June 1967).

5. Quarterly #2, June 1976, ERDA/JPL-954352-76/2, p. 10.

6. Handy, R. J. , Solid State Electronics, pp. 765-775, 10, 1967.

7. Burrill, J. F., King, W. J., Harrison, S. and McNally, P., "Ion Implantation as a Production Technique", presented at Fifth Photovoltaic Specialists Conference, Greenbelt, MD, (Oct. 1965); IEEE Transactions on Electron Devices, ED-14, p. 10(1967).

APPENDIX 1

SOLAR ARRAY MANUFACTURING INDUSTRY COSTING STANDARDS

FORMAT A

PROCESS DESCRIPTION

JET PROPULSION LABORATORY
California Institute of Technology
4800 Oak Grove Dr / Pasadena, Calif 91103

A1 Process Referent: ICP

A2 Description (Optional): Single Machine Manufacture of Integral Structure Solar Cells

PART 1 – PRODUCT DESCRIPTION

A3 Product Referent: ISC

A4 Name or Description: Integrated Solar Cells

A5 Units Of Measure: m^2 (Batch Size = 3.85 E 2 m^2)

PART 2 – PROCESS CHARACTERISTICS

A6	Output Rate	6.60 E-1	Units (given on line A5) Per Operating Minute
A7	Average Time at Station	6.00 E2	Calendar Minutes
A8	Process Usage Time Fraction	0.83	Average Number of Operating Minutes Per Minute

PART 3 – EQUIPMENT COST FACTORS

A9	Component Referent	ISCMACH		
A10	Base Price Year For Purchase Price	1975		
A11	Purchase Price ($ Per Component)	7.50 E6		
A12	Anticipated Useful Life (Years)	15		
A13	Salvage Value ($ Per Component)	1.50 E6		
A14	Cost of Removal & Installation ($ Component)	0.75 E6		

ORIGINAL PAGE IS
OF POOR QUALITY

Format A Process Description (Continued)

A15 Process Referent (From Page 1) ICP

PART 4 – DIRECT REQUIREMENTS PER MACHINE

A16 Catalog Number	A17 Requirement Description	A18 Amount Required Per Machine	A19 Units
A2064 D	Manufacturing Space(Type A)	6.40 E3	$ft.^2$
B3240 B	Mechanical Engineer	1	PRSN*yrs
B3704 D	Electronics Technician Automated Processes	4	PRSN*yrs

PART 5 – DIRECT REQUIREMENTS PER BATCH (A continuous process has a "batch" of one unit)

A20 Catalog Number	A21 Requirement Description	A22 Amount Required Per Batch	A23 Units
C1032B	Electricity	1.00 E4	kW-hr
C1128 D	Water-Cooling	9.00 E3	kW-hr
D1160D	Warm Cooling Water	2.40 E4	Gallons
D1176 D	Rejected Cells	1.93 E1	m^2
EG1088D	Alumina	5.40	Oz.
E1096D	Aluminum	2.07 E1	lbs.
EG1396D	Nickel	1.14 E1	lbs.
E1592D	Silver	2.02 E3	grams

PART 6 – INTRA-INDUSTRY PRODUCT(S) REQUIRED

A24 Product Reference	A25 Product Name	A26 Yield Factor (Usable Output Input)	A27 Units
CSGPS	Clean Solar Grade Polycrystalline Silicon	0.95	m^2 Cell Material / m^2 CSGPS

Prepared by _____ Date _____

REVERSE SIDE JPL 3037-S 11 77

SOLAR ARRAY MANUFACTURING INDUSTRY COSTING STANDARDS

FORMAT B

COMPANY DESCRIPTION

JET PROPULSION LABORATORY
California Institute of Technology
4800 Oak Grove Dr / Pasadena Calif 91103

B1 Company Referent CELLCO A

B2 Description (Optional) Manufacture of Photovoltaic Cells From Polycrystalline Silicon

B3 Product Produced ISC

B4 Process ICP

B5 Intermediate Product Process

Intermediate Product Process

Intermediate Product Process

Intermediate Product Process

Intermediate Product Process

Intermediate Product Process

Intermediate Product Process

Intermediate Product Process

Intermediate Product Process

Intermediate Product Process

Intermediate Product Process

B6 Purchased Product Clean Solar Grade Polycrystalline Silicon (CSGPS)

B7 Supplier Company Reference WAFERCO A Percent Supplied 250%*

Supplier Company Reference Percent Supplied

* WAFERCO A produces 50% of the solar grade material for the industry, hence 250% of that used by CELLCO A, which produces 20% of the industry's cells.

Prepared by _____ Date _____

JPL 3038 - [illegible]

SOLAR ARRAY MANUFACTURING INDUSTRY COSTING STANDARDS

FORMAT C

INDUSTRY DESCRIPTION

JET PROPULSION LABORATORY
California Institute of Technology
4800 Oak Grove Dr / Pasadena Calif 91103

C1 Industry Referent Samics - 86

C2 Description (Optional) 1986 Standard Industry

INDUSTRY OBJECTIVE

C3 Industry Result New Photovoltaic Power Capacity

C4 Quantity Produced 525×10^6 Peak-Watts/Year

DESCRIPTION OF THE FINAL PRODUCT OF THE INDUSTRY

C5 Reference ISC Name Integrated Solar Cells

C6 Production is Measured in m^2/year

C7 Hardware Performance 100 Watts/m^2 AM1 (C4 per C6)

C8 Product Design Description (Optional) Integral Structure Solar Cells

MAKERS OF THE FINAL PRODUCT OF THE INDUSTRY

C9 Company Reference CELLCO A Market Share 20%

Company Reference CELLCO B Market Share 20%

Company Reference * Market Share

* Three remaining companies each produce 20% of the industry's output.

Prepared by _____ Date _____

PRECEDING PAGE BLANK NOT FILMED

JPL 3039-S 11/77

JET PROPULSION LABORATORY
California Institute of Technology
4800 Oak Grove Dr. / Pasadena, Calif. 91103

PROCESS WORK SHEET

P1 PROCESS REFERENCE ICP

LABOR PRICES AND COSTS PER MACHINE

P2 Catalog Number	P3 Inflated Price	P4 Cost
B3240B	5.08 E4	5.08 E4
B3704D	2.38 E4	9.52 E4

P2 Catalog Number	P3 Inflated Price	P4 Cost

BYPRODUCTS PER CYCLE

P5 Catalog Number	P6 Annual Quantity	P7 Uninflated Price	P8 Inflated Price	P9 Byproduct Expense	P10 Byproduct Revenue
D1160D	6.72E7 gal.	2.87E-4 $/gal	1.34E-3 $/gal	8.98 E4	
D1176D	5.55E4 m^2	-9.50E-1 $/m^2$	-1.63 $/m^2$		9.05 E4

COMMODITIES PER CYCLE

P11	P12	P13	P14	P15
Catalog Number	Annual Quantity	Uninflated Price	Inflated Price	Commodities Expense
EG1088D	1.51 E4 oz.	6.07E-1 $/oz	2.33 $/oz	3.52 E4
E1096D	5.80 E4 lbs.	6.43E-1 $/lb	1.50 $/lb	8.70 E4
EG1396D	3.19 E4 lbs.	2.76 $/lb	1.06E-1 $/lb	3.38 E5
E1592D	5.66 E6 gr.	1.26E-1 $/gr	4.85E-1 $/gr	2.75 E6
E1608D	$ 2.80 E5	----	----	4.80 E5

UTILITIES PER CYCLE

P16	P17	P18	P19	P20
Catalog Number	Annual Quantity	Uninflated Price	Inflated Price	Utilities Expense
C1032B	2.80 E7 kW-hr	2.54 E-2 $/kW-hr	8.84 E-2 $/kW-hr	2.48 E6
C1128D	2.52 E7 kW-hr	4.28 E-3 $/kW-hr	1.99 E-2 $/kW-hr	5.01 E5

Prepared by _____ Date _____

W1 COMPANY REFERENCE CELLCO A

W2 PRODUCT PRODUCED ISC

ANNUAL AMOUNT 1.05 E6 (QUAN) m^2 (units)

1986 W30 INFLATED PRICE 86.8 $/$m^2$

1975 W31 DEFLATED PRICE 45.3 $/$m^2$

JPL JET PROPULSION LABORATORY California Institute of Technology 4800 Oak Grove Dr. / Pasadena, Calif. 91109

COMPANY WORK SHEET

W3 Process	W4 Product	W5 Yield	W6 Annual Amount	W7 Req'd Machine Minutes Per Year	W8 Minutes Per Machine	W9 Number of Machines	W10 Cost Per Machine	W11 Equipment Cost	W12 Floor Space Per Machine	W13 Total Floor Space	W14 Labor Cost Per Machine	W15 Total Direct Labor	W16 Total Byproduct Expense	W17 Total Direct Materials & Supplies	W18 Total Direct Utilities	W19 Byproduct Revenue
ICP	CSGPS	0.95	1.11 E6 m^2	1.68 E6	4.12 E5	4.08	1.42 E7	5.79 E7	6.40 E3	2.61 E4	1.46 E5	5.96 E5	8.98 E4	3.69 E6	2.98 E6	9.05 E4
								5.79 E7		2.61 E4		5.96 E5		3.96 E6	2.98 E6	9.05 E4
								W20 EQPT		W21 SQFT		W22 DLAB	W23	8.98 E4	W25 UTIL	W26 BYP

W24 → 3.96 E6

W27 Price of Purchased Product 34.9 $/$m^2$

W28 Purchased Product Expense 3.87 E7

4.25 E7

W29 MATS

Prepared by _____ Date _____

JPL 3001-5 11/71 E-3

ORIGINAL PAGE IS OF POOR QUALITY